Forensic age prediction using inter-platform analysis of DNA methylation with bisulfite-converted DNA quantitation

Sae Rom Hong

Department of Medical Science

The Graduate School, Yonsei University

Forensic age prediction using inter-platform analysis of DNA methylation with bisulfite-converted DNA quantitation

Sae Rom Hong

Department of Medical Science

The Graduate School, Yonsei University

Forensic age prediction using inter-platform analysis of DNA methylation with bisulfite-converted DNA quantitation

Directed by Professor Kyoung-Jin Shin

The Doctoral Dissertation
Submitted to the Department of Medical Science
and the Graduate School of Yonsei University
in partial fulfillment of the
requirements for the degree of
Doctor of Philosophy in Medical Science

Sae Rom Hong

June 2021

This certifies that the dissertation
of Sae Rom Hong is approved.

Thesis Supervisor : Kyoung-Jin Shin

Thesis Committee Member#1 : Hyoung-Pyo Kim

Thesis Committee Member#2 : Hwan Young Lee

Thesis Committee Member#3: Kyung Hee Chun

Thesis Committee Member#4: Sangwoo Kim

The Graduate School
Yonsei University

June 2021

ACKNOWLEDGEMENTS

5년 넘게 공부한 긴 길 위에 큰 이정표를 세우고 가게 되었습니다. 그동안 배우고 익히고 웃고 힘들어한 정든 시간이 쌓여 지금의 제가 있다고 생각합니다. 제가 되기까지 도와주신 분들에게 그동안의 감사함을 담아 이 글을 바칩니다.

부족한 저를 여러 모로 지도해주시고 지혜를 가르쳐 주신 신경진 교수님, 연구실에 들어오는 계기를 만들어주시고 제가 전공하는 분야를 만나게 해주신 이환영 교수님. 두 분께 배울 수 있어서 제게 참 큰 행운이었습니다. 지도해주시고 부족한 부분을 가르쳐주셔서 감사드립니다. 또 바쁘신 와중에도 연구와 논문을 좋은 방향으로 이끌어주신 김형표 교수님과 전경희 교수님, 김상우 교수님께도 깊이 감사드립니다. 그리고 멀리서 든든하게 챙겨주신 양우익 교수님과 많은 관심을 주신 박종필 교수님, 매번 신경 써주신 이숭덕 교수님께도 감사드립니다.

항상 응원의 말씀해주시고 다독여 주신 정상은 선생님, 많은 것을 같이 해주시고 챙겨주신 이은희 선생님, 정말 많이 가르쳐주신 이은영 선생님과 늘 응원을 보내주시는 이지현 선생님, 언제고 연락 드려도 항상 도와주시는 조소희 교수님, 바쁘신데도 늘 도와주신 배수진 선생님과 김모아 선생님께도 감사드립니다. 멀리 계셔도 매번 관심 갖고 연락해주시는 박명진, 정욱희, 심정은, 최아진, 김은혜, 권소연 선배님과 김나영 선생님께도 감사의 말을 전합니다.

학위 과정을 함께하면서 정도 많이 들고 언제나 든든했던 보민씨, 미현씨, 예림씨와 수민씨, 모두 다 건강하고 씩씩하게 학위 과정 잘 마치길 계속 응원합니다! 또, 항상 응원하고 고민을 들어준 생화학과 캡틴정 다은언니, 재영, 진영, 민혁오빠, 한유 모두 힘든 시기 잘 넘기고 행복해지면 좋겠습니다. 그리고 언제나 용감한 모습을 보여주면서 같이 버텨준 혜인이, 룸메로 만나 좋은 친구가 되어줘서 고맙습니다.

언제나 넘치는 사랑과 응원, 기도를 보내주는 우리 가족! 엄마, 아빠와 동생 종현, 종범 정말 고맙고 사랑합니다. 마지막으로 언제나 곁에서 가장 많은 응원과 지지를 해준 남자친구에게도 고마움과 사랑을 전합니다. 그동안 제가 받은 사랑과 지지를 늘 감사히 생각하며 베푸는 사람이 되겠습니다. 정말 감사합니다.

TABLE OF CONTENTS

ABSTRACT ····· v

I. INTRODUCTION ····· 1

II. MATERIALS AND METHODS ····· 5
1. BisQuE ····· 5
A. Sample and bisulfite conversion ····· 5
B. Selection of markers and internal positive control ····· 6
C. Standard DNA and C-T indicators ····· 9
D. BisQuE ····· 10
E. Statistical analysis ····· 11
2. Inter-platform DNAm analysis ····· 12
A. Sample and bisulfite conversion ····· 12
B. Inter-platform DNAm analysis ····· 12
(A) MPS ····· 15
ⓐ Library construction ····· 15
ⓑ MPS Sequencing and DNAm extraction ····· 16
(B) SBE ····· 17
(C) Pyrosequencing ····· 18
(D) Statistical analysis ····· 20
3. Age prediction model ····· 21
A. Data splitting ····· 21
B. Adjustment of SBE and pyrosequencing ····· 21
C. Five-CpG model ····· 22
D. Multiple CpGs model ····· 22

III. RESULTS ····· 23
1. BisQuE ····· 23
A. Standard DNA, C-T indicator, and commercial BS-DNA ····· 23
B. Conversion efficiency ····· 26
C. Degradation level ····· 27
D. Recovery from BisQuE and Qubit ····· 28
2. Inter-platform DNAm analysis ····· 30
A. MPS ····· 30
(A) MPS coverage ····· 30
(B) Age correlations of 69 CpG sites ····· 32
B. SBE ····· 37
C. Pyrosequencing ····· 39
D. Comparison between three platforms ····· 43
(A) MPS vs SBE ····· 43
(B) MPS vs SBE vs pyrosequencing ····· 45
3. Age prediction model ····· 49
A. Adjustment of SBE and pyrosequencing ····· 49
B. Five-CpG model ····· 53
C. Multiple CpGs models ····· 55

IV. DISCUSSION ····· 58
V. CONCLUSION ····· 72

REFERENCES ····· 74
APPENDICES ····· 82
ABSTRACT (IN KOREAN) ····· 99
PUBLICATION LIST ····· 102

LIST OF FIGURES

Figure 1. Concept of a multiplex quantitative real-time PCR evaluation system for bisulfite conversion (BisQuE) and an example ····· 7

Figure 2. Schematic workflow of inter-platform analysis of DNAm ·····13

Figure 3. Schematic PCR step for pyrosequencing·····19

Figure 4. Box-scatter plot of the BS conversion kit ·····25

Figure 5. Difference between BisQuE and Qubit·····29

Figure 6. Basic result of MPS ·····31

Figure 7. Age correlations of common five CpG markers using MPS ·····36

Figure 8. Electropherogram of SBE result ·····37

Figure 9. Age correlations of five CpG markers using SBE ·····38

Figure 10. Pyrogram of FHL2 ·····39

Figure 11. Age correlations of five common CpG markers using pyrosequencing ·····40

Figure 12. Five CpG markers of MPS and SBE from 250 sample ·····44

Figure 13. Boxplots of each marker of three DNAm analysis platforms ·····46

Figure 14. Training and test set of adjustment model for CpGs of SBE ·····50

Figure 15. Five-CpG model result·····54

Figure 16. Multiple CpGs model result·····57

LIST OF TABLES

Table 1. Primer and probe sequences for qPCR ····· 8

Table 2. C-T indicator, and IPC sequence for real-time qPCR ····· 9

Table 3. Primers of 1st PCR ····· 14

Table 4 Index primer for MPS ····· 15

Table 5. SBE primers for five genes ····· 17

Table 6. Pyrosequencing PCR primers and sequencing primers ····· 19

Table 7. Six BS conversion kits and an overview of the results ····· 24

Table 8. Age correlation values of 69 CpG sites from MPS data ····· 33

Table 9. Age correlation values of 40 CpG sites from pyrosequencing data ····· 41

Table 10. Intra-class coefficient and Passing-Bablok regression analysis of common five CpGs from MPS and SBE data ····· 43

Table 11. Intra-class coefficient analysis of three platforms ····· 45

Table 12. Passing-Bablok regression analysis of MPS and pyrosequencing ····· 47

Table 13. Adjustment models for SBE ····· 49

Table 14. Adjustment models for pyrosequencing ····· 51

Table 15. The constructed five-CpG model ····· 53

Table 16. The constructed multiple CpGs model ····· 55

Table 17. Amount of BS-DNA based on the long-sized BisQuE result ····· 64

Table 18. Target sizes of previous works ····· 66

ABSTRACT

Forensic age prediction using inter-platform analysis of DNA methylation with bisulfite-converted DNA quantitation

Sae Rom Hong

Department of Medical Science
The Graduate School, Yonsei University

(Directed by Professor Kyoung-Jin Shin)

Recently, DNA methylation (DNAm) is vigorously studied for its potential to applicate in forensic genetics, such as an age prediction for investigation leads. Researchers have suggested various age predictive models using many DNAm analysis platforms for several forensically relevant body fluids including blood. Even though a lot of age prediction models have been suggested, there are some several concerns considering forensic context: poor quality and low quantity of DNA; continuity of age and DNAm level; and loss of accuracy while applying inter-platform data to different platforms. To deal with the concerns, three concepts was come up with in this study: bisulfite (BS) converted DNA quantitation; forensic age prediction models based on massively parallel sequencing sequencing (MPS) data; and adjustment method for inter-platform analysis of widely used platforms, single-base extension (SBE), and pyrosequencing.

First, BS conversion is a prerequisite to most DNAm analysis methods, and it leads to the degradation or loss of DNA, which can hinder the further downstream analysis. By adopting Cytosine-free PCR primers for two differently sized multicopy regions, a multiplex quantitative real-time PCR system named BisQuE was suggested to simultaneously analyze three important aspects of the conversion step: BS conversion efficiency, recovery, and degradation level. By using the BisQuE, six different BS converting kits were tested with 20 DNA samples.

Since the detected DNAm level can be different according to its analysis platform, the same amplicon strategy was developed in this study for three commonly used platforms: MPS, SBE, and pyrosequencing. This system contained five different amplicons on *ELOVL2, FHL2, KLF14, MIR29B2C,* and *TRIM59*, respectively. Based on the long-sized BisQuE results, DNA from 250 human blood samples were converted and prepared to containing 1.5 ng of BS-converted DNA, which can be the minimum amount to have reliability of DNAm result.

Then DNAm data of 250 individuals were obtained successfully from MPS and SBE, and 20 samples for each five markers were pyrosequenced and analyzed. Thanks to the same amplicon strategy, DNAm differences due to platforms were compared and the ELOVL2 marker seemed to be interchangeable in all three methods; however, the platform-adjusted models of SBE and pyrosequencing were calculated for rest of markers to be fitted to MPS data.

Finally, considering the continuities of age and DNAm, two age prediction models based on DNAm detected with MPS were constructed: 5-CpG model and multiple CpGs model. The 5-CpG model was simplified one containing common five CpGs which were overlapped to targets of SBE showing high accuracy in the adjusted SBE data, 3.99 years of mean absolute error. The multiple CpG model can be used in both MPS and pyrosequencing and showed 2.85 years and 5.43 years of error, respectively.

This study provides the guideline for age prediction modelling in forensic context based on quantitation of BS-DNA and the same amplicon strategy, and it is the first study to quantify BS-DNA for entire samples and analyze the difference between DNAm platforms with same amplicons. By following the recommendations, accurate and reliable age prediction modelling can be done by whom trying to suggest the model in forensic fields, and trustworthy age prediction reports can be generated by who dealing with forensic DNA from crime scenes.

Key words : age prediction, bisulfite conversion, DNA methylation, massively parallel sequencing, pyrosequencing, quantitative real-time PCR, single-base extension

Forensic age prediction using inter-platform analysis of DNA methylation with bisulfite-converted DNA quantitation

Sae Rom Hong

Department of Medical Science
The Graduate School, Yonsei University

(Directed by Professor Kyoung-Jin Shin)

I. INTRODUCTION

DNA methylation (DNAm) is widely-studied epigenetic phenomena for aging[1-7], development[8], and diseases[9]. As DNAm has potential implications in various fields, researchers bring it to forensic fields to get more information from evidences in crime scenes[10-15]. For decades, short-tandem repeat (STR) typing is used for personal identification[16]. When the identification is impossible, however, the case can be remained as a cold case for a long time. To prevent this effort- and time-consuming case, many researchers have attempted to utilize DNAm data for investigation leads such as body fluid identification[10, 12, 17, 18], and age prediction[1, 19-45]. This trend leads to rise of forensic epigenetics, and this new field is expanding the realm of forensic genetics.

Many works report numerous age-correlated CpG sites and suggest age prediction models based on DNAm data from forensic-relevant materials such as blood[2, 3, 23, 25, 27, 33, 35, 38-50], saliva[1, 26, 28, 32, 33], semen[17, 30], and bone[36, 37, 43, 44, 49, 51, 52] using various analysis platforms, e.g. pyrosequencing[23, 25, 31, 39, 42, 45, 47, 50, 53], single-base extension (SBE) [20, 26, 32, 33, 35, 36, 47], massively parallel sequencing (MPS) [29, 32, 34, 38, 44, 49], and EpiTYPER (based on MALDI-TOF mass spectrometry) [24, 31, 46-48, 54]. As many age-predictive models have been suggested, the accuracy of the models is getting higher and higher. Also, exploiting the age information as the investigation leads allows to narrow the range of the suspects and save

the time and effort.

Even though a lot of age prediction models have been suggested, there are some limitations due to forensic context: low quantity of DNA, vague quantity of bisulfite (BS) conversion step before analysis[13, 29, 55], and the loss of accuracy while inter-platform applications[29, 31, 32, 47]. Since the amount of forensic DNA samples is fairly low and its' quality cannot be guaranteed as intact DNA from regular laboratories, it is important to consider the low limit of DNA input for DNAm analysis in forensic epigenetics. Naue et al.[56] simulated *in silico* the margin of error at a 95% confidence of DNAm level depending on input of DNA. In their study, 5% of margin of error at 95% confidence level was shown in 1.36ng, assuming when the original DNAm level is 50%. Aliferi et al.[29] demonstrated that 10ng of starting material (~2ng of PCR input) showed quite successful to obtain reliable predicted age. Heiddeger et al.[34] showed the duplicated had a difference more than 10% when input is 10ng or less by using MPS. Most studies have used more than 100ng of genomic DNA (gDNA) for their starting material and consumed some part of it.

BS conversion, which includes a series of chemical reactions using bisulfite, is a prerequisite to most of the methods, therefore it is considered to be an essential step in the associated research process. Unfortunately, BS conversion occurs under harsh conditions (acidic and high temperature) and thus leads to the degradation or loss of DNA, which can hinder the further downstream analysis[57-59]. Additionally, the incomplete BS conversion can have crucial implications as it causes an exaggeration of the DNAm level, which might affect the results[13, 46, 55]. For these reasons, many researchers have attempted to quantify the BS conversion efficiency[34, 60-65], recovery[59, 62, 63], and the degradation level[57, 59, 64]. Previous studies have attempted to develop many methods which showed to be highly accurate, although all of them had hardships with providing key information of the BS conversion: the BS conversion efficiency, recovery, and degradation level. However, three key features cannot be obtained in a single assay, it should be needed at least two different assays. Also, most forensic age prediction model studies offered their gDNA input, not BS-converted DNA (BS-DNA). Researchers recommended the quantitation of BS-DNA[13, 55] and *in silico*

simulation[56] was not taken into account the loss of DNA, so quantitation is important for forensic DNAm analysis.

When it comes to forensic age prediction models, researchers have made use of a few age-predictive markers for constructing the model as the DNA and usable resources are limited in forensic laboratories. Thanks to rapid developments in technologies of DNAm analysis, forensic age prediction models have been developed based on a wide array of DNAm analysis platforms.; however, it showed quite large errors when applying DNAm data which were from different platforms. To increase applicability, many researchers have tried to suggest the integrated model for two or more platforms [31, 32, 38, 47]. Vidaki et al.[38] applied MPS data into a generalized regression neural network (GRNN) model with HumanMethylation27/450 data from blood but mean absolute error (MAE) was quite larger (7.45 yrs) than the beadchip array data (4.6 yrs). Feng et al.[31] transformed pyrosequencing data with z-score transformation, and then applied it to the EpiTYPER-based model to get 2.76 yrs of mean absolute deviation (MAD). Additionally, Hong et al.[32] induced platform variable to construct the age prediction model based on both MPS and SBE data and got 3.16 yrs of MAD in the test set, but it was merely making a model not integrating both platforms. Freire-Aradas et al.[47] suggested a quantile regression model based on EpiTYPER, pyrosequencing, and MPS data, also they presented a model based on EpiTYPER, MPS, and SBE.

However, previous studies merely showed the possible way to application of the models and the prediction accuracy will be higher if the data is applied into the single-platform model of which the platform is the same with the data. Unfortunately, forensic age prediction has innate obstacles to apply those models: poor quality and low quantity of DNA. Due to distinctive features of DNA samples from case work, large amount of starting materials are quite challenging for routine forensic works. Furthermore, amplification of more than 300bp long amplicon might be hindered because of the poor quality-DNA from evidence. Therefore, an age prediction model based on the least amount of DNA is needed.

In this study, we tried to propose how to construct age prediction models considering in

forensic context to provide reliable and accurate age prediction results independent to three platforms: MPS, SBE, and pyrosequencing. Firstly, a multiplex quantitative real-time PCR system for the evaluation of the BS conversion (BisQuE) was developed for simultaneously analyzing three important aspects of the conversion step to guarantee the quality of the BS conversion step and quantify the amount of BS-DNA. For the exploitation of the constructed qPCR system, six BS conversion kits were tested in 20 samples to investigate the conversion efficiency, recovery, and degradation levels of the various kits and select the kit for the experiment. Then, 250 samples were BS converted and quantified with the BisQuE to be used as template for the target specific (1st multiplex) PCR in the same amount. With this PCR product, each downstream experiment steps were performed for three DNAm analysis platforms: MPS and SBE data of 250 samples, and pyrosequencing data of 20 samples for five markers were analyzed. This five markers are on the *ELOVL2, FHL2, KLF14, MIR29B2C,* and *TRIM59* genes, respectively and those are common age predictive markers for blood demonstrated in several population groups in three platforms: pyrosequencing[25, 47, 50], MPS[34, 44], and SBE[33, 35].

Based on the result, adjustment models of SBE and pyrosequencing data to MPS data were suggested; the SBE adjusting model was tested with independent test set, but the pyrosequencing model was not due to small numbers of samples. Lastly, with statistical modellings, two MPS-based age prediction models were proposed by the training set of MPS data; five-CpG model and multi CpG model. The five-CpG model was constructed with common five CpGs for MPS, SBE, and pyrosequencing, and the multi-CpG model was for MPS and pyrosequencing. In the independent test, two model showed high accuracies in MPS test set, 4.29 yrs and 2.85 yrs of MAE, respectively. Also, five-CpG model showed 3.99 yrs of MAE in SBE data, and 4.97 yrs of MAE in pyrosequencing data. The multiple CpG model presented somewhat low accuracy in pyrosequencing data (5.43 yrs of MAE).

II. MATERIALS AND METHODS

1. BisQuE[66]

A. Sample and bisulfite conversion

Peripheral blood samples of 20 Korean (10 males and 10 females) were obtained from a biobank of the Asian Sample Network under the approval of the Institutional Review Board of Severance Hospital, Yonsei University in Seoul, Korea (4-2019-0707). DNA was extracted from a 200 μl of whole blood sample using a QIAamp® DNA Mini Kit (Qiagen, Hilden, Germany) following the instructions of the manufacturer. The extracted DNA was quantified using the Quantifiler™ Duo Kit (Thermo Fisher Scientific, Waltham, MA, USA) and stored at −20°C until further usage.

For the 20 samples, each sample was diluted to 5 ng/μl based on the Quantifiler Duo Kit result for BS conversion and the BisQuE step. The BS-DNA was obtained through the modification of 50 ng of gDNA with six BS conversion kits: EZ DNA Methylation-Lightning Kit (Zymo Research, Irvine, CA, USA; Z-EZ), Premium Bisulfite kit (Diagenode, Seraing, Belgium; D-PB), MethylEdge® Bisulfite Conversion System (Promega, Madison, WI, USA; P-ME), EpiJET Bisulfite Conversion Kit (Thermo Fisher Scientific; T-EJ), EpiTect Fast DNA Bisulfite Kit (Qiagen; Q-EF), and NEBNext® Enzymatic Methyl-seq Conversion Module (New England Biolabs, Ipswich, MA, USA; N-NE). Detailed specifications of six kits were in Appendix 1. The BS conversion as well as subsequent purification steps were performed according to the protocol of the respective kit and the BS-DNA was eluted with 10 μl of 1 × TE buffer except for the N-NE, which was eluted with 20 μl of 1 × TE buffer. Converted DNA was stored at −20°C and used within 1–3 days. Besides, 1 μl of BS-DNA samples were measured with Qubit™ ssDNA Assay Kit (Thermo Fisher Scientific) two times using a Qubit™ 4 Fluorometer from the same manufacturer.

B. Selection of markers and internal positive control

To achieve a measurement with high accuracy and sensitivity, multicopy regions that showed relatively constant copy numbers among several populations[67] were considered. Based on in silico BS-converted genomic reference sequences, Cfree PCR primer candidates and probe candidates were designed with Primer3 v. 0.4.0 (http://bioinfo.ut.ee/primer3-0.4.0/) and subsequently adjusted manually (Table 1). The region on introns of two genes, *CCDC29* and *FLJ39739* were targeted to amplify 104bp and 238bp, respectively. Two types of CCDC29 probes, the short-C probe and the short-T probe were designed to separate BS-converted T and unconverted C on the same site in non-CpG context. (Figure 1). These probes had the same sequence except only one base: C for C probe, and T for T probe (Table 1). Meanwhile, the probe of longer amplicon, FLJ39739, included no cytosine nucleotide in its' sequence, so that it can be detected both gDNA and BS-DNA.

An IPC sequence was generated with a Random DNA Sequence Generator (Table 2) (https://faculty.ucr.edu/~mmaduro/random.htm) to obtain a random sequence free from human DNA to avoid interaction with other primers or probes. IPC was synthesized by gBlocks Gene Fragments (Integrated DNA Technologies, Coralville, IA, USA), and calculated to be 500 copies for each qPCR reaction.

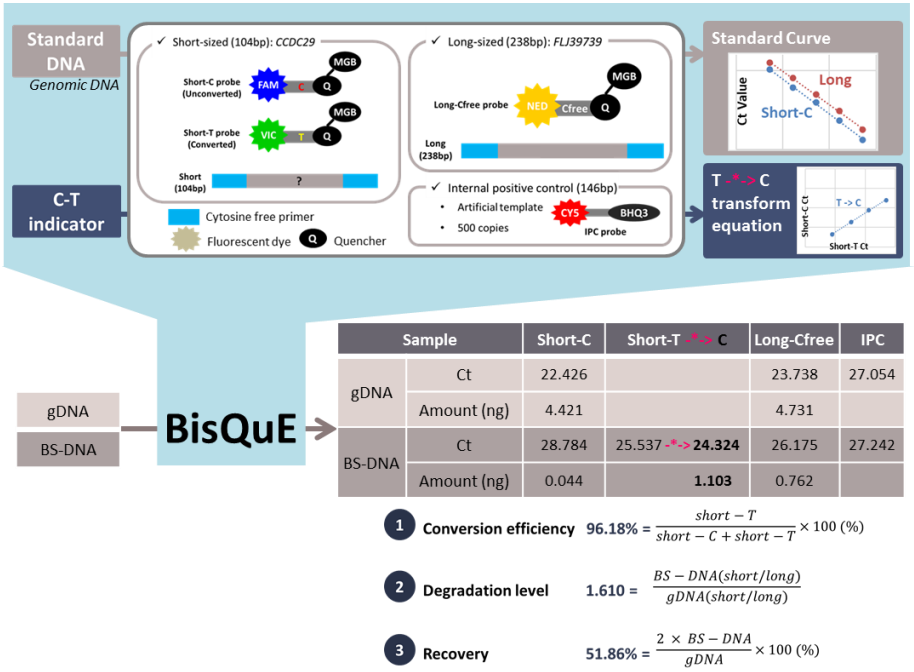

Sample		Short-C	Short-T -*-> C	Long-Cfree	IPC
gDNA	Ct	22.426		23.738	27.054
	Amount (ng)	4.421		4.731	
BS-DNA	Ct	28.784	25.537 -*-> **24.324**	26.175	27.242
	Amount (ng)	0.044	**1.103**	0.762	

1 **Conversion efficiency** 96.18% = $\frac{short - T}{short - C + short - T} \times 100\ (\%)$

2 **Degradation level** 1.610 = $\frac{BS - DNA(short/long)}{gDNA(short/long)}$

3 **Recovery** 51.86% = $\frac{2 \times BS - DNA}{gDNA} \times 100\ (\%)$

Figure 1. Concept of a multiplex quantitative real-time PCR evaluation system for bisulfite conversion (BisQuE) and an example. Figure 1 from Hong et al.[66] Genomic DNA (gDNA) and bisulfite-converted DNA (BS-DNA) undergoes the developed BisQuE method, which including cytosine free PCR primers and probes for two different sized targets. Also, standard curves and the short-T to C transforming equation (-*->, highlighted in pink color) were obtained with standard DNA and C-T indicators, respectively. With those results of each gDNA and BS-DNA, the three key features (conversion efficiency, degradation level, and recovery) were calculated.

Table 1. Primer and probe sequences for qPCR

Target	PCR amplification			Probe		
	Primer sequences (5′ > 3′)	Conc. (μM)	Amplicon size (bp)	Probe sequence (5′ > 3′)	Conc. (μM)	Length (nt)
Short	F: gaa atg gtt aag aga aag gga aa	0.6	104	C: FAM-tgg gtg aat a**C**t tag aat g-NFQ MGB	0.1	19
*CCDC29**	R: ccc att aca ttt ttc atc ctc a	0.6		T: VIC-tgg gtg aat a**T**t tag aat g-NFQ MGB	0.1	19
Long	F: ggg aaa atg agg aag tga tga	1.0	238	Cfree: NED-aat gtt gta tgt tat ttg tgg-NFQ MGB	0.15	21
*FLJ39793***	R: aca caa aaa acc ctt caa aaa a	1.0				
IPC	F: aac tgc tag aaa acc gcg tc	0.8	147	Probe: CY5-tcc agg cag tgc gtc t gc tgt-BHQ3	0.2	21
	R: gag gca ggc tct tgc tat gt	0.8				

* chr9:67907355-67907458 and 8 other loci (GRCh38, UCSC in silico PCR)

** chr1:149482287+149482524 and 10 loci (GRCh38, UCSC in silico PCR)

Table 2. C-T indicator, and IPC sequence for real-time qPCR

C-T indicator (single strand) 104 nt	GAA ATG GTT AAG AGA AAG GGA AAA ACT GAA ACC TGT GGG TGA ATA **Y**TT AGA ATG ACA GTA TTT AGC TCA GCC TGA AGA CAG ATG AGG ATG AAA AAT GTA ATG GG
IPC (dsDNA) 450bp	CTCTAACTAGTATGGATAACCGTGTTTTCACTGTGCTGCGGT TACCCATCGCCTGAAATCCAGTTGGTGTCAAGCCATTCCCTG TCTAGGACGCCGCATGTAGTAAAACATATACATTGCTCGGG TTCACTCCGGTCCGTTCTGAGTCGACCAAGGACACAATCGA GCTCCGATCTGTATTGTCGAGAAACTTGTATCCAACCCCCGC AGCTTGCCAGCTCTTCGGGTATCATGGAGCCTATGGTTGAA CAAGGCCCATACGCGAGATAAACTGCTAGAAAACCGCGTCT TTACGACTGGTGCTTAATTTAATTTCGCTGACGTGATGACAT TCCAGGCAGTGCGTCTGCTGTCGGGTCCCTCTCGTGATTGGG TAGTTGGACATGCCCTTGAAAAACATAGCAAGAGCCTGCCT CTCTATTGATGTCACGGCGAATGTCGGGGAGACAG

C. Standard DNA and C-T indicators

Standard DNA samples were prepared from Quantifiler Duo DNA Standard by serial dilution with TE buffer: 10 ng, 2 ng, 400 pg, 80 pg, and 16 pg per 1 μl. Additionally, 1 ng/μl of BS-converted, methylated sample (Epi-M) and 1 ng/μl of BS-converted, unmethylated sample (Epi-U) were obtained from the EpiTect Control DNA and Control DNA Set (Qiagen), which were diluted according to the concentration given by the manufacturer, and were utilized as reference samples. C-T indicators (Table 2) were synthesized by Macrogen (Seoul, Korea) and 10^6, 10^5, 10^4, and 10^3 copies per μl were freshly prepared to obtain the relation between the C to T. As the indicator sequence contained a degenerate base Y, it supposed to consist of 50% of C and 50% of T for simple calculation (Table 2).

D. BisQuE

The BisQuE was performed with an Applied Biosystems 7500 Real-Time PCR System (Thermo Fisher Scientific) and the results were analyzed with the Applied Biosystems 7500 Real-Time PCR Software v2.3 from the same manufacturer. As most of the ready-made real-time PCR systems contain uracil N-glycosylase or uracil-DNA glycosylase to prevent carryover contamination, so BS-DNA could not be amplified in this system. To analyze features of BS-DNA, each reaction contained 5 μl of 2X Platinum™ II Hot-Start PCR Master Mix (Thermo Fisher Scientific), 0.6–1.0 uM of each primer, 0.1–0.2 uM of each TaqMan probe (Thermo Fisher Scientific) (Table 1), 500 copies of IPC, 0.5 μl of 1/10 diluted ROX passive reference dye (Thermo Fisher Scientific), and 1 μl of the template: 16 pg/μl–10 ng/μl of five DNA standards; 1 ng/μl of Epi-M; 1 ng/μl of Epi-U; 5 ng/μl of gDNA; BS-DNA; and 10^3–10^6 copies/μl of four C-T indicators. The thermal cycling conditions were set to 94℃ for 2 min, followed by 40 cycles at 94℃ for 15 s and 60℃ for 45 s. All the reactions were amplified in a duplicate.

Cycle threshold (Ct) values were determined using the automatic baseline algorithm. The slope of the standard plot regression line was used to calculate qPCR amplification efficiencies. The content of each 104bp of the CCDC29 and 238bp of the FLJ39739 amplicon was calculated from the Ct value of the C probe of the CCDC29 (short-C) and the Cfree probe of the FLJ39739 (long-Cfree), respectively. The T probe of the CCDC29 (short-T) was subsequently computed from the relation between the Ct values of the short-C and the short-T from the results of the C-T indicators.

The conversion efficiency, degradation level, and recovery of BS conversion were acquired based on the calculated content of each amplicon. The ratio of short-T amount and sum of the short-C and the short-T amount (%) described the BS conversion efficiency, and the ratio of the division of the short by the long amplicon of gDNA and BS-DNA led to the calculation of the degradation level. Besides, the double of the short amplicon ratio of the gDNA and BS-DNA (%) was recovered from the BS conversion step (The recovery

of the N-NE samples was doubled again due to that its eluted volume was 20 μl, whereas others were 10 μl). (Figure 1) Those values were obtained for 120 BS-converted samples from 20 gDNA samples undergoing six different BS conversion kits.

E. Statistical analysis

To show if there were significant differences between BS conversion kits in each of conversion efficiency, degradation level, recovery from BisQuE, and recovery tested with Qubit. All statistical analyses were performed with IBM SPSS 25 and Microsoft Excel Office 365. Shapiro-Wilk test was done to test normality of the three features and Qubit recovery, then Levene's test was done for testing equal variance. Following tests were applied by its' results: Kruskal–Wallis one-way analysis of variance (ANOVA) for conversion efficiency; Welch's one-way ANOVA for degradation level and Qubit recovery; one-way ANOVA for recovery from BisQuE. Post hoc analysis were performed to confirm the differences between the kits: Bonferroni-corrected method for conversion efficiency; Games-Howell test for degradation level and Qubit recovery; Tukey's honest significant difference test for BisQuE recovery.

2. Inter-platform DNAm analysis

A. Sample and bisulfite conversion

Peripheral blood samples of 250 Korean (125 males and 125 females) aged 20–74 yrs old were obtained from a biobank of the Asian Sample Network under the approval of the Institutional Review Board of Severance Hospital, Yonsei University in Seoul, Korea (4-2019-0707). DNA was extracted from a 200 μl of whole blood sample using a QIAamp® DNA Mini Kit (Qiagen) following the instructions of the manufacturer. The extracted DNA was quantified using the Quantifiler™ Duo Kit (Thermo Fisher Scientific) and stored at −20℃ until further usage. The BS-DNA was obtained through the modification of 50 ng of gDNA with Z-EZ and eluted with 10 μl of 1 × TE buffer. All BS-DNA samples were quantified with the BisQuE.

B. Inter-platform analysis of DNAm

Five loci on the five genes (*ELOVL2*, *FHL2*, *KLF14*, *MIR29B2C*, and *TRIM59*) were selected. To achieve the inter-platform DNAm analysis, the concept of a same amplicon strategy for library generation used. The first round PCR was performed with target-specific primers compatible with TruSeq® DNA Library Prep Kit (Illumina, San Diego, CA, USA). (Table 3) Using those primers, multiplex PCR reactions were performed in 20 μl reaction volumes containing 1.5 ng (based on the amount of long-Cfree) of BS-DNA, 10 μl of 2X Platinum™ II Hot-Start PCR Master Mix (Thermo Fisher Scientific), 0.17–1.8 μM of each primer. PCR cycling was conducted using a Veriti™ 96-Well Thermal Cycler under the following conditions: 94˚C for 2 min; 27 cycles of 94˚C for 15 s, 59˚C for 1 min, and 68˚C for 15 s; and a final extension at 68˚C for 1 min.

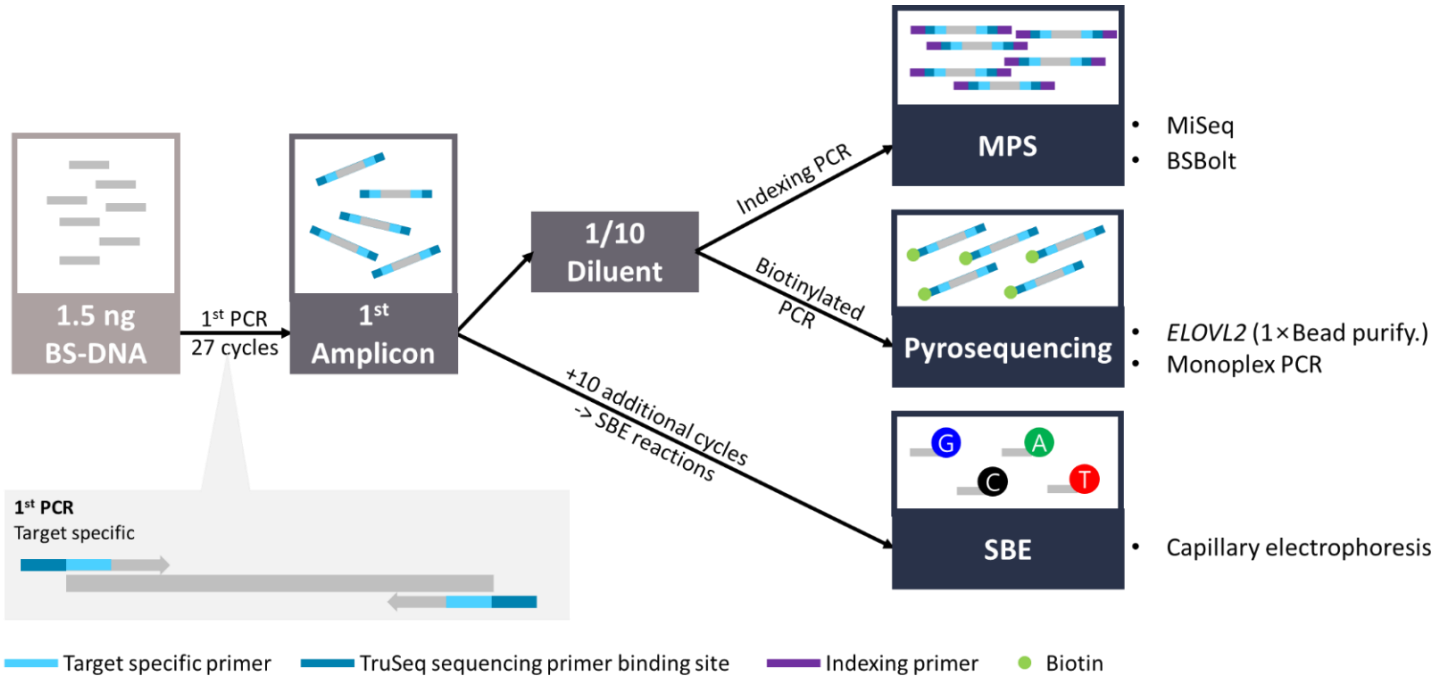

Figure 2. Schematic workflow of inter-platform analysis of DNAm. MPS, pyrosequencing, and SBE results were from the same 1st PCR amplicon. 1.5 ng of BS-DNA was prepared based on the quantified amount of the long-Cfree of the BisQuE. Three different DNAm analysis were done with the same 1st PCR amplicons and its' steps were briefly presented.

Table 3. Primers of 1st PCR

Gene	Sequence (5'>3')	Conc. (μM)	Amplicon size (bp)
ELOVL2	F: ACACTCTTTCCCTACACGACGCTCTTCCGATCTggggYgtagggtaagtgagg	1.8	254 (187)
	R: GTGACTGGAGTTCAGACGTGTGCTCTTCCGATCTcaacRaataaatattcctaaaactcc	1.8	
FHL2	F: ACACTCTTTCCCTACACGACGCTCTTCCGATCTgggttttgggagtatagtagtt	0.21	195 (128)
	R: GTGACTGGAGTTCAGACGTGTGCTCTTCCGATCTcctaaaaccaaacaaaaatccc	0.21	
KLF14	F: ACACTCTTTCCCTACACGACGCTCTTCCGATCTaggttgttgtaatttagaagttt	0.5	181 (114)
	R: GTGACTGGAGTTCAGACGTGTGCTCTTCCGATCTatatttaacaacctcaaaaattatcttatc	0.5	
MIR29B2C	F: ACACTCTTTCCCTACACGACGCTCTTCCGATCTtgggggaagaaggggggtta	0.7	200 (133)
	R: GTGACTGGAGTTCAGACGTGTGCTCTTCCGATCTttaataaaaccaaattctaaaacattc	0.7	
TRIM59	F: ACACTCTTTCCCTACACGACGCTCTTCCGATCTgtggtttgggggagaggtt	0.17	189 (122)
	R: GTGACTGGAGTTCAGACGTGTGCTCTTCCGATCTtccacaacataacaaMaaaccc	0.17	

(A) MPS

ⓐ Library construction

Table 4. Index primer for MPS

MPS index primer	Sequence (5'>3')*	Conc. (μM)
rhAmpSeq i7 index	CAAGCAGAAGACGGCATACGAGAT [N8] GTGACTGGAGTTCAGACGTGT	0.5
rhAmpSeq i5 index	AATGATACGGCGACCACCGAGATCTACAC [N8] ACACTCTTTCCCTACACGAC	0.5

*[N8] is 8-base index sequence.

In the second PCR step, 1 μl of 10-fold diluted PCR product, 10 μl of 2X Platinum™ SuperFi II Master Mix (Thermo Fisher Scientific), 0.5 μM of each rhAmpSeq Index Primer (Integrated DNA Technologies, Coralville, IA, USA) containing P5 and P7 Illumina index primer sequences (Table 4). PCR cycling was conducted using a Veriti™ 96-Well Thermal Cycler under the following conditions: 98˚C for 30 s; 15 cycles of 98˚C for 10 s, 61˚C for 10 s, and 72˚C for 20 s; and a final extension at 72˚C for 5 min. All the constructed libraries were checked with an Agilent 2100 Bioanalyzer and a DNA 1000 Kit (both Agilent Technologies, Santa Clara, CA, USA). Then pooled libraries were undergone PCR cleanup with 1.2× Agencourt® AMPure® XP beads (Beckman Coulter, Indianapolis, IN, USA), and quantified using KAPA library quantification kits (KAPA Biosystems, Wilmington, MA, USA). Then, the size of the amplicons was checked using the DNA 1000 Kit (Agilent Technologies).

ⓑ MPS Sequencing and DNAm extraction

Sequencing was conducted on a MiSeq® system using MiSeq Reagent Kit v3 (600 cycles) (Illumina). The obtained fastq data were trimmed with cutadapt v1.9.1 (https://cutadapt.readthedocs.org/), and the base quality was checked by FastQC v0.11.4 (http://www.bioinformatics.babraham.ac.uk/projects/fastqc/). The obtained reads from 250 individuals were aligned to *in silico* bisulfite-converted genomic reference sequences of seven markers using BSbolt v1.4.5 and BWA with the following parameters: single-end, non-directional alignment, and other conditions set to default values. The DNAm values of the CpG and the non-CpG sites were extracted using the BSbolt (both base quality and mapping quality > 30) and SAMtools, and BS conversion efficiency of each sample was calculated by subtracting the level from 100% using the non-CpG C context levels.

(B) SBE

Table 5. SBE primers for five genes

Gene	Sequence (5'>3')	Conc. (μM)	Amplicon size (bp)
ELOVL2	(T)7 gggIggIgatttgtaggtttagt	0.8	30
FHL2	(T)21 gttttgggagtatagtagttat	0.7	43
KLF14	(T)34 cctcaaaaattatcttatctcc	0.3	56
MIR29B2C	(T)46 aaaccaaaatttaaatctac	1.2	66
TRIM59	(T)51 ctcaaaaaccItcIaccaccRac	0.3	74

*I denotes for inosine and R does for degenerate base containing G and A.

SBE primers for selected CpG markers were adjusted (Table 5). Additional PCR was performed in 10 μl reaction volumes from the first target-specific PCR. PCR cycling was conducted using a Veriti™ 96-Well Thermal Cycler under the following conditions: 94˚C for 15 s; 10 cycles of 94˚C for 15 s, 59˚C for 1 min, and 68˚C for 15 s; and a final extension at 68˚C for 5 min. The, 5 μl aliquots of PCR products were purified with 1 μl of ExoSAP-IT™ (Thermo Fisher Scientific) by incubation at 37˚C for 45 min, followed by heat inactivation at 80˚C for 15 min. An SBE reaction was performed using 1 μl of purified PCR product, 0.3–1.2 μM of SBE primers (Table 5), and a SNaPshot™ Kit (Thermo Fisher Scientific) according to the manufacturer's instructions. Extension products were analyzed using an ABI PRISM 3130 Genetic Analyzer and GeneMapper ID software v3.2 (Thermo Fisher Scientific). Methylation level (0–1) at each CpG site was calculated by dividing methylated signal (nucleotide C or G) intensity by sum of both methylated and unmethylated signal (nucleotide T or A) intensities.

(C) Pyrosequencing

Similar to II.B.(A).ⓐ, 1 μl of 10-fold diluted PCR product, 10 μl of 2X Platinum™ SuperFi II Master Mix (Thermo Fisher Scientific), each of the primers including biotinylated primer. (Table 6, Figure 3) PCR cycling was conducted using a Veriti™ 96-Well Thermal Cycler under the following conditions: 98˚C for 30 s; 27 cycles (for *ELOVL2*) or 25 cycles (for four genes) of 98˚C for 10 s, 61˚C for 10 s, and 72˚C for 20 s; and a final extension at 72˚C for 5 min. The product of *ELOVL2* purified with 1.0× Agencourt® AMPure® XP beads (Beckman Coulter). All the constructed products were checked with 8% polyacrylamide gel electrophoresis. The template prepared from biotinylated PCR product was sequenced with a PyroMark Q96ID system with the Pyro Gold reagents kit (both Qiagen) according to the manufacturer's instructions. The generated pyrograms were automatically analyzed using PyroMark analysis software.

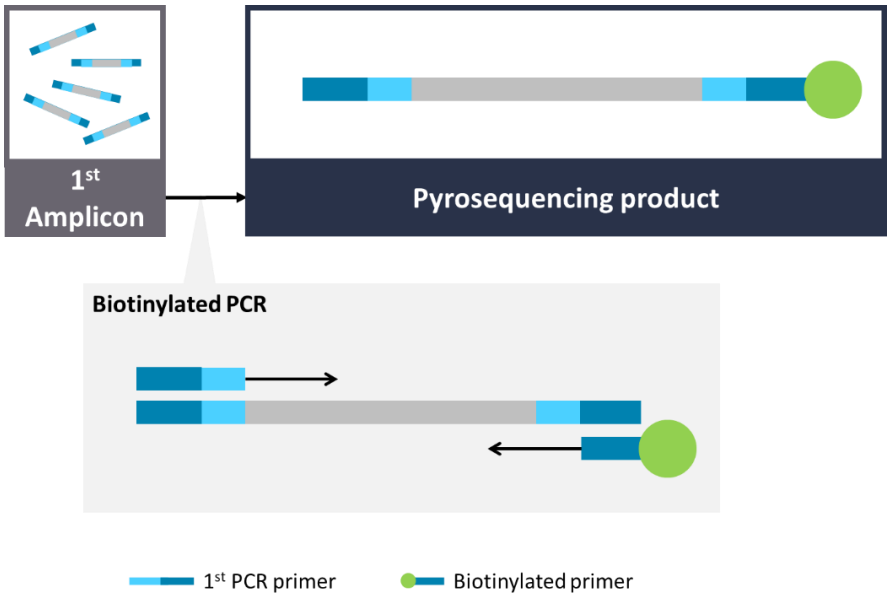

Figure 3. Schematic PCR step for pyrosequencing.

Table 6. Pyrosequencing PCR primers and sequencing primers

Gene	Sequence (5'>3')*	Conc. (μM)	Amplicon size (bp)
ELOVL2	F: Same with 1st PCR F primer	1.8	254 (187)
	R: Biotin-R	1.8	
	Seq: gggIggIgatttgtaggtttag	0.5	
FHL2	F: Same with 1st PCR F primer	0.5	195 (128)
	R: Biotin-R	0.5	
	Seq: ggttttgggagtatagtagtta	0.5	
KLF14	F: Biotin-F primer	0.6	181 (114)
	R: Same with 1st PCR R	0.6	
	Seq: acctacaaaattatcttatctt	0.5	
MIR29B2C	F: Biotin-F primer	0.8	200 (133)
	R: Same with 1st PCR R	0.8	
	Seq: aaaccaaaatttaaatcta	0.5	
TRIM59	F: Same with 1st PCR F primer	0.6	189 (122)
	R: Biotin-R	0.6	
	Seq: aaaccaaaatttaaatcta	0.5	

Biotinylated primer	Sequence (5'>3')
Biotin-F	Biotin-ACACTCTTTCCCTACACGACGCTCTTCCGATC
Biotin-R	Biotin-GTGACTGGAGTTCAGACGTGTGCTCTTCCGATC

*The sequence of the 1st PCR F or R primer of each marker were on Table 3.

**I denotes for inosine.

(D) Statistical analysis

Statistical analysis was performed using R project with R studio and Microsoft EXCEL. The age-related correlations of methylation level at all CpG sites were assessed using Pearson's correlation coefficient (68 CpGs for MPS, 5 CpGs for SBE, and 40 CpGs for pyrosequencing). Normality was tested using a Shapiro-Wilk or Kolomogorov-Smirnov normality test for DNAm levels of each CpGs from three platforms. To check agreement, intra-class correlation coefficient (ICC)[68] and Passing-Bablok regression[69] were applied using psych and mcr packages. ICC estimates and their 95% confident intervals were calculated based on a single-rating (k = 1), absolute-agreement, 2-way random-effects model. To compare the differences between three platforms, one-way repeated measures ANOVA test or Friedman test (FHL2) were applied using rstatix package, and paired t-test with Bonferroni correction or Wilcoxon signed rank test with Bonferroni correction (FHL2 only) were done as post-hoc analysis.

3. Age prediction model

A. Data splitting

To separate the training set and test set, caret package in R was used to partitioned samples into 200 and 50 samples, respectively. To prevent the over-fitting problem, 20 samples, which were commonly tested in MPS, SBE, and pyrosequencing, were assigned to the test set. Then all models were trained via 5-time repeated 10-fold cross validation to reduce overfitting effect except the adjustment of pyrosequencing data.

B. Adjustment of SBE and pyrosequencing

To adjust the difference between MPS-SBE and MPS-pyrosequencing, polynomial regression method was used for each five CpG sites. For MPS-SBE adjustment, linear or cubic equations were selected based on their accuracy and residual errors. Shapiro-Wilk normality test was applied to test the normality of residual errors. The adjustment models were tested with 50 samples of test set from SBE. For MPS-pyrosequencing adjustment, all 20 common samples were used to construct the equations, as the number of samples was not enough to partition the training set and test set. The models of each CpGs were trained with 10-time repeated 5-fold cross validation.

C. Five-CpG model

Partitioned 200 samples (training set) of MPS were used to train the model based on ELOVL2_CpG20, FHL2_CpG1, KLF14_CpG6, MIR29B2C_CpG6, and TRIM59_CpG5 (which were same targets of SBE). With R package MASS, stepwise regression was adopted to quadratic term. The model was selected based on its' accuracy and residual error, and it was tested with 50 samples of test set from MPS; 250 samples of adjusted SBE; 20 samples of adjusted pyrosequencing data.

D. Multiple CpGs model

Using the training set of MPS data with R pacakage MASS, stepwise linear regression was adopted to select the markers. By using the chosen markers, 5-time repeated 10-fold cross validation for linear regression was done for two models. The model involved quadratic terms based on its' accuracy and residual error, and it was tested with 50 samples of test set from MPS; 250 samples of adjusted SBE; 20 samples of adjusted pyrosequencing data.

III. RESULTS

1. BisQuE

A. Standard DNA, C-T indicator, and commercial BS-DNA

Data generated for the standard DNA showed a consistent assay sensitivity and reproducibility[35]. Among five individual assays, 10 ng to 16 pg of standard per well exhibited an average Ct of 21.247 to 29.899 in short-C, and 22.595 to 31.077 in long-Cfree, respectively. Consistency of the results and assay reproducibility were also exhibited in high R-squared values, as well as the PCR efficiency, slope, and y-intercept were constant. With this result, standard curves of short-C and long-Cfree were obtained for each assay, and then applied to quantify the amount of short amplicons containing cytosine (gDNA or unconverted DNA) and long amplicons, respectively. C-T indicator data also demonstrated similar results for the standard DNA in terms of the Ct values of each successive dilution, R-squared value, and PCR efficiency. The Ct transforming formula (highlighted in pink color in Figure 1) of short-T to short-C were generated with the relative ratio of Ct between short-C and short-T in four different amounts of diluted C-T indicators. The Ct value of the short-T of BS-DNA was substitute into the formula to convert Ct of short-T into that of short-C, so that transformed Ct can be applied to the standard curve of short-C. Meanwhile, each 1 ng of Epi-M and Epi-U sample was analyzed in common among five assays, and their Ct values and calculated amount were similar in comparison with the standard DNA. Also, both of the two commercial samples showed a high average conversion rate of more than 99%. Those samples came out to have a much smaller amount (about 0.2 ng) than expected.

Table 7. Six BS conversion kits and an overview of the results

No.	Kit	DNA input (ng)	Elution vol. (μl)	qPCR						Qubit
				Conversion Efficiency (%)	Conversion rank	Degradation Level	DL rank	Recovery (%)	Recovery rank	Recovery (%)
1	Z-EZ	50	10	99.90	1	1.495	4	50.58	1	62.57
2	D-PB		10	99.74	4	1.762	6	43.79	4	61.67
3	P-ME		10	99.78	3	1.577	5	44.42	3	49.12
4	T-EJ		10	99.61	5	1.479	3	48.39	2	47.12
5	Q-EF		10	99.89	2	1.279	2	39.65	5	58.66
6	N-NE		20*	94.24	6	0.857	1	18.24	6	27.90

*Due to the bead purification step, the converted DNA was eluted with 20 μl of TE buffer by following the manufacturers' guide.

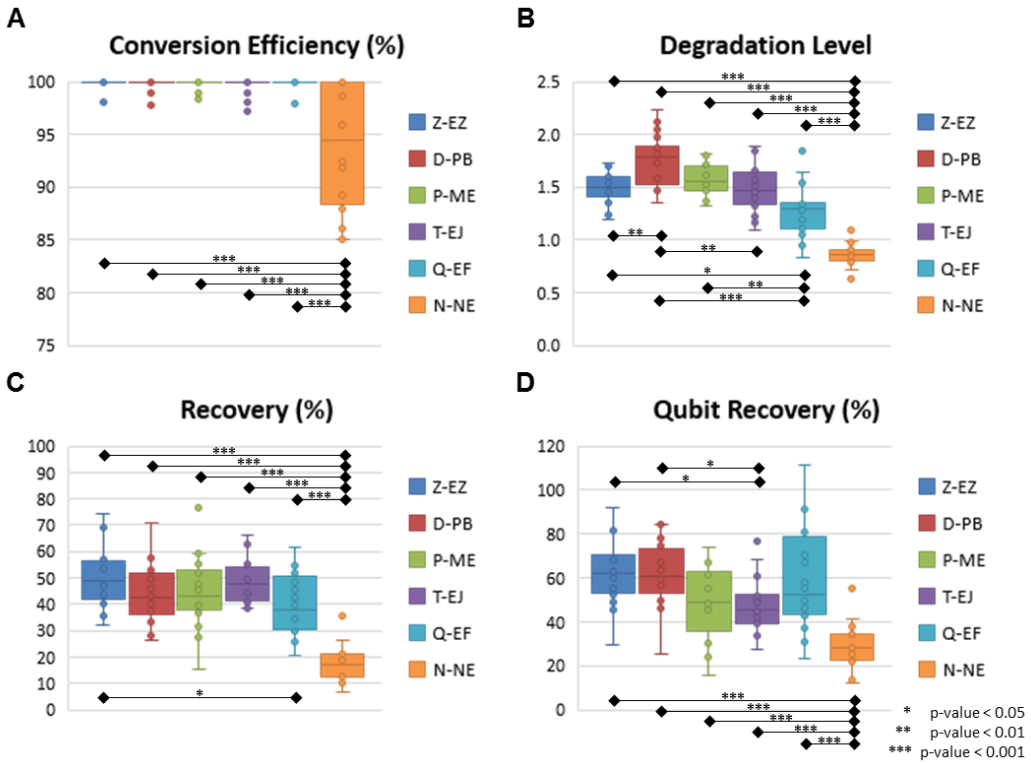

Figure 4. Box-scatter plot of the BS conversion kit. (A) Conversion efficiency of each kit. (B) Degradation level of each kit. (C) Recovery calculated based on the qPCR data of each kit. (D) Recovery measured with the Qubit ssDNA assay. In all three key features of bisulfite conversion, N-NE showed the lowest performance, and it was significantly different with other five kits.

B. Conversion efficiency

The conversion efficiency of each kit was calculated by the short-T amount divided by the sum of the short-C and the short-T amount. Since standard DNA, which is human DNA, only provided the standard curves of short-C and long-Cfree, the Ct values of the short-T were modified into those of the short-C with the application of the relation formula obtained from the C-T indicator. As shown in Figure 4A, most of the BS-DNA exhibited more than 99% of conversion efficiency. In this study, Z-EZ was the highest efficiency in BS conversion followed by the Q-EF, P-ME, D-PB, T-EJ, and N-NE. All samples converted with kits except the N-NE had a higher efficiency than 95%, but 7 out of 20 samples from the N-NE showed less than 90% of the rate. In statistics analysis, there was a significant difference between N-NE and the other kits (p-value < 0.001) and no significant differences were observed among the five kits.

C. Degradation level

Before computing the degradation level, it is the first step to calculate the ratio of short amplicons (both short-C and short-T) divided by the long amplicons (long-Cfree). Degradation levels were computed from BS-DNA out of gDNA of this ratio. This concept is inspired from the degradation index of quantifiler HP and Trio DNA Quantification kit. Degradation level will be 1, when the ratio is same in both gDNA and BS-DNA. However, if the amount of long fragment is smaller in the BS-DNA, the short/long ratio will be bigger leading to the degradation level will be >1. Therefore, the degradation level > 1 implies that the BS-DNA was degraded during the BS conversion step. Shown in Table 7 and Figure 4B, D-PB exhibited the highest degradation level and N-NE showed the lowest degradation level, less than 1.000, among the tested six kits. Obviously, N-NE was significantly different from the other five kits (Games-Howell's $p < 0.001$). Other kits demonstrated average degradation levels ranging between 1.279 and 1.577. There was no difference between Z-EZ, P-ME, and T-EJ. Meanwhile, Q-EF showed significant difference with four kits including N-NE, Z-EZ ($p < 0.05$), D-PB ($p < 0.001$), and P-ME ($p < 0.01$). D-PB showed differences with Z-EZ and T-EJ, respectively ($p < 0.01$).

D. Recovery from BisQuE and Qubit

In this study, the recovery of each kit was calculated by the ratio of the content of the short amplicon from BS-DNA (short-T and short-C, representing converted U and unconverted C, respectively) divided by gDNA (short-C), and subsequently multiplied by two[59] (Figure 1). Because both the sense and the antisense strand of the gDNA worked as template, whereas only the sense strand of the BS-DNA could be amplified. Additionally, BS-DNA from the N-NE was eluted in 20 μl of TE buffer, so the recovery of the N-NE had to be multiplied by two again.

As shown in Table 7 and Figure 4C, Z-EZ exhibited the highest recovery and N-NE showed the lowest recovery, 50.58% and 18.24%, respectively. The average recovery rates of the remaining kits, except for the Q-EF were highly similar ranging between 43.79% and 48.39%. In statistics analysis, there was a highly significant difference (Tukey's p-value < 0.001) between N-NE and the other kits, also Z-EZ and Q-EF showed significant difference ($p < 0.05$). However, the rest of each kit in this study was insignificantly different (Figure 4C).

Besides the usage of the developed qPCR system, the recovery was also measured with the Qubit ssDNA assay. As shown in Figure 4D, N-NE was significantly different with the other five kits (Games-Howell's p-value < 0.001), and T-EJ showed significant difference with Z-EZ and D-PB ($p < 0.05$). However, there is no difference in the other kits. There were one sample showed recovery rate larger than 100% in the Q-EF kit, which showed 54.55% in the BisQuE result. Also, shown in Table 7 and Figure 5, the low correlation between the qPCR result (Pearson's rho = 0.446) as well as the rank by the Qubit assay and that by the qPCR were somewhat different.

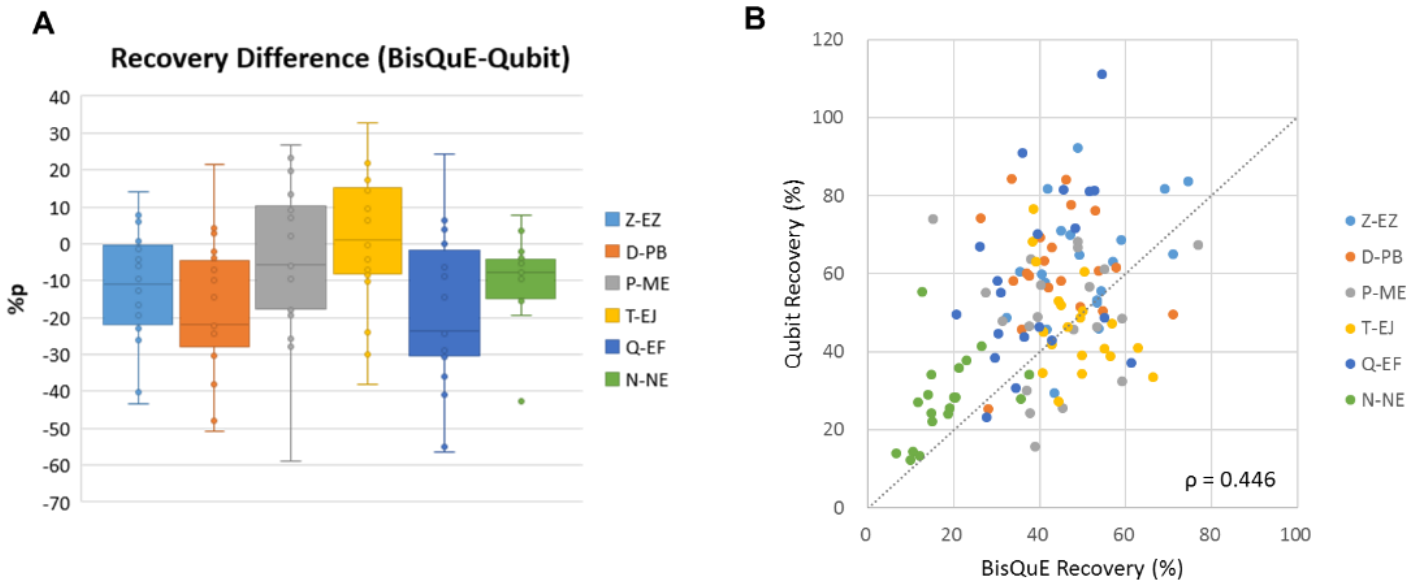

Figure 5. Difference between BisQuE and Qubit. (A) Recovery difference between BisQuE and Qubit (B) Scatter plot of recovery measured by BisQuE and Qubit with y=x line. There was a difference between the recovery by BisQuE and Qubit. Generally, the recovery by BisQuE was smaller than that by Qubit. (A) is a boxplot for the value that recovery of BisQuE subtracted by that of Qubit, and its' medians are < 0 except T-EJ, which showed large variance. As shown in (B), there was a low correlation between two methods (Pearson correlation coefficient = 0.446).

2. Inter-platform DNAm analysis

A. MPS

(A) MPS coverage

In this study, a total of 1250 bisulfite-converted amplicons from 250 blood samples were sequenced. Approximately 24 million of reads were obtained, and more than 92% of bases had a base quality > Q30. On average, samples showed read depth of 90,000, ranged 58,528-120,744. Average of total mapped reads per sample was 85,000, and the highest (sample 094) and lowest (sample 133) were around 115,000 and 55,500, respectively (Figure 6A). The average of each marker was plotted in Figure 6B. *ELOVL2* showed the lowest coverage about 10%, and the rest of four markers exhibited even coverage among them. As MPS data can show sequences of amplicons, it is possible to check bisulfite conversion efficiency of each sample. The average of conversion rate was 99.7%, in the range of 99.6% to 99.8%.

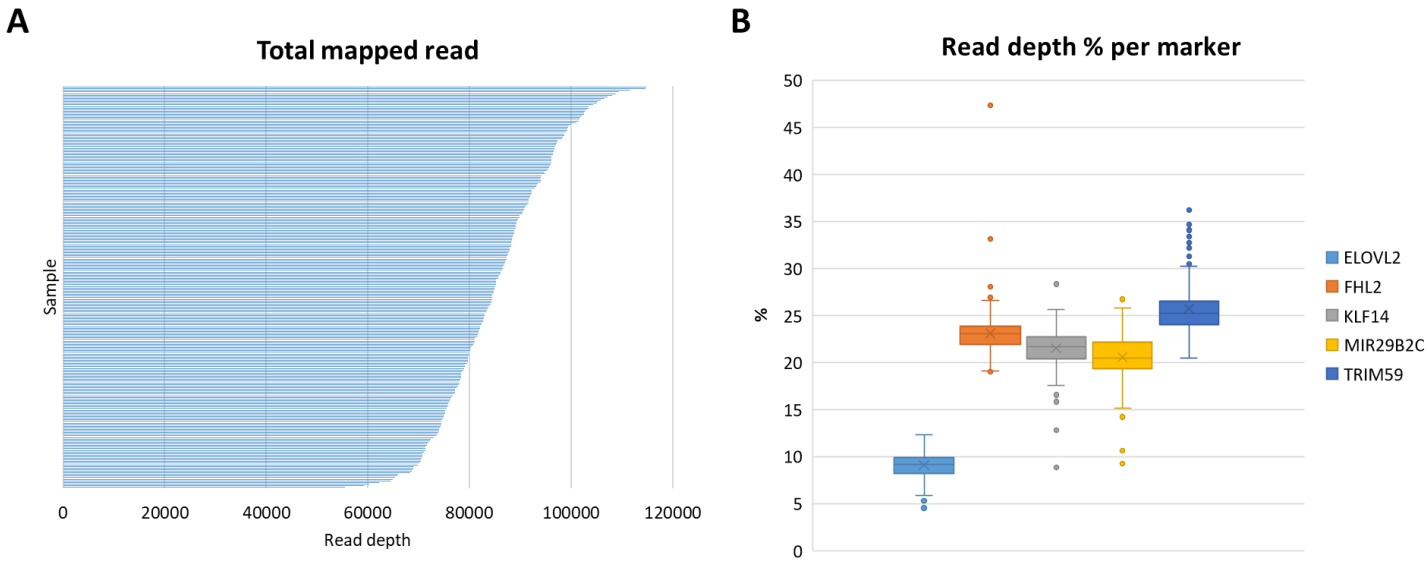

Figure 6. Basic result of MPS. (A) Mapped read depth of 250 samples. Average of mapped reads per sample was 85,000 and the highest numbers of mapped reads were 2.1 times of the lowest numbers of mapped reads. (B) Percentage of read depth per each marker of 250 samples. *ELOVL2* showed the lowest percentage of coverage among markers, but the highest (*TRIM59*) percentage was 2.5 times than ELOVL2.

(B) Age correlations of 69 CpG sites

The DNAm profiles of 69 CpG sites within the five amplicons were analyzed to determine the correlations between DNAm and chronological age (Table 8). Among 69 CpGs, CpG22 of *ELOVL2* (ELOVL2_P3 in pyrosequencing) showed the highest age-correlation, and at least three CpG sites of each genes were highly age-correlated (Spearman's rank correlation coefficient $r_s > 0.8$). As shown in Table 8, most neighbor CpG sites located within a same amplicon exhibited similar age-correlations, but some CpGs showed age associations different from those of adjacent CpGs within the same amplicon. furthermore, FHL2_CpG13 showed $p > 0.05$, so both highly age-correlated region and scarcely correlated region are co-existent even in the same amplicon.

In Figure 7, the commonly overlapped five CpGs (marked in Table 8) were plotted. As mentioned above, those markers showed high correlations with chronological age; however, there were outliers in them, and sample 172 was a common outlier in the result. Particularly, sample 172 showed the highest DNAm level in FHL2_CpG1 among all samples.

Table 8. Age correlation values of 69 CpG sites from MPS data

Gene	Location (GRCh38)	No.	ID	r_s	p-value	SBE*	Pyro**
ELOVL2	11044521	1		0.4120	< 0.001		
(chr6)	11044524	2		0.3322	< 0.001		
	11044531	3		0.3343	< 0.001		
	11044539	4		0.3870	< 0.001		
	11044545	5		0.3553	< 0.001		
	11044547	6		0.1783	0.005		
	11044549	7		0.2977	< 0.001		
	11044563	8		0.4694	< 0.001		
	11044567	9		0.6445	< 0.001		
	11044573	10		0.6411	< 0.001		
	11044579	11		0.6220	< 0.001		
	11044581	12		0.5289	< 0.001		
	11044585	13		0.8252	< 0.001		
	11044587	14		0.5493	< 0.001		
	11044590	15		0.6117	< 0.001		
	11044600	16		0.5676	< 0.001		
	11044604	17		0.6721	< 0.001		
	11044608	18		0.6336	< 0.001		
	11044611	19		0.7511	< 0.001		
	11044628	20		0.8795	< 0.001	V	P1
	11044631	21		0.8616	< 0.001		P2
	11044634	22		0.9156	< 0.001		P3
	11044640	23		0.8914	< 0.001		P4
	11044642	24		0.8897	< 0.001		P5
	11044644	25	cg16867657	0.9045	< 0.001		P6
	11044647	26		0.8833	< 0.001		P7
	11044655	27	cg24724428	0.8602	< 0.001		P8
	11044661	28	cg21572722	0.8396	< 0.001		P9

Table 8 (continued)

FHL2	105399282	1	cg06639320	0.8853	< 0.001	V	P1
(chr2)	105399288	2	cg17268658	0.8801	< 0.001		P2
	105399291	3		0.8635	< 0.001		P3
	105399297	4		0.8852	< 0.001		P4
	105399300	5		0.8759	< 0.001		P5
	105399310	6	cg22454769	0.8619	< 0.001		P6
	105399314	7	cg24079702	0.7835	< 0.001		P7
	105399316	8		0.7721	< 0.001		P8
	105399323	9		0.7641	< 0.001		P9
	105399327	10		0.6535	< 0.001		P10
	105399338	11		0.2309	< 0.001		P11
	105399340	12		0.4716	< 0.001		P12
	105399360	13		0.1237	0.051		
	105399363	14		0.2738	< 0.001		
KLF14	130734356	1		0.6681	< 0.001		
(chr7)	130734358	2		0.7618	< 0.001		P5
	130734373	3	cg09499629	0.7543	< 0.001		P4
	130734376	4	cg08097417	0.8334	< 0.001		P3
	130734399	5		0.8183	< 0.001		P2
	130734413	6	cg14361627	0.8303	< 0.001	V	P1
MIR29B2C	207823637	1		-0.8307	< 0.001		
(chr1)	207823657	2		-0.6804	< 0.001		P5
	207823660	3		-0.7520	< 0.001		P4
	207823672	4		-0.8507	< 0.001		P3
	207823675	5	cg10501210	-0.8268	< 0.001		P2
	207823681	6		-0.8926	< 0.001	V	P1
	207823702	7		-0.8775	< 0.001		
	207823705	8		-0.8520	< 0.001		
	207823715	9		-0.8977	< 0.001		
	207823723	10		-0.8717	< 0.001		

Table 8 (continued)

TRIM59	160450172	1		0.7894	< 0.001		P1
(chr3)	160450174	2		0.8108	< 0.001		P2
	160450179	3		0.8583	< 0.001		P3
	160450184	4		0.8576	< 0.001		P4
	160450189	5	cg07553761	0.8733	< 0.001	V	P5
	160450192	6		0.8890	< 0.001		P6
	160450199	7		0.8698	< 0.001		P7
	160450202	8		0.8566	< 0.001		P8
	160450231	9		0.6109	< 0.001		P9
	160450238	10		0.5834	< 0.001		
	160450243	11		0.5658	< 0.001		

* The overlapped loci with SBE.

** The overlapped loci with pyrosequencing.

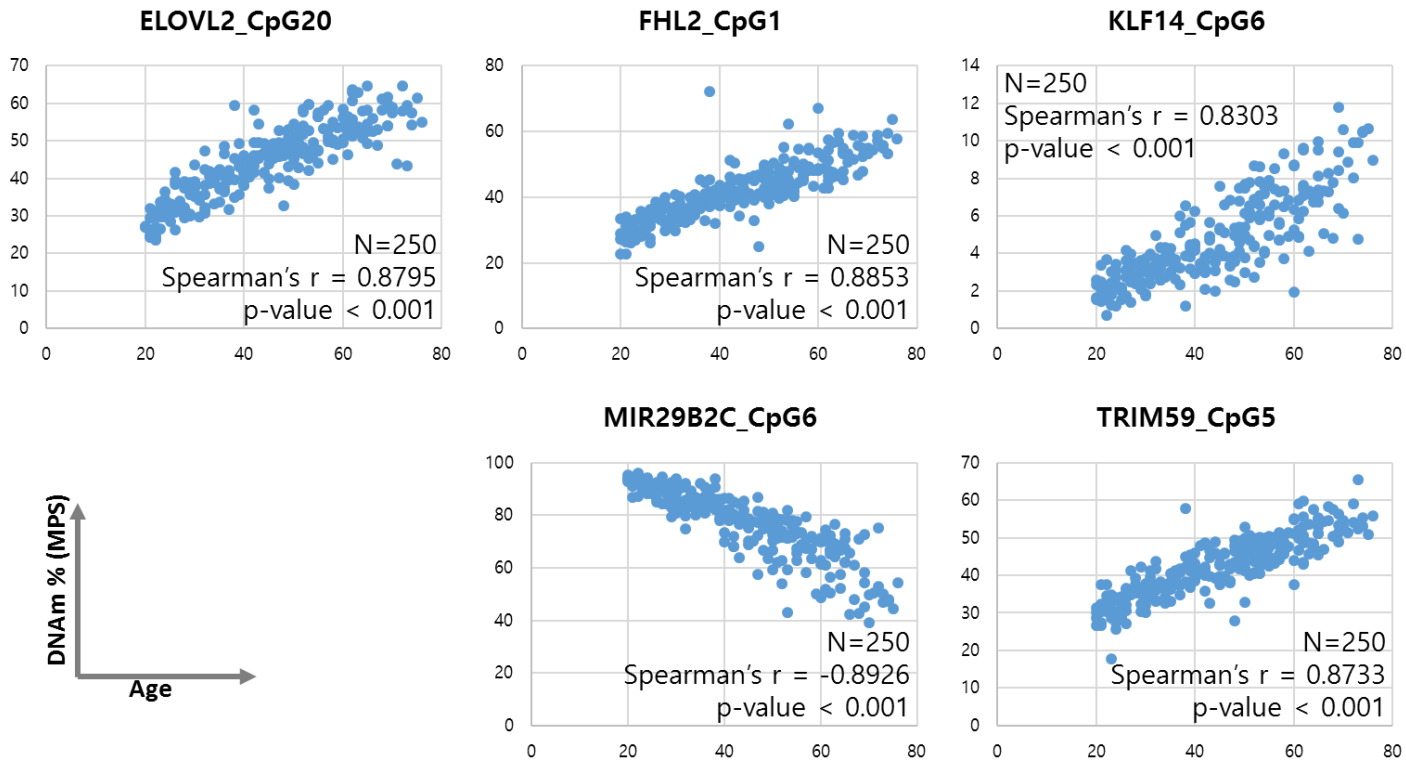

Figure 7. Age correlations of common five CpG markers using MPS. Each marker was overlapped in MPS, SBE, and pyrosequencing. KLF14_CpG6 showed the lowest age correlation and ELOVL2_CpG20 showed the highest.

B. SBE

Age associations of the five CpG markers were investigated in 250 samples using a developed methylation SNaPshot assay (Figure 8). The DNAm level of all markers showed a significant correlation with age $|r_s| > 0.8$ (Figure 9). Among them, *MIR29B2C* showed the highest age-correlation followed by *TRIM59* and *ELOVL2*. *FHL2* and *KLF14* also showed high age correlations despite the outliers. There were outliers in each five CpGs, and sample 172 was a commonly observed outlier in Figure 9 and Appendix 2. Particularly, there were three samples having 0% of DNAm in *KLF14* marker due to their heights of G peaks were under the threshold (50 rfu). Similarly, two samples of MIR29B2C presented 100% of DNAm due to their height of A peaks were under the threshold (50 rfu). Meanwhile, age correlations of markers from SBE data were lower than those of MPS, except KLF14; however, the difference of r_s was quite small (0.8303 for MPS and 0.8329 for SBE).

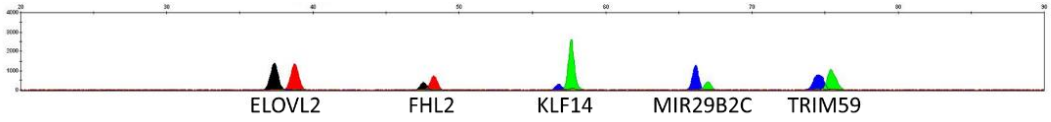

Figure 8. Electropherogram of SBE result. It was analyzed in 3130 Genetic Analyzer and the y-axis is ranged 0-4000 rfu.

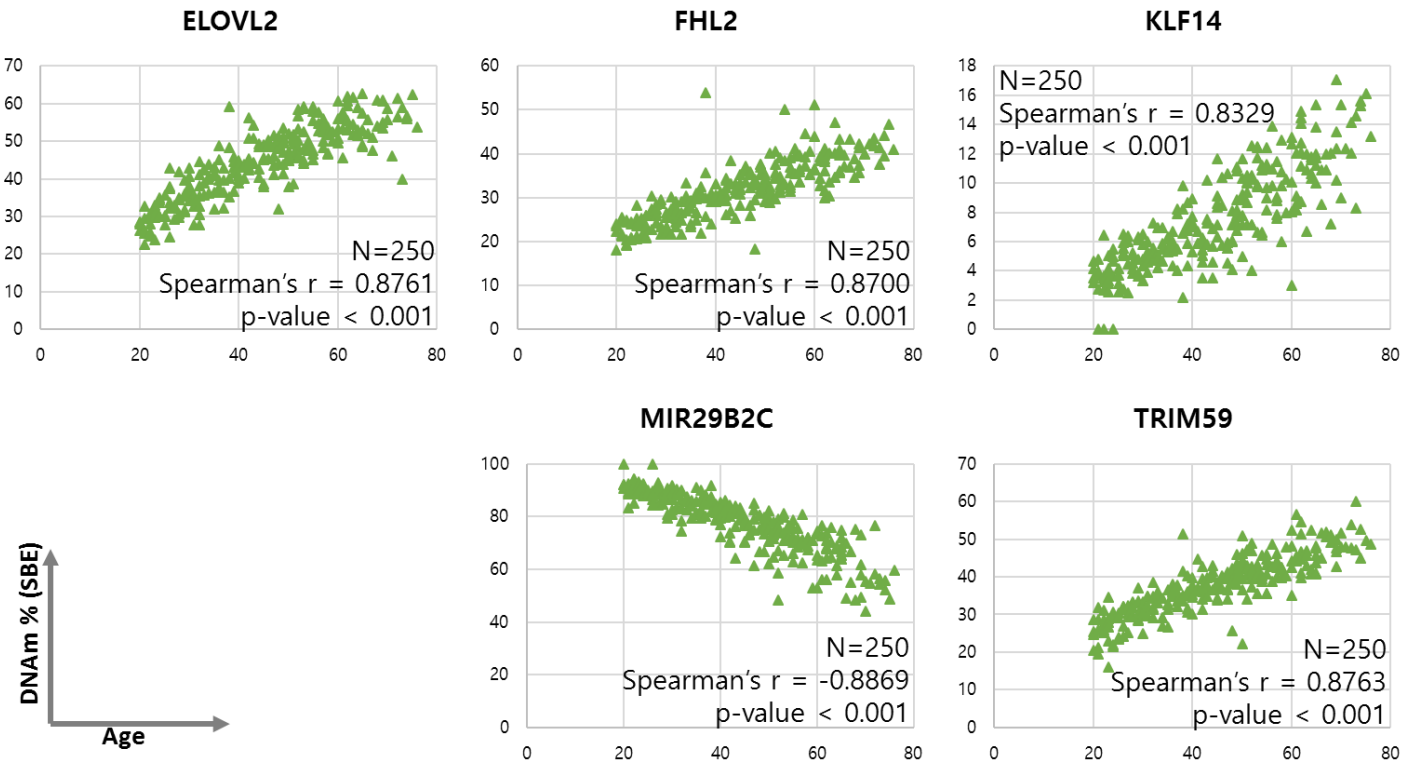

Figure 9. Age correlations of five CpG markers using SBE. TRIM59 showed the highest age correlation and KLF14 showed the lowest. Three samples in KLF14 and two samples in MIR29B2C showed 0% and 100% of DNAm due to low signal intensity.

C. Pyrosequencing

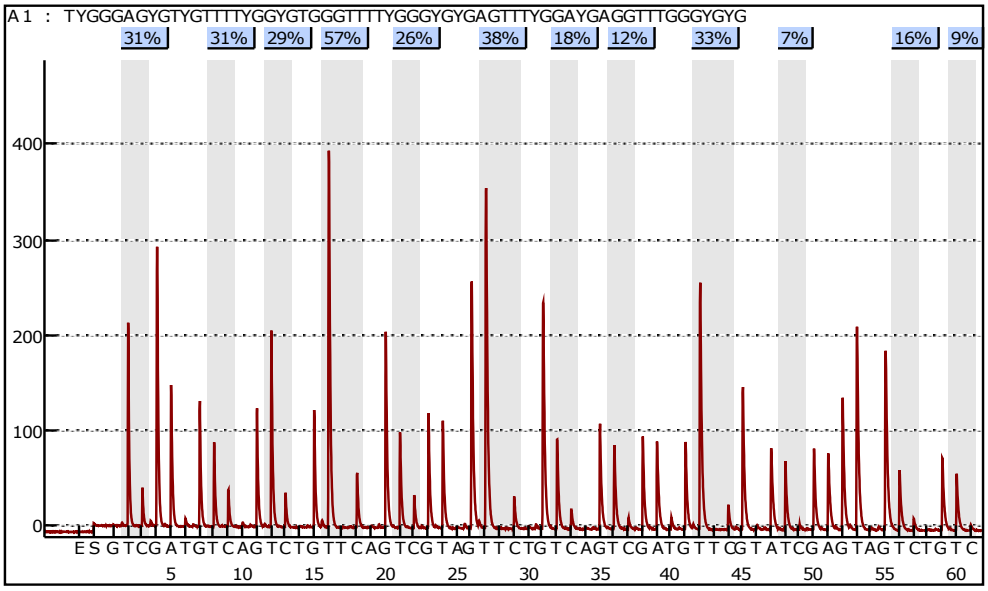

Figure 10. Pyrogram of FHL2. An example pyrogram of FHL2 from sample 013. DNAm percentage of each CpG sites were presented on top of the pyrogram. It was sequenced on PyroMark Q96ID system.

Age associations of the five CpG markers were investigated in 20 samples using a pyrosequencing. The DNAm level of all markers showed a significant correlation with age (Figure 10, Table 9). Among them, KLF14_P1 (cg14361627, KLF14_CpG6) showed the highest age-correlation followed by KLF14_P2 (KLF14_CpG5) and MIR29B2C_P1 (MIR29B2C_CpG6). One sample (sample 172) showed outlier values in ELOVL2_P1, FHL2_P1, KLF14_P1, TRIM59_P5. It showed similar values in MPS and SBE as well.

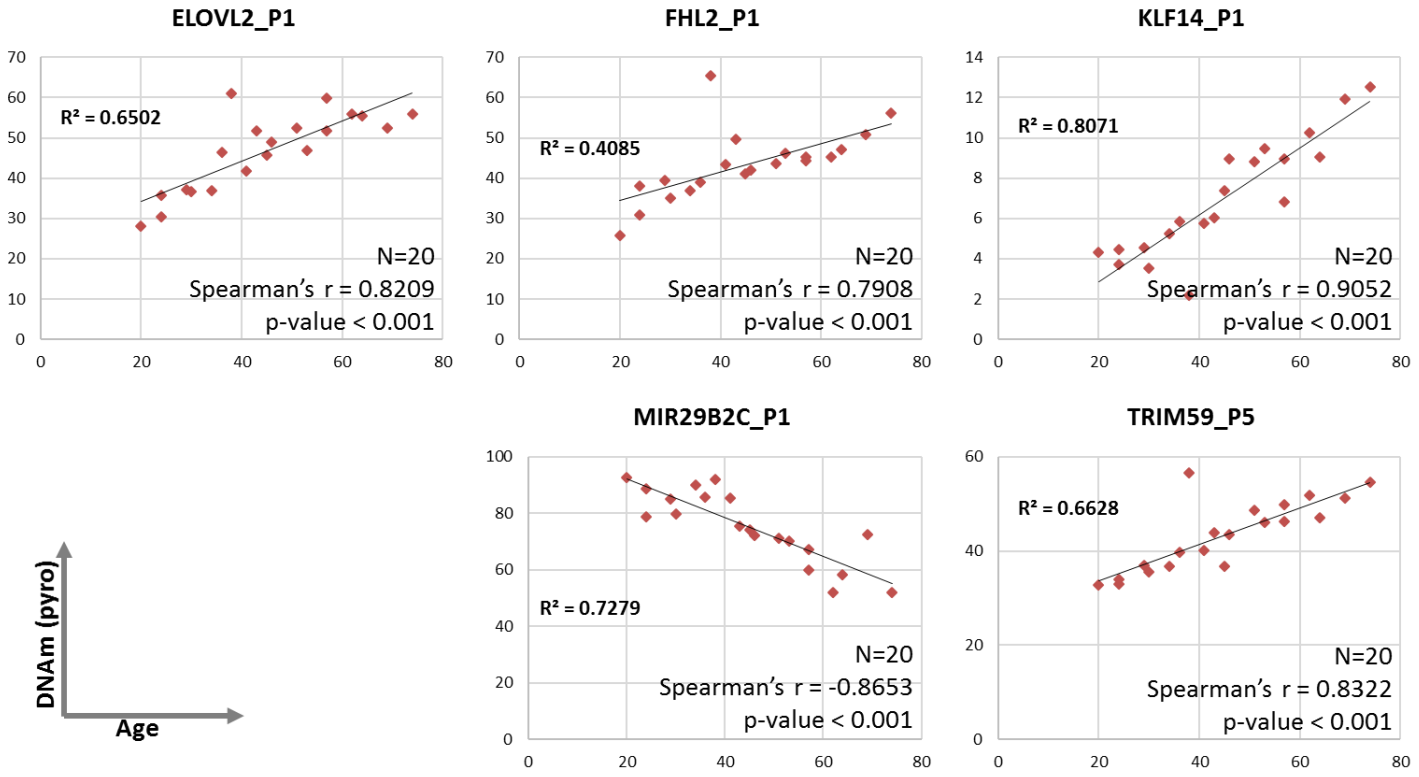

Figure 11. Age correlations of five common CpG markers using pyrosequencing. There are common outliers (sample 172) in ELOVL2_P1, FHL2_P1, KLF14_P1, and TRIN59_P5.

Table 9. Age correlation values of 40 CpG sites from pyrosequencing data

Gene	No.	ID	r_s	p-value	SBE*	MPS**
ELOVL2	P1		0.8209	< 0.001	V	CpG20
	P2		0.8322	< 0.001		CpG21
	P3		0.7991	< 0.001		CpG22
	P4		0.8600	< 0.001		CpG23
	P5		0.7434	< 0.001		CpG24
	P6	cg16867657	0.6742	0.001		CpG25
	P7		0.7637	< 0.001		CpG26
	P8	cg24724428	0.5322	0.016		CpG27
	P9	cg21572722	0.7798	< 0.001		CpG28
FHL2	P1	cg06639320	0.7908	< 0.001	V	CpG1
	P2	cg17268658	0.8194	< 0.001		CpG2
	P3		0.8209	< 0.001		CpG3
	P4		0.7381	< 0.001		CpG4
	P5		0.8375	< 0.001		CpG5
	P6	cg22454769	0.7856	< 0.001		CpG6
	P7	cg24079702	0.7457	< 0.001		CpG7
	P8		0.7547	< 0.001		CpG8
	P9		0.6305	0.003		CpG9
	P10		0.5600	0.010		CpG10
	P11		0.2972	0.202		CpG11
	P12		0.5576	0.011		CpG12
KLF14	P1	cg14361627	0.9052	< 0.001	V	CpG6
	P2		0.8721	< 0.001		CpG5
	P3	cg08097417	0.7901	< 0.001		CpG4
	P4	cg09499629	0.5245	0.018		CpG3
	P5		0.5988	0.005		CpG2

Table 9 (continue)

MIR29B2C	P1		-0.8653	< 0.001	V	CpG6
	P2	cg10501210	-0.8014	< 0.001		CpG5
	P3		-0.7788	< 0.001		CpG4
	P4		-0.7171	< 0.001		CpG3
	P5		-0.7013	< 0.001		CpG2
TRIM59	P1		0.7698	< 0.001		CpG1
	P2		0.6998	< 0.001		CpG2
	P3		0.8059	< 0.001		CpG3
	P4		0.8284	< 0.001		CpG4
	P5	cg07553761	0.8322	< 0.001	V	CpG5
	P6		0.8465	< 0.001		CpG6
	P7		0.7991	< 0.001		CpG7
	P8		0.7908	< 0.001		CpG8
	P9		0.5561	0.011		CpG9

*The overlapped loci with SBE.

**The overlapped loci with MPS.

D. Comparison between three platforms

(A) MPS vs SBE

Table 10. Intra-class coefficient and Passing-Bablok regression analysis of common five CpGs from MPS and SBE data

Gene	ICC(2,1)		Slope (95% CI)*		Intercept (95% CI)*	
	Value	p-value	Lower	Upper	Lower	Upper
ELOVL2	0.99	< 0.001	0.9644	1.0026	-0.3855	1.5541
FHL2	0.48	< 0.001	0.7303	0.7891	-1.7677	0.7821
KLF14	0.63	< 0.001	1.4156	1.4787	0.4893	0.7697
MIR29B2C	0.98	< 0.001	0.8375	0.8650	10.9629	13.2226
TRIM59	0.82	< 0.001	0.9485	1.0120	-5.2816	-2.4901

* Slope and intercept were calculated by Passing-Bablok regression analysis, and CI is abbreviation of confidential interval.

DNAm data of the overlapped five CpGs from MPS and SBE were shown in Figure 12. There were significant differences between FHL2 ($p < 0.001$), KLF14 ($p < 0.001$), MIR29B2C ($p = 0.0015$), and TRIM59 ($p < 0.001$) confirmed by paired-t test or Wilcoxon signed rank test. Intriguingly, ELOVL2 and MIR29B2C showed extremely high ICC values which indicate excellent reliability[68], 0.99 and 0.98, respectively (Table 10), showing the possibility of interchangeability between MPS and SBE data . In MIR29B2C, 95% confidential interval (CI) of slope was lesser than 1 and that of intercept was more than 0, so MIR29B2C cannot be fitted to y=x unlike ELOVL2. Therefore, only SBE data of ELOVL2 can be used directly to MPS-based age prediction model. TRIM59 showed 0.82 of ICC and it's 95% CI of slope was around 1, but that of intercept was lesser than 0. FHL2 and KLF14 showed low ICC, and their Passing-Bablok regression results also presented that MPS and SBE data cannot be interchangeable (Table 10 and Figure 12).

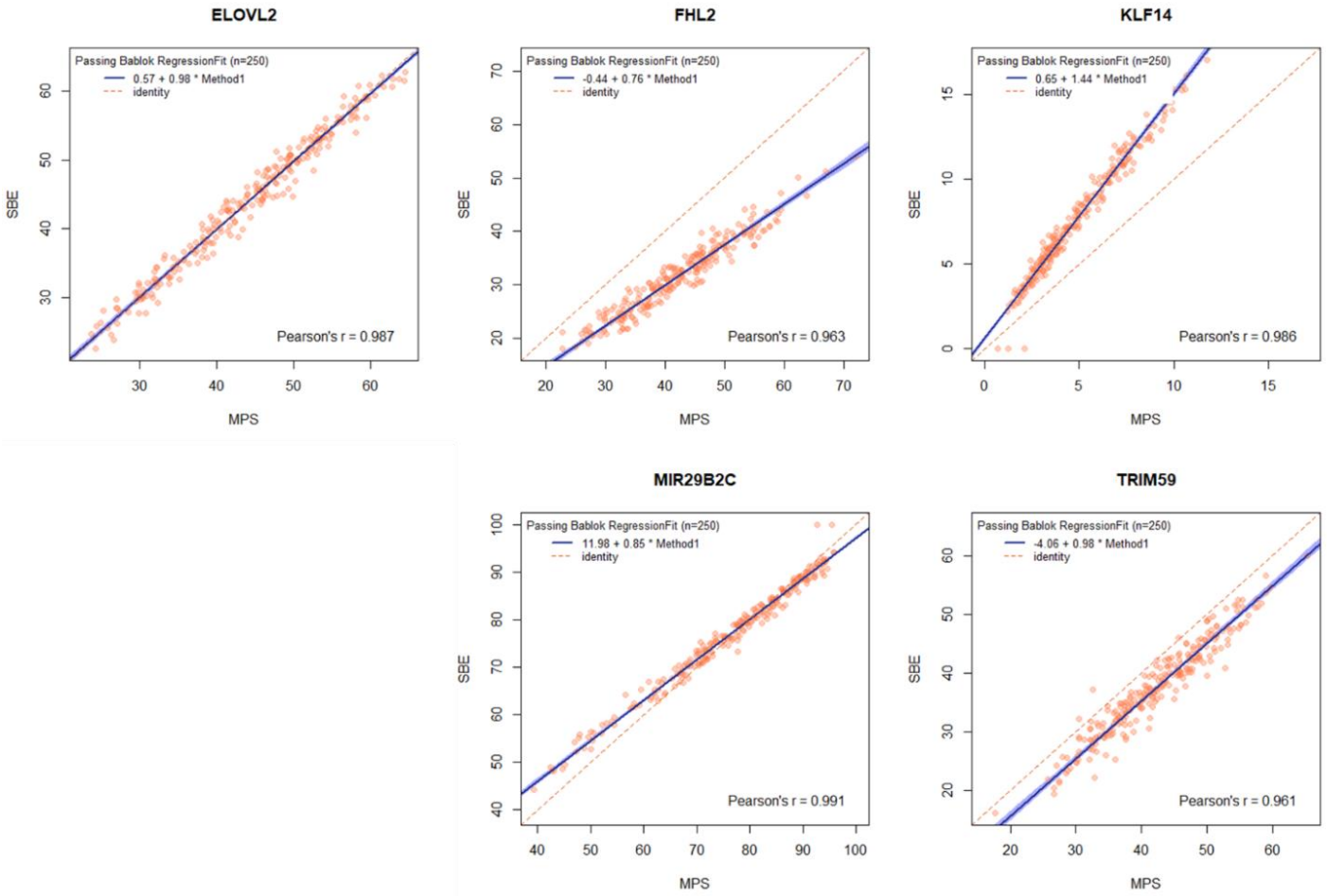

Figure 12. Five CpG markers of MPS and SBE from 250 samples.

(B) MPS vs SBE vs pyrosequencing

As shown in Figure 13, there were DNAm differences between each platform. SBE showed differences except MIR29B2C: pyrosequencing in ELOVL2, both MPS and pyrosequencing in FHL2, both MPS and pyrosequencing in KLF14, both MPS and pyrosequencing in TRIM59. MPS and pyrosequencing showed no significant difference except KLF14. DNAm data from three platforms were somewhat different, though those were from the same 1st PCR product.

Table 11. Intra-class coefficient analysis of three platforms

Marker	ICC(2,1)	
	Value	p-value
ELOVL2_P1	0.99	< 0.001
FHL2_P1	0.65	< 0.001
KLF14_P1	0.76	< 0.001
MIR29B2C_P1	0.96	< 0.001
TRIM59_P5	0.90	< 0.001

Table 11 presented ICC values of 5 common CpGs in all three platforms. Like ELOVL2 in Figure 13, ICC of ELOVL2 was 0.99 and Passing-Bablok regression result (Table 12) of ELOVL2 showed that pyrosequencing data of ELOVL2 can be interchangeable to MPS data; however other four markers cannot be interchangeable.

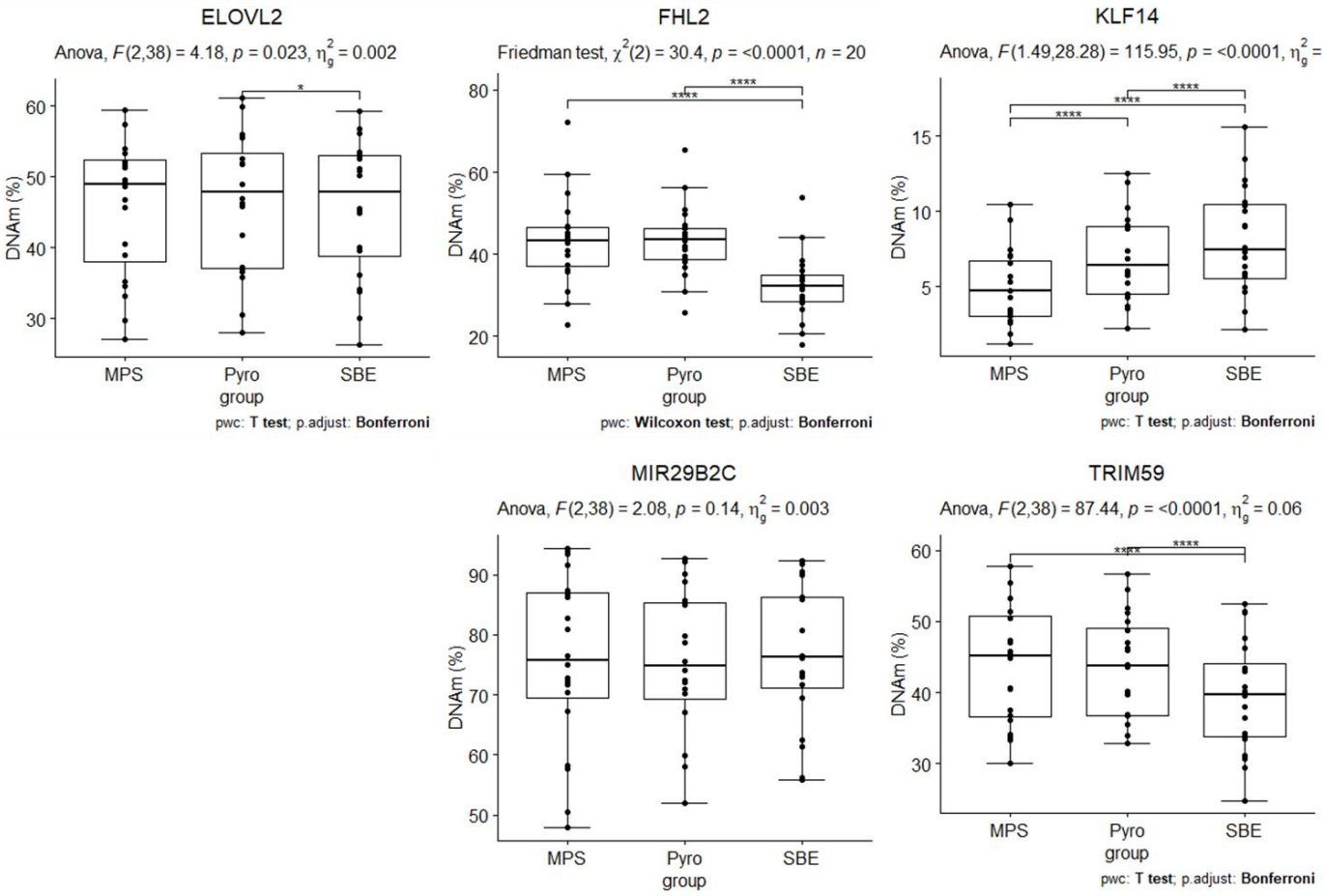

Figure 13. Boxplots of each marker of three DNAm analysis platforms. Pyro indicated pyrosequencing. The applied statistical methods were under the plot.

Table 12. Passing-Bablok regression analysis of MPS and pyrosequencing

Gene	MPS	Pyro	Slope (95% CI)		Intercept (95% CI)	
			Lower	Upper	Lower	Upper
ELOVL2	CpG20	P1	0.9101	1.1097	-4.6266	4.7705
	CpG21	P2	0.7494	0.9498	0.6324	7.4290
	CpG22	P3	0.8444	1.2891	-30.1984	5.9564
	CpG23	P4	0.8809	1.0755	-7.1303	6.5542
	CpG24	P5	0.7658	0.8961	1.4834	6.0747
	CpG25	P6	0.9261	1.0378	-6.4424	0.8785
	CpG26	P7	0.8675	1.0531	-12.0148	2.1399
	CpG27	P8	0.7365	0.9597	-2.9440	5.6175
	CpG28	P9	0.8196	1.3558	-7.3808	8.5387
FHL2	CpG1	P1	0.7404	0.8594	6.5632	11.7078
	CpG2	P2	0.7648	0.8738	5.1168	10.4006
	CpG3	P3	0.7552	0.8696	3.7682	9.6692
	CpG4	P4	0.5414	0.9596	6.8076	34.7603
	CpG5	P5	0.6824	0.8114	1.2722	6.8908
	CpG6	P6	0.6908	0.9773	7.5958	18.8202
	CpG7	P7	0.6772	0.8958	0.4714	6.5502
	CpG8	P8	0.7327	0.8833	3.5561	5.6868
	CpG9	P9	0.6648	0.9796	4.6453	15.2764
	CpG10	P10	0.8336	1.1793	1.4050	4.6684
	CpG11	P11	0.8015	1.1831	2.8992	8.3989
	CpG12	P12	0.8220	1.1848	0.3519	3.3218
KLF14	CpG2	P5	0.8860	1.6780	-0.9011	1.5486
	CpG3	P4	0.9360	1.7352	0.5384	2.0429
	CpG4	P3	0.7742	1.1493	1.2208	2.8697
	CpG5	P2	1.0397	1.3237	0.4024	1.6448

Table 12 (continue)

	CpG6	P1	1.0666	1.2757	0.5673	1.7401
MIR29B2C	CpG2	P5	0.6623	0.9506	-1.8345	8.8690
	CpG3	P4	0.6070	0.9496	-2.6641	10.7642
	CpG4	P3	0.5228	0.8427	-1.4401	15.9959
	CpG5	P2	0.6673	0.8824	0.3481	12.7695
	CpG6	P1	0.8687	0.9756	1.5097	9.3122
TRIM59	CpG1	P1	0.8937	0.9967	1.2851	3.6627
	CpG2	P2	0.8020	1.0163	0.2193	3.5033
	CpG3	P3	0.8554	0.9930	1.0372	4.0549
	CpG4	P4	0.8396	0.9284	3.2932	7.4670
	CpG5	P5	0.8100	0.9539	1.0494	7.6082
	CpG6	P6	0.8980	1.0182	0.1326	5.1030
	CpG7	P7	0.8371	1.0068	1.7074	7.8626
	CpG8	P8	0.8806	1.0739	0.4205	6.0376
	CpG9	P9	0.7639	1.0088	3.0728	7.5376

As shown in Figure 13, 40 overlapped CpG sites of MPS and pyrosequencing showed high consistencies. Despite those high correlations, few CpGs can be considered interchangeable referring to Passing-Bablok regression data (Table 12). Pyrosequencing data of ELOVL2_CpG20/P1 (common CpG with SBE) might be interchangeable to MPS data; however, most of CpGs showed slightly different to y=x line.

3. Age prediction model

A. Adjustment of SBE and pyrosequencing

Table 13. Adjustment models for SBE

Coefficient	ELOVL2	FHL2	KLF14	MIR29B2C	TRIM59
intercept	0	2.8338	0.9405	78.7512	6.0255
x	1	1.2435	0.1787	-3.0022	0.9666
x^2			0.0552	0.0612	
x^3			-0.0020	-0.0003	

Adjustment model for SBE was constructed and tested. The models contained quadratic or cubic terms to fit the data from MPS. All p-values of coefficients in Table 13 were < 0.001. Since ELOVL2 showed interchangeability between MPS and SBE, there was no adjustment model for ELOVL2. In the training set (Figure 14), five adjusted models showed high accuracies and each model, but TRIM59 showed relatively lower R-squared value than other models. In the test set (Figure 14), these models also showed high accuracies like the training set.

Figure 14. Training and test set of adjustment model for CpGs of SBE. X-axis denoted for DNAm of MPS and Y-axis denoted for adjusted DNAm value.

Table 14. Adjustment models for pyrosequencing

Gene	No.	intercept	p-value	x	p-value	x^2	p-value
ELOVL2	P1	0		1			
	P2	-3.6014	0.025	1.1426	< 0.001		
	P3	10.4272	0.082	0.9478	< 0.001		
	P4	0.3691	0.901	1.0125	< 0.001		
	P5	-3.3458	0.097	1.1771	< 0.001		
	P6	5.3107	0.430	0.9507	< 0.001		
	P7	5.8957	0.046	1.0323	< 0.001		
	P8	-53.9202	< 0.001	4.7042	< 0.001	-0.0560	<0.001
	P9	4.3799	0.132	0.8129	< 0.001		
FHL2	P1	-11.4794	< 0.001	1.2632	< 0.001		
	P2	-9.5798	< 0.001	1.2230	< 0.001		
	P3	-7.9639	< 0.001	1.2138	< 0.001		
	P4	-13.2900	0.077	1.1210	< 0.001		
	P5	-5.2693	0.001	1.3284	< 0.001		
	P6	-13.5865	< 0.001	1.1488	< 0.001		
	P7	4.0330	0.240	0.6089	0.022	0.0132	0.007
	P8	-7.6407	< 0.001	1.3495	< 0.001		
	P9	-8.3111	0.009	1.1113	< 0.001		
	P10	-2.3503	0.004	0.9484	< 0.001		
	P11	-5.5483	0.001	1.0108	< 0.001		
	P12	-2.2024	0.034	1.0412	< 0.001		
KLF14	P1	0.8762	0.006	0.8450	< 0.001		
	P2	-0.8503	< 0.001	0.8276	< 0.001		
	P3	0.3578	0.842	0.0887	0.894	0.0805	0.181
	P4	0.1955	0.884	0.1595	0.837	0.0650	0.546
	P5	0.6871	0.129	0.5505	< 0.001		

Table 14 (continue)

MIR29B2C	P1	-5.2354	0.341	1.0799	< 0.001		
	P2	-39.4782	0.105	2.6106	0.012	-0.0134	0.161
	P3	-2.9800	0.6830	1.3260	< 0.001		
	P4	-31.4220	0.109	2.7888	0.014	-0.0201	0.151
	P5	-2.3453	0.462	1.1888	< 0.001		
TRIM59	P1	-2.5759	< 0.001	1.060	< 0.001		
	P2	-1.290	0.059	1.052	< 0.001		
	P3	-2.4132	0.015	1.0642	< 0.001		
	P4	-5.3902	< 0.001	1.1173	< 0.001		
	P5	-4.6611	0.008	1.1216	< 0.001		
	P6	-2.5164	0.008	1.0340	< 0.001		
	P7	-4.2515	0.050	1.0585	< 0.001		
	P8	-3.4808	0.019	1.0270	< 0.001		
	P9	-6.0474	< 0.001	1.1294	< 0.001		

Adjustment models for pyrosequencing was constructed only due to small number of samples. The models contained linear or quadratic terms to fit the data from MPS. As the number of samples was small, the models were might not be highly accurate; also, it is inappropriate to generalize this model.

B. Five-CpG model

Table 15. The constructed five-CpG model

Markers	Coefficient	p-value
(intercept)	13.3067	0.094
ELOVL2	0.3996	< 0.001
KLF14	2.1018	0.002
MIR29B2C	0.3657	0.143
$(FHL2)^2$	0.0025	0.001
$(KLF14)^2$	-0.0950	0.073
$(MIR29B2C)^2$	-0.0053	0.003
$(TRIM59)^2$	0.0031	< 0.001

Table 15 showed the constructed 5-CpG model. As DNAm data from three platforms, MPS, SBE, and pyrosequencing, had the overlapped five CpGs in common, the constructed model can be applied into all DNAm data. This model was constructed with 200 sample of training set from MPS, so MPS data can be directly applied. SBE data and pyrosequencing data can be applied after adjustment. As shown in Table 15, this model contained quadratic terms of four markers.

Plotted in Figure 15, this model can explain more than 90% of age in training set of MPS and SBE data. The test set of MPS and pyrosequencing data showed more than 0.87 of R-squared values. Mean absolute errors (MAE) of both MPS sets were 2.90 yrs and 4.29 yrs and root mean square errors (RMSE) were 3.85 yrs and 5.36 yrs, respectively. Additionally, adjusted SBE data showed high accuracy (R-Squared value > 0.91) and presented 3.99 yrs of MAE and 4.90 yrs of RMSE as shown in Figure 15. The adjusted pyrosequencing data showed the highest MAE (4.97 yrs) and RMSE (5.97 yrs) among data.

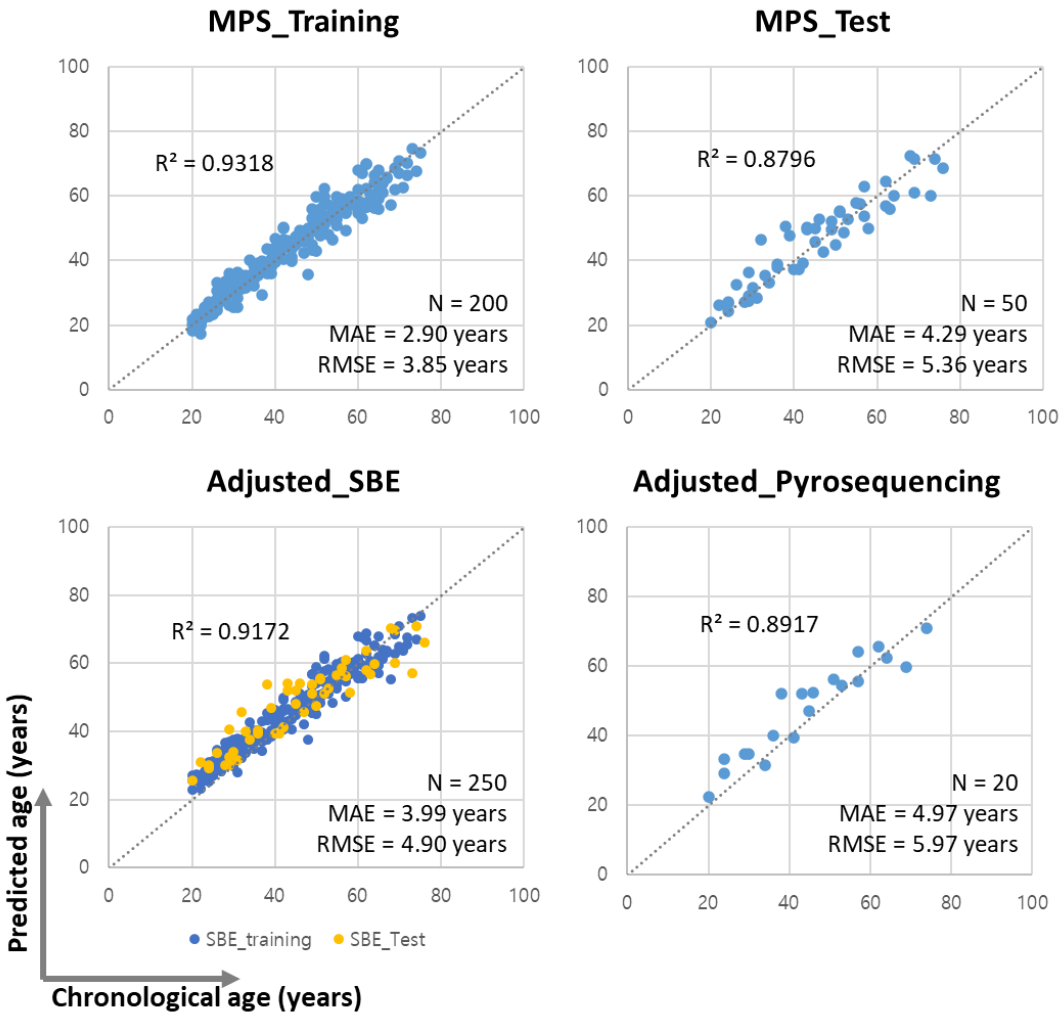

Figure 15. Five-CpG model result. As the model was constructed with the training set of MPS, it can be applied into the test set of MPS directly unlike SBE and pyrosequencing data, which needed to be adjusted before application.

C. Multiple CpGs model

Table 16. The constructed multiple CpGs model

Markers	Coefficient	p-value	Markers	Coefficient	p-value
(intercept)	68.8319	< 0.001	$(ELOVL2\_CpG22)^2$	0.0106	0.001
ELOVL2_CpG20	0.0888	0.1996	$(FHL2\_CpG1)^2$	0.0034	0.015
ELOVL2_CpG22	-1.5047	0.002	$(FHL2\_CpG2)^2$	0.0273	< 0.001
ELOVL2_CpG24	0.2245	0.004	$(FHL2\_CpG5)^2$	-0.0214	0.005
ELOVL2_CpG25	0.1532	0.053	$(FHL2\_CpG7)^2$	0.0428	0.003
FHL2_CpG2	-2.4518	< 0.001	$(FHL2\_CpG9)^2$	-0.0351	< 0.001
FHL2_CpG5	1.8159	0.006	$(FHL2\_CpG10)^2$	0.0308	< 0.001
FHL2_CpG7	-2.3358	0.004	$(KLF14\_CpG2)^2$	-0.5583	< 0.001
FHL2_CpG9	2.1946	0.003	$(KLF14\_CpG4)^2$	0.0861	0.013
KLF14_CpG2	2.9904	0.007	$(KLF14\_CpG6)^2$	-0.1626	0.002
KLF14_CpG3	1.1452	0.020	$(MIR29B2C\_CpG2)^2$	-0.0006	0.513
KLF14_CpG6	2.0308	< 0.001	$(MIR29B2C\_CpG4)^2$	-0.0029	< 0.001
TRIM59_CpG4	0.2341	0.039	$(MIR29B2C\_CpG5)^2$	-0.0007	0.454
TRIM59_CpG5	-0.3118	0.003	$(TRIM59\_CpG2)^2$	0.0151	0.002
TRIM59_CpG8	0.1963	0.123	$(TRIM59\_CpG9)^2$	-0.0239	0.008
TRIM59_CpG9	0.8307	0.038			

Table 16 showed the constructed multiple CpGs model. As DNAm data from MPS and pyrosequencing had the overlapped 40 CpGs in common, the marker selection was done for modelling. To increase the accuracy of age-predictive model, the model was developed to contain quadratic term of CpG sites. This model was constructed with 200 sample of training set from MPS, so MPS data can be directly applied and pyrosequencing data can be applied after adjustment.

Shown in Figure 16, this model can explain more than 90% of age in both training and test sets of MPS data; also, 81.48% of age variation in pyrosequencing. Also, both training and test sets of MPS data showed lower MAEs and RMSEs than pyrosequencing data. MAEs of both MPS data sets were less than 3 yrs, and RMSEs were 2.87 yrs and 3.64 yrs, respectively. Meanwhile, pyrosequencing data showed 5.43 yrs of MAE and 7.45 yrs of RMSE in this study. The model showed higher accuracies in MPS data but it was rather lower in pyrosequencing data.

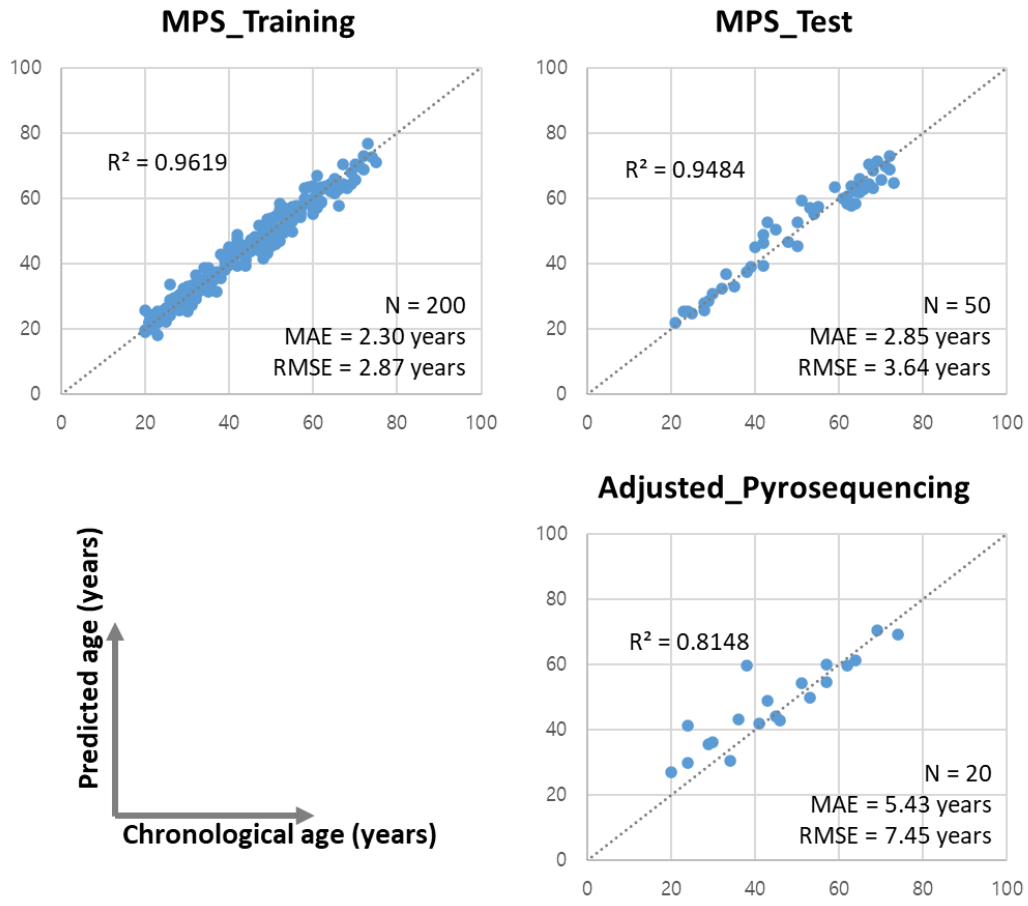

Figure 16. Multiple CpGs model result. As the model was constructed with the training set of MPS, it can be applied into the test set of MPS directly unlike SBE and pyrosequencing data, which needed to be adjusted before application. This model contained quadratic terms.

IV. DISCUSSION

In this study, we came up with BS-DNA quantitation, forensic age prediction models based on MPS data, and adjustment method for inter-platform DNAm analysis to show how can we deal with concerns under forensic context: poor quality and low quantity of DNA; continuity of age and DNAm level; and loss of accuracy while applying inter-platform data to different platforms. Aforementioned, the BisQue was developed and it could measure the quantity and status of BS-DNA to be able to guarantee downstream analysis. Then based on the result of previous studies[26, 29, 56], 1.5 ng of BS-DNA was set as the minimum input for age prediction and all BS-DNA samples were prepared by using the BisQuE to construct age prediction model with MPS data. Lastly, the adjustment models for SBE and pyrosequencing were suggested by adopting the same amplicon strategy.

First, forensic DNA samples are usually low quantity and it is well-known that the BS conversion step affects the quantity and quality. Moreover, BS conversion is a key step for entire DNAm analysis as its' quality affects the downstream result and BS conversion is still prerequisite to common DNAm analysis platforms[70]. Therefore, it is important to quantify the BS conversion efficiency, recovery, and the degradation level for successful downstream studies. BisQuE consisted of three sets of Cfree primers, and four different probes (including IPC) was performed in this research (Figure 1). As the Cfree primers amplified both the BS-converted and the unconverted DNA, the analysis of the gDNA and BS-DNA in a single assay was possible. Cfree primer systems were already exploited[59, 63, 64] but those were not able to obtain information regarding the BS conversion efficiency, degradation level, and recovery at the same time.

Additionally, this assay aimed to amplify the multicopy region to achieve high sensitivity and reliability. Remarkably, standard DNA, which was from human genomic DNA, and gDNA had no Ct value in the short-T, as well as the short-C and short-T showed relatively constant patterns for the C-T indicator. On the other hand, the Ct value of IPC can indicate the presence of a PCR inhibitor, although there was no significant outlier Ct value of IPC

in this research. IPC Ct values were found to be highly constant among samples, implying that there was an ineffective amount of PCR inhibitor in the 1 μl of the eluted DNA or buffering capacity of the used PCR master mix enabled to overcome it.

The C-T indicator is essential in this method. Since the standard curve of the Short-T was not available, only indirect quantification with the standard curve of the short-C was possible by applying short-T Ct values to the transforming formula. If the R-squared value of the transforming formula was less than 0.99, the performed qPCR assay was unreliable. Therefore, the formula of the C-T indicator should be regarded to be as important as the standard curves of the method. It is highly recommended to check the R-squared value of it and the PCR efficiency of C-T indicators. However, C-T indicator contains a degenerate base Y, and it supposed to consist of 50% of C and 50% of T for simple calculation in this study. As the Y in the middle of the sequence was synthesized, it is likely to have bias during the oligo synthesis process. But the purpose of the indicator was to induce the transforming formula for short-T to short-C to calculate the amount of converted DNA indirectly, not to separate them to have the same Ct values. Therefore, this assumption of 50%-50% would be acceptable.

All of the six kits used in this study showed high conversion efficiency, and this result was concordant with previous studies. D-PB and P-ME were found to exhibit the highest conversion efficiency, more than 99%, by MPS[62]. Similarly, high conversion rates of Q-EF were reported based on MPS results[64, 65] and Sanger sequencing data[59]. D-PB exhibited more than 99% of efficiency in MPS[34] and ddPCR[63], which also exhibited the T-EJ as well as had a high conversion rate.

However, the efficiency of the Z-EZ was somewhat different in the studies. Tierling et al.[65] suggested that Z-EZ unconverted 23% of cytosines in their study, but Holmes et al.[59] and Kint et al.[64] reported high a conversion efficiency of more than 99%. Izzi et al.[61] showed that there was no significant difference between the Z-EZ and the EZ DNA Methylation Gold kit from the same manufacturer, which was reported to have the highest conversion rate[59, 64, 65]. In our study, Z-EZ was observed to have the highest efficiency in BS conversion.

Since N-NE was quite recently introduced, it is less studied. To be precise, N-NE does not chemically alter C into U by using bisulfite in contrast with the other five kits, but it rather utilizes APOBEC for the enzymatic deamination of cytidine as well as bead purifications. Therefore, its performance might differ depending on the experience of the researchers or the given laboratory conditions.

It is widely known that incomplete BS conversion leads to exaggeration in the DNA methylation analysis, so choosing a BS conversion kit that guarantees high and stable conversion efficiency is one of the key steps in the preparation of a DNA methylation study. Five kits investigated in this study demonstrated extremely high conversion efficiency (average efficiency > 99.5%), whereas the other showed a high conversion rate (average > 94%). However, the application of the developed qPCR could be still useful before downstream experiments when it is necessary to confirm the success or failure of the BS conversion step due to mistakes of the researchers or mistreated reagents.

In this study, the short/long ratio only provide the glimpse of the severe degradation; because the content of the short amplicon would be much higher than that of the long amplicon if there was severe degradation in association with the converted DNA. But to be precise, the copy number ratio of short and long amplicons can vary from individual to individual, the accurate determination of the quantity of degraded BS-DNA might be vague. Therefore, degradation level of BisQuE needed the simultaneous analysis of both the gDNA and the BS-DNA, so that it can normalize the individual copy number variation and enable the acquisition of a precise degradation level. Therefore, the degradation level > 1 implies that the BS-DNA was degraded during the BS conversion step.

As shown in Table 7 and Figure 4B, the degradation level of the N-NE was lower than 1, meaning that the proportion of the long amplicons increased during the process. As the BS-DNA from the N-NE was purified by beads, therefore these findings might result from the bead purification step as the concentration of the beads contributed to the selective elimination of a specific size of DNA. The lower concentration of the beads led to a larger size of purified DNA. 1.0× bead purification during the conversion could remove some of

the small-sized DNA. The method using larger volume of the bead, such as 2.0× or 3.0×, or standard column purification method might enable to recover the short-fragments of enzyme-treated DNA more than the manufacturer's guide. However, this study was the first study to measure the conversion efficiency, degradation level, and recovery of N-NE, so it was hard to modify the guide. The suggested methods of the cleanup step would be recommended after testing the three features of the kit.

Other kits demonstrated average degradation levels ranging between 1.279 and 1.577 to be subtly different. Kint et al.[64] reported a similar result in the fragmentation of three kits: Q-EF, Z-EZ, and D-PB in less degraded order. They compared the degradation of each kit with gel electrophoresis, qPCR, and dPCR. In particular, during the comparison of the absolute quantification dPCR results of pre- and post-BS conversion samples, they found that BS-treated DNA had lost about 97% of the fragments longer than 227bp, which observation was quite similar to that of this study. Additionally, gel electrophoresis data[24] and Bioanalyzer data[31] presented that the Q-EF was less fragmented than the Z-EZ on a longer scale (>500bp). On the other hand, Worm Ø rntoft et al.[63] reported that T-EJ and D-PB were the least fragmented kit, but T-EJ was slightly less degraded than D-PB, which was in concordance with the findings of this research. However, Q-EF showed larger variance even in case of its lower degradation level, therefore those instabilities should be considered by the researchers.

On the other hand, larger target sizes, such as 500bp, are not guaranteed by this system as the size of the long amplicon is 238bp. The BS conversion step is well-known for degradation and as one of the impeding step of amplifying the large size of genes. Therefore, if the interested region is quite large, for example it is more than 500bp, the degradation level can be confirmed with other methods, such as gel electrophoresis (2 ug of gDNA and BS-DNA[59]) or Bioanalyzer (500 ng of gDNA for starting material[65]). In this study, only 50 ng of gDNA was used as starting material in the BS step and eluted with 10 µl (20 µl for N-NE) of TE buffer. Therefore, methods using gel electrophoresis and bioanalyzer was not suitable to direct confirmation. But our preliminary test result using Agilent DNA 1000 kit

with Bioanalyzer showed that the large amplicon (FLJ39739) was obviously less amplified than the short amplicon (CCDC29) in BS-DNA. So, it is highly recommended for studying larger sized targets to check the degradation level with other methods and start with enough DNA. Furthermore, the amplification of small-sized amplicons that are less than 300bp is common in forensic genetics. This small amplicon strategy can be suited to the BisQuE.

In this study, the recovery of each kit was calculated by the ratio of the short amplicon content of the gDNA and the BS-DNA. Concerning DNAm studies, such as forensic fields studies that inevitably require to deal with a limited amount of input DNA, an insufficient amount of BS-DNA can lead to a pitfall called the stochastic effect, therefore a certain amount of BS-DNA depending on the purpose of the study must be present to obtain reliable DNA methylation data[71]. Therefore, the recovery of the BS conversion kit should be thoroughly investigated to determine the minimum input of gDNA for conversion.

As shown in Table 7 and Figure 4C, N-NE showed the lowest recovery, 18.24%. Since the N-NE requires bead purification two times during the conversion process, a severe DNA loss can occur, the extent of which depends on the skillfulness of the researchers. For the remaining kits, except for the Q-EF, average recoveries were highly similar, ranging between 43.79% and 48.39%. Like these results, Holmes et al.[59] reported a higher recovery of Z-EZ than Q-EF by using qPCR, as well as Worm Ø rntoft et al.[63] investigated the recovery by qPCR and found a slightly higher recovery rate for the T-EJ compared to that of the D-PB. Although the order of recovery was somewhat different, the average recovery of each kit in this study was relatively similar to each other, except for the N-NE (Figure 4C). Besides, the qPCR amplicon sizes varied for each study, therefore it is recommended to apply the method which targets the appropriate size.

The Qubit assay was used to obtain the recovery of BS-treated DNA[62, 64]. Leontiou et al.[62] reported that the D-PB had the highest recovery, followed by the P-ME, and both were observed to be about 55%. Furthermore, Kint et al.[64] showed the recovery rank by Qubit measurement to be the highest for D-PB, followed by Z-EZ, and Q-EF. In this study, Z-EZ was the highest, followed by D-PB and Q-EF in order, showing > 55% of recovery

measured by Qubit. There was a low correlation between the results of the qPCR and the Qubit assay (Table 7, Figure 4D, and Figure 5). Moreover, one sample converted with Q-EF showed more than 100% of Qubit recovery though it showed 54.55% of recovery rate in BisQuE. This might be due to that the constructed qPCR system quantifies functional (amplifiable) DNA, whereas the Qubit assay measures fluorescent dye signal intercalating ssDNA specifically. If the amount provided by the Qubit assay is low, it could imply that the amount of BS-DNA quantified by the BisQuE is low. However, it cannot guarantee that the amount of amplifiable the converted DNA even though the results of the Qubit seem to be promising. Consequently, the acquisition of the right amount of amplifiable DNA for obtaining reliable data when the amount of input DNA is low should be considered.

By the way, we tried to use 50 ng as a starting material of BS-conversion, and 1.5 ng of DNA (detected with BisQuE's long-cfree amplicon unlike short amplicon) was amplified in the common target specific PCR step of three DNAm analysis platforms. Since Naue et al.[56] demonstrated *in silico* that accuracy of detected DNAm level depends on the amount of input DNA, and they also emphasized the input DNA amount for age prediction should be considered as the detected DNAm level which cannot reflect the real DNAm value can lead to inaccurate predictions. Previous studies exploited more than 100 ng of gDNA for BS-conversion and used some of eluted BS-DNA, however it is quite challenging amount of forensic case work. As age predictive markers are continuous value as well as DNAm level, the balance between high detection accuracy and amount of available DNA should be considered.

In Table 17, the amount of BS-DNA used in Zbiec-Piekarska et al.[50] and Jung et al.[33] cannot be calculated the result based on the long-sized BisQuE due to lack of information about the used kits. In the study of Zbiec-Piekarska et al.[50], they described that 20 ng of BS-DNA was used as a template for PCR; however, it was hard to know how much volume of BS-DNA eluent was used or how BS-DNA was measured. Jung et al.[33] used 1 µl of BS-DNA eluent (20 µl) from 200 ng of gDNA. The kit they used was not been tested with the BisQuE, but Worm Ø rntoft[63] showed that the long sized recovery rate of Imprint DMA

Modification kit (Sigma-Aldrich) was similar to D-PB, the amount of BS-DNA might be around 1.2 ng. Meanwhile, the works of Naue et al.[27] used EZ DNA Methylation-Gold Kit (Zymo research; Z-MG), but there was no significant difference between the Z-EZ and the Z-MG from the same manufacturer referring to Izzi et al.[61]. Therefore, the BisQuE-based BS-DNA was calculated with the result of Z-EZ.

Table 17. Amount of BS-DNA based on the long-sized BisQuE result

Study	Conversion kit	Input gDNA (ng)	Elution vol. (µl)	BS-DNA vol. for PCR	BS-DNA* (ng)
Zbiec-Piekarska[50]	Q-E96[a]	2000		20 ng[d]	-
Cho[25]	Z-EZ	500	50	2 µl	6.766
Naue[27]	Z-MG[b]	300		10 ng (Qubit)	5.407
Aliferi[29]	P-ME	50	10	2 µl	1.243
Hong[26]	Q-EF	500	50	1 µl	1.550
Hong[32]	Q-EF	200	20	1 µl	1.550
Jung[33]	S-ID[c]	200	20	1 µl	(1.2)[e]
VISAGE[34, 44]	D-PB	200	10	2 µl	4.970

*The quantity of BS-DNA was measured using the long-sized amplicon of the BisQuE.

[a]Q-E96 is EpiTect 96 Bisulfite kit (Qiagen).

[b]Z-MG is EZ DNA Methylation-Gold Kit (Zymo research).

[c]S-ID is Imprint DMA Modification kit (Sigma-Aldrich, St. Louis, MO, USA).

[d]There was no description about the measurement.

[e]Based on the result of Worm Ø rntoft[63], the long sized recovery rate of S-ID was calculated to be around 1.2 ng.

As in Table 17, previous works have used somewhat enough amount of BS-DNA. Cho et al.[25], Naue et al.[27], and VISAGE project[34, 44] used around 5 ng or more of BS-DNA, but 200-500 ng of gDNA was exploited for BS-conversion step. Aliferi et al.[29], Hong et al.[32], and Jung et al.[33] amplified similar amount of BS-DNA with this study. They successfully constructed age-predictive models with high accuracy and assessed their models as well, so it can be the trustworthy BS-DNA quantity for age prediction in forensic context.

On the other hand, the amount of DNA which was less than 1 ng presented the larger difference with high BS-DNA input in this study. (Appendix 5) As shown, there were small differences between 5 ng and 1.5 ng of BS-DNA which were measured with the long-sized amplicon of the BisQuE. The DNAm level detected from 1 ng of BS-DNA also showed low discrepancy with 5 ng, but the input which was less than 1 ng showed large differences.

Not surprisingly, it is concordance with previous reports of Hong et al.[26], Naue et al.[56], Aliferi et al.[29], and Heidegger et al.[34]. Approximately, 0.48 ng of BS-DNA based on the long-sized BisQuE (4 ng, which the researchers supposed that there had been no loss while converting) showed unreliable SBE result in the work of Hong et al.[26]. Aliferi et al.[29] described 0.248 ng of BS-DNA (10 ng of starting material, gDNA, and eluted with 10 µl, and then used 2 µl of eluent) can compromise for PCR input for most markers in MPS. Also, Heidegger et al.[34] performed the sensitivity test with 8 µl of BS-converted eluent (200, 100, 50, 20, 10, and 1 ng of gDNA with D-PB kit eluted with 10 µl), which can be calculated into 19.880, 9.940, 4.970, 1.988, 0.994, and 0.099 ng. They reported that down to 1.988 ng (20 ng of gDNA) of BS-DNA, there was no DNAm difference exceeding 10 %, while less BS-DNA input showed much larger deviations. Therefore, it is tremendously important to use at least more than 1 ng of BS-DNA, measured in the long-sized BisQuE, for the reliable result of age prediction. As Naue et al.[56] and Heidegger et al.[34] pointed out that stochasticity affects the detected DNAm level, the quantitation of BS-DNA for 1st PCR is highly recommended and it should be described in every age prediction report.

Not only the quantity of BS-DNA, but continuity and DNAm analysis platforms should be taken count into when reporting age prediction result. Since SBE is widely known for

its' semi-quantitative result[33, 47, 72] and pyrosequencing can analyze only one amplicon a reaction, so MPS was chosen for constructing age prediction models out of three DNAm analysis platforms: MPS, SBE, and pyrosequencing. Moreover, when it comes to inter-platform DNAm analysis, this study was based on the same 1st amplicon strategy (Figure 2), so only DNAm difference from platforms can be managed in this study.

Table 18. Target sizes of previous works

Gene	Zbiec-Piekarska[50]	Cho[25]	Jung[33]	VISAGE[34, 44]	this study
ELOVL2	308bp	303bp	187bp	267bp	187bp
FHL2	167bp	191bp	191bp	167bp	128bp
KLF14	128bp	101bp	114bp	128bp	114bp
MIR29B2C	146bp	326bp	116bp	146bp	133bp
TRIM59	141bp	148bp	148bp	141bp	122bp

First of all, the same 1st amplicon strategy (Figure 2) was adopted to analyze samples in three platforms: MPS, SBE, and pyrosequencing. To achieve it, 1st PCR primers contained TruSeq sequencing primer (Rd1 and Rd2) binding sequence in 5' end for further indexing PCR for MPS (Table 3 and 18) in this study. Neglecting those sequences, most targeted amplicon sizes in this study were smaller than previous works, and deviations of amplicon sizes were much lesser (Table 18). During the MPS, extreme size-difference can lead the imbalance of markers and it might cause severe loss of read depth of the larger sized marker. Also, as shown in Figure 4 and Table 7, BS-conversion step causes degradation. Therefore, smaller sized amplicon strategy is highly recommended in DNAm analysis.

As well as the target size, CpG site in target-specific primer binding site also should be considered, which can might lead the PCR bias[55]. It is the best if there is no CpG on primers, but primers containing CpG have been used due to difficulties of primer designing for BS-DNA. Therefore, using degenerate base Y (C and T) and R (G and A) or using base independent of DNA can be an option for avoiding it.

SBE is working on capillary electrophoresis (CE) so it is much easier to be integrated routine forensic laboratory works, and much simpler to analyzed than MPS or pyrosequencing. Furthermore, bodyfluid ID system based on SBE[17, 18] showed high accuracy of classification and it is simple and easy to understand as its' on-off pattern. Nonetheless, SBE has several limitations in constructing a model for age prediction. First, DNAm level of SBE system is calculated with fluorescent intensity of ddNTP[32, 33], but this intensity of each base is not equal; the ratio of G:A:C:T is 4:2:1:1[15, 73, 74]. Therefore, target of reversed SBE primer cannot help having exaggerated DNAm values due to fluorescent inequality[15, 32, 33].

Second, the location of SBE primers is fixed as SBE can only detect one base, and this limitation increases complexity of designing SBE primers: neighboring CpG sites and interference between primers. For example, degenerate base was also used in SBE primers for previous studies[26, 33, 35]; however, inosine was used instead of Y or R (Table 5), except one R on the 3' end of *TRIM59* primer due to its' binding affinity. Since, Jung et al.[33] and So et al.[72] pointed out that degeneracy of *TRIM59* primer can cause the broad or split peaks of *TRIM59* in electropherogram, adopting inosine instead of mixed base seemed to be similar with other peaks shown in Figure 8. However, the stability of inosine and base is highly affected by neighboring A/T or C/G pairs[75], it needs to be considered thoroughly.

Also unknown interaction might affect the detected DNAm level or peak heights. Referring to Appendix 2 and 6, there were differences between DNAm values of *MIR29B2C* though its' 1st PCR products were same; the only difference was primers of SBE. However, the DNAm result of four markers were almost same, so this discrepancy would be from unveiled interaction of SBE primer set. Therefore, the model suggested in Jung et al.[33] showed different accuracies in 20 same samples listed in Appendix 6: 5.04 of MAE and 5.71 of RMSE from developed method (Table 5); 3.54 of MAE and 4.20 of RMSE from SBE primer set of Jung et al.[33]. Moreover, depending on the CE software and the hardware, this ratio can be changed[72].

Pyrosequencing is widely used for DNAm analysis and it is quantitative method. Unlike SBE, sequencing primers of pyrosequencing is relatively free from those constraints due to its' sequencing-by-synthesis chemistry. However, it needs to be prepared for single amplicons to analyze. In Cho et al.[25], quite large amount of DNA was used to amplify five amplicons and it might be burdensome for forensic researchers to attain from crime scenes. To avoid the quantity problem, Fleckhaus et al.[53] amplified BS-DNA with general multiplex PCR primer and then amplified with biotinylated primer, which was similar with this study (Figure 3). They showed none of difference was observed with this pyrosequencing adopting nested PCR and conventional pyrosequencing method. Nonetheless, lack of multiplexing ability is one of biggest disadvantages of pyrosequencing.

Meanwhile, data processing can be one of the biggest obstacles in MPS. Analysis of MPS is quite burdensome but much easier analysis tools arise these days. In addition, MPS offers quantitative and absolute DNAm level by counting the methylated and un-methylated reads. It also can analyze multiple samples with multiple markers all at once. Therefore, this study used MPS data to construct age prediction models.

Based on this same amplicon technique, DNAm level and discrepancies between platforms can be analyzed. SBE data showed differences with MPS data as shown in Table 10 and Figure 12. Except *ELOVL2* marker, DNAm level from SBE data of four markers cannot be interchangeable to MPS data, and vice versa. *ELOVL2* marker, which is ELOVL2_P1 (pyrosequencing) and ELOVL2_CpG20 (MPS), was interchangeable and this result is concordant with previous work[47]. Therefore, the adjustment models for SBE to MPS were suggested (Table 13) and tested (Figure 14) for *FHL2, KLF14, MIR29B2C*, and *TRIM59*.

Similar to SBE, ELOVL2_P1 from pyrosequencing and ELOVL2_CpG20 from MPS were interchangeable, which is concordant with Freire-Aradas et al.[47] but rest of markers were hard to substitute. Unlike SBE, only 20 samples were analyzed with pyrosequencing. Therefore, these discrepancies between MPS and pyrosequencing might be reduced if more samples were tested since Bock et al.[76] showed the good agreement between these two

platforms. Anyway, adjustment model for pyrosequencing to MPS was suggested based on the result.

By the way, pyrosequencing data of 20 samples can be applied into the model of Zbiec-Piekarska et al.[50] and the best five model of Cho et al.[25] to get 5.98 yrs and 5.02 yrs of MAEs, respectively. Since predicted ages in Korean from the model of Zbiec-Piekarska et al.[50] showed 4.18 yrs of MAE[25], those MAEs seem to be quite large; however, MAEs reduce to 5.78 yrs (Zbiec-Piekarska et al.[50]) and 3.85 yrs (Cho et al.[25]) without outlier sample 172. Also, small number of samples might affect to the accuracy.

For age prediction models in this study showed high accuracy. First, 5-CpG model showed less than 3 yrs of MAE in training set, the test set of MPS, adjusted SBE data, and adjusted pyrosequencing showed 4.29 yrs, 3.99 yrs, and 4.97 yrs of MAE. (Figure 15). It is promising result for users of SBE as semi-quantitative data can be applied into the MPS-based model with quite high accuracy. However, pyrosequencing data showed somewhat bigger error than others even after adjustment.

One of the reasons is outliers; sample 172. This sample showed outlier values in all 5 CpG sites in three platforms constantly. As sample 172 was analyzed in pyrosequencing, it was assigned to test set of MPS data not to construct overfitted model for MPS. If the outlier is removed from the datasets, MAE and RMSE of the MPS test set decrease to 4.12 yrs and 5.11 yrs, respectively. Also, R-squared value of pyrosequencing data increases to 0.9202 and MAE and RMSE of it reduce to 4.49 yrs and 5.19 yrs, repectively; however, sample of SBE data set is quite large (N=250), removal of sample 172 reduces MAE and RMSE to 3.95 yrs and 4.81 yrs, respectively.

Meanwhile, multiple CpGs models showed similar result to the 5-CpG model. The model showed high accuracy in training and test set of MPS data, but less accurate in the adjusted pyrosequencing data (Figure 16). Like 5-CpG model, sample 172, the outlier, affected the results a lot. Without sample 172, the model shows 0.9040 of R-squared value, 4.58 yrs of MAE, and 5.82 yrs of RMSE. Therefore, containing outlier samples in training set should be considered and robust modelling methods are highly recommended. Also,

researchers who try to predict age based on DNAm should take into account outlier.

On the other hand, both age prediction models in this study were trained with linear regression using quadratic terms. There are many models using a wide range of statistical modeling methods such as neural network[29, 31, 32, 38], random forest regression[27, 45], quantile regression[47], and supportive vector regression[28, 31, 40], and linear regression[20, 25, 26, 33, 35, 42, 44]. Aliferi et al.[29] compared several statistical modeling methods and finally chose the supportive vector machine with polynomial function, which presented the best performance. They suggested that the major prediction error was sample specific in their data set. Unlike the study of Aliferi et al, Montesanto et al.[45] reported that a ridge linear regression model was selected as the best predictive method in their data. It implies that the best model for each data can be changed when applying to other dataset.

However, a linear regression method, which is the simplest way to predict age, showed relatively similar performances through data sets around the world, so it was used in this study. Also, two models suggested in this work showed quite similar or better performance compared to previous works. It suggests that the major factors which highly contribute to the performance of model are good age-predictive markers and accurately detected DNAm levels, so those should be put high on the list. As more and more complicated machine learning models and statistical models have risen, the statistical methods should be considered and tested thoroughly before its' usages; the basic assumptions or conditions need to be checked.

By the way, inter-platform analysis was possible by applying adjustment models. It is different from previous studies[32, 38, 47] as those works merely attempted to apply DNAm data to the model from different platforms[38, 47] or trained data which combined with two or more platforms[32]. Especially, Hong et al.[32] introduced the platform variable and just trained the model with both MPS and SBE data, but we adjusted semi-quantitative SBE data to absolute MPS data and the adjusted data were used as the test set of MPS-based model. This concept is similar to Feng et al.[31], but they trained the model using EpiTYPER and applied z-score transformed pyrosequencing data. Freire-Aradas et al.[47] also reported that

z-score transformation can improve the performances by data scaling in SBE, which was different from other platforms.

Without adjustment models, unadjusted SBE data showed 3.96 yrs of MAE and 5.10 yrs of RMSE in the 5-CpG model. It seemed to have similar performance but the error terms were not normalized, which implies the model cannot explain the age variance well. In the multiple CpGs model, unadjusted pyrosequencing data presented 8.93 yrs of MAE and 11.11 yrs of RMSE, which showed a great loss of accuracy. It might be due to that the number of pyrosequenced samples was small. Nonetheless, adjustment models should be provided for end users who are not able to do MPS and more studies are needed to suggest adjustment models as age prediction model should be constructed based on MPS data due to continuity of age and DNAm; accuracy; and multiplexing capability.

To develop the age prediction model considering forensic context, quantitation of BS-DNA is highly recommended as the number of BS-DNA molecules affects on the result of DNAm analysis and accuracy of predicted age. The performance of BS conversion also needs to be checked to guarantee the reliability of downstream analysis. Moreover, the age prediction model should be constructed based on MPS data, and it is desirable to analyzed DNAm data for age prediction with MPS; however, for who cannot use MPS, the adjustment model to support inter-platform analysis should be provided, and it can be achieved by adopting the same 1st amplicon strategy.

V. CONCLUSION

In this study, age prediction under forensic context was suggested in aspects of quantitation of BS-DNA; MPS based model due to continuity of DNAm and age; and inter-platform analysis methods adopting the same 1st amplicon strategy. To quantify the BS-DNA and assess the performance of BS conversion step, the BisQuE system was developed. The BisQuE is a simple single assay to measure the amount of both gDNA and BS-DNA and give three key information of the conversion step: BS conversion efficiency, the degradation level, and the recovery). Exploiting the constructed qPCR system, six BS conversion kits were tested in 20 samples. Five kits were shown similar conversion efficiency more than 99% and degradation level, whereas the other kit showed the lowest efficiency and degradation level. Kit recovery was also investigated and found to range between 18% and 50%. Furthermore, the amount of amplifiable DNA cannot be guaranteed by the converted DNA either, even though the results of the Qubit seem to be promising.

Based on the BisQuE result, the minimum amount to get reliable DNAm data was determined, and MPS was chosen for training the age prediction model considering continuity of DNAm and age; SBE is semi-quantitative and pyrosequencing cannot analyze multiple amplicons. Then 250 BS-DNA samples were quantified and used as template for the same amplicon strategy to analyzed with MPS and SBE. Additional pyrosequencing was done with 20 samples from the same 1st PCR amplicon. By using the same amplicon strategy, differences between platforms can be compared thoroughly. ELOVL2 marker can be interchangeable in all three platforms but rest of markers needed to be adjusted to perform inter-platform analysis.

Using DNAm data from MPS, two types of age prediction models were constructed: 5-CpG and multiple CpGs model. The 5-CpG model can support both SBE and pyrosequencing data by platform adjustment model. This model showed 4.29 yrs of MAE in the independent test set of MPS, but 3.99 yrs and 4.97 yrs of MAE in the adjusted SBE and pyrosequencing, respectively. The multiple model can support pyrosequencing, and its'

performance was highly accurate in the MPS test set (2.85 yrs of MAE) and slightly less accurate in the adjusted pyrosequencing (5.43 yrs of MAE).

This study provides the guideline for age prediction modelling in forensic context based on quantitation of BS-DNA and the same amplicon strategy. To the best of our knowledge, it is the first study to quantify BS-DNA for entire samples and analyze the difference between DNAm platforms with same amplicons. By following the recommendations, accurate and reliable age prediction modelling can be done by whom trying to suggest the model in forensic fields, and trustworthy age prediction reports can be generated by who dealing with forensic DNA from crime scenes.

REFERENCES

1. Bocklandt S, Lin W, Sehl ME, Sanchez FJ, Sinsheimer JS, Horvath S, et al. Epigenetic predictor of age. PLoS One. 2011;6(6):e14821.
2. Horvath S. DNA methylation age of human tissues and cell types. Genome biology. 2013;14(10):R115.
3. Hannum G, Guinney J, Zhao L, Zhang L, Hughes G, Sadda S, et al. Genome-wide methylation profiles reveal quantitative views of human aging rates. Mol Cell. 2013;49(2):359-67.
4. Horvath S, Raj K. DNA methylation-based biomarkers and the epigenetic clock theory of ageing. Nat Rev Genet. 2018;19(6):371-84.
5. Ciccarone F, Tagliatesta S, Caiafa P, Zampieri M. DNA methylation dynamics in aging: how far are we from understanding the mechanisms? Mech Ageing Dev. 2018;174:3-17.
6. McCartney DL, Zhang F, Hillary RF, Zhang Q, Stevenson AJ, Walker RM, et al. An epigenome-wide association study of sex-specific chronological ageing. Genome Med. 2019;12(1):1.
7. Bell CG, Lowe R, Adams PD, Baccarelli AA, Beck S, Bell JT, et al. DNA methylation aging clocks: challenges and recommendations. Genome biology. 2019;20(1):249.
8. Cedar H, Bergman Y. Linking DNA methylation and histone modification: patterns and paradigms. Nat Rev Genet. 2009;10(5):295-304.
9. Greenberg MVC, Bourc'his D. The diverse roles of DNA methylation in mammalian development and disease. Nat Rev Mol Cell Biol. 2019;20(10):590-607.
10. Lee HY, Lee SD, Shin KJ. Forensic DNA methylation profiling from evidence material for investigative leads. BMB reports. 2016;49(7):359-69.
11. Zubakov D, Liu F, Kokmeijer I, Choi Y, van Meurs JBJ, van IWFJ, et al. Human age estimation from blood using mRNA, DNA methylation, DNA rearrangement, and telomere length. Forensic Sci Int Genet. 2016;24:33-43.

12. Jung S-E, Shin K-J, Lee HY. DNA methylation-based age prediction from various tissues and body fluids. BMB Reports. 2017;50(11):546-53.
13. Vidaki A, Kayser M. Recent progress, methods and perspectives in forensic epigenetics. Forensic Sci Int Genet. 2018;37:180-95.
14. Parson W. Age Estimation with DNA: From Forensic DNA Fingerprinting to Forensic (Epi)Genomics: A Mini-Review. Gerontology. 2018;64(4):326-32.
15. Freire-Aradas A, Phillips C, Lareu MV. Forensic individual age estimation with DNA: From initial approaches to methylation tests. Forensic science review. 2017;29(2):121-44.
16. Butler JM. Advanced topics in forensic DNA typing: methodology: Academic press; 2011.
17. Lee HY, An JH, Jung SE, Oh YN, Lee EY, Choi A, et al. Genome-wide methylation profiling and a multiplex construction for the identification of body fluids using epigenetic markers. Forensic Sci Int Genet. 2015;17:17-24.
18. Lin YC, Tsai LC, Lee JC, Liu KL, Tzen JT, Linacre A, et al. Novel identification of biofluids using a multiplex methylation-specific PCR combined with single-base extension system. Forensic Sci Med Pathol. 2016;12(2):128-38.
19. An JH, Shin K-J, Choi A, Yang WI, Lee HY. DNA Methylation-Based Age Estimation in the Forensic Field. Korean Journal of Legal Medicine. 2013;37(1).
20. Lee HY, Jung SE, Oh YN, Choi A, Yang WI, Shin KJ. Epigenetic age signatures in the forensically relevant body fluid of semen: a preliminary study. Forensic Sci Int Genet. 2015;19:28-34.
21. Giuliani C, Cilli E, Bacalini MG, Pirazzini C, Sazzini M, Gruppioni G, et al. Inferring chronological age from DNA methylation patterns of human teeth. Am J Phys Anthropol. 2016;159(4):585-95.
22. Eipel M, Mayer F, Arent T, Ferreira MR, Birkhofer C, Gerstenmaier U, et al. Epigenetic age predictions based on buccal swabs are more precise in combination with cell type-specific DNA methylation signatures. Aging. 2016;8(5):1034-48.

23. Park JL, Kim JH, Seo E, Bae DH, Kim SY, Lee HC, et al. Identification and evaluation of age-correlated DNA methylation markers for forensic use. Forensic Sci Int Genet. 2016;23:64-70.
24. Freire-Aradas A, Phillips C, Mosquera-Miguel A, Giron-Santamaria L, Gomez-Tato A, Casares de Cal M, et al. Development of a methylation marker set for forensic age estimation using analysis of public methylation data and the Agena Bioscience EpiTYPER system. Forensic Sci Int Genet. 2016;24:65-74.
25. Cho S, Jung SE, Hong SR, Lee EH, Lee JH, Lee SD, et al. Independent validation of DNA-based approaches for age prediction in blood. Forensic Sci Int Genet. 2017;29:250-6.
26. Hong SR, Jung SE, Lee EH, Shin KJ, Yang WI, Lee HY. DNA methylation-based age prediction from saliva: High age predictability by combination of 7 CpG markers. Forensic Sci Int Genet. 2017;29:118-25.
27. Naue J, Hoefsloot HCJ, Mook ORF, Rijlaarsdam-Hoekstra L, van der Zwalm MCH, Henneman P, et al. Chronological age prediction based on DNA methylation: Massive parallel sequencing and random forest regression. Forensic Sci Int Genet. 2017;31:19-28.
28. Hamano Y, Manabe S, Morimoto C, Fujimoto S, Tamaki K. Forensic age prediction for saliva samples using methylation-sensitive high resolution melting: exploratory application for cigarette butts. Sci Rep. 2017;7(1):10444.
29. Aliferi A, Ballard D, Gallidabino MD, Thurtle H, Barron L, Syndercombe Court D. DNA methylation-based age prediction using massively parallel sequencing data and multiple machine learning models. Forensic Science International: Genetics. 2018;37:215-26.
30. Lee JW, Choung CM, Jung JY, Lee HY, Lim SK. A validation study of DNA methylation-based age prediction using semen in forensic casework samples. Leg Med (Tokyo). 2018;31:74-7.
31. Feng L, Peng F, Li S, Jiang L, Sun H, Ji A, et al. Systematic feature selection improves

accuracy of methylation-based forensic age estimation in Han Chinese males. Forensic Sci Int Genet. 2018;35:38-45.

32. Hong SR, Shin KJ, Jung SE, Lee EH, Lee HY. Platform-independent models for age prediction using DNA methylation data. Forensic Sci Int Genet. 2019;38:39-47.
33. Jung SE, Lim SM, Hong SR, Lee EH, Shin KJ, Lee HY. DNA methylation of the ELOVL2, FHL2, KLF14, C1orf132/MIR29B2C, and TRIM59 genes for age prediction from blood, saliva, and buccal swab samples. Forensic Sci Int Genet. 2019;38:1-8.
34. Heidegger A, Xavier C, Niederstatter H, de la Puente M, Pospiech E, Pisarek A, et al. Development and optimization of the VISAGE basic prototype tool for forensic age estimation. Forensic Sci Int Genet. 2020;48:102322.
35. Dias HC, Cordeiro C, Pereira J, Pinto C, Real FC, Cunha E, et al. DNA methylation age estimation in blood samples of living and deceased individuals using a multiplex SNaPshot assay. Forensic Sci Int. 2020;311:110267.
36. Lee HY, Hong SR, Lee JE, Hwang IK, Kim NY, Lee JM, et al. Epigenetic age signatures in bones. Forensic Science International: Genetics. 2020;46:102261.
37. Shi L, Jiang F, Ouyang F, Zhang J, Wang Z, Shen X. DNA methylation markers in combination with skeletal and dental ages to improve age estimation in children. Forensic Sci Int Genet. 2018;33:1-9.
38. Vidaki A, Ballard D, Aliferi A, Miller TH, Barron LP, Syndercombe Court D. DNA methylation-based forensic age prediction using artificial neural networks and next generation sequencing. Forensic Sci Int Genet. 2017;28:225-36.
39. Weidner CI, Lin Q, Koch CM, Eisele L, Beier F, Ziegler P, et al. Aging of blood can be tracked by DNA methylation changes at just three CpG sites. Genome biology. 2014;15(2):R24.
40. Xu C, Qu H, Wang G, Xie B, Shi Y, Yang Y, et al. A novel strategy for forensic age prediction by DNA methylation and support vector regression model. Sci Rep. 2015;5:17788.

41. Yi SH, Xu LC, Mei K, Yang RZ, Huang DX. Isolation and identification of age-related DNA methylation markers for forensic age-prediction. Forensic Sci Int Genet. 2014;11:117-25.
42. Zbiec-Piekarska R, Spolnicka M, Kupiec T, Makowska Z, Spas A, Parys-Proszek A, et al. Examination of DNA methylation status of the ELOVL2 marker may be useful for human age prediction in forensic science. Forensic Sci Int Genet. 2015;14:161-7.
43. Bekaert B, Kamalandua A, Zapico SC, Van de Voorde W, Decorte R. Improved age determination of blood and teeth samples using a selected set of DNA methylation markers. Epigenetics. 2015;10(10):922-30.
44. Woźniak A, Heidegger A, Piniewska-Róg D, Pośpiech E, Xavier C, Pisarek A, et al. Development of the VISAGE enhanced tool and statistical models for epigenetic age estimation in blood, buccal cells and bones. Aging. 2021;13(5):6459-84.
45. Montesanto A, D'Aquila P, Lagani V, Paparazzo E, Geracitano S, Formentini L, et al. A new robust epigenetic model for forensic age prediction. Journal of forensic sciences. 2020;65(5):1424-31.
46. Freire-Aradas A, Phillips C, Giron-Santamaria L, Mosquera-Miguel A, Gomez-Tato A, Casares de Cal MA, et al. Tracking age-correlated DNA methylation markers in the young. Forensic Sci Int Genet. 2018;36:50-9.
47. Freire-Aradas A, Pośpiech E, Aliferi A, Girón-Santamaría L, Mosquera-Miguel A, Pisarek A, et al. A Comparison of Forensic Age Prediction Models Using Data From Four DNA Methylation Technologies. Front Genet. 2020;11:932.
48. Garagnani P, Bacalini MG, Pirazzini C, Gori D, Giuliani C, Mari D, et al. Methylation of ELOVL2 gene as a new epigenetic marker of age. Aging Cell. 2012;11(6):1132-4.
49. Naue J, Sanger T, Hoefsloot HCJ, Lutz-Bonengel S, Kloosterman AD, Verschure PJ. Proof of concept study of age-dependent DNA methylation markers across different tissues by massive parallel sequencing. Forensic Sci Int Genet. 2018;36:152-9.
50. Zbiec-Piekarska R, Spolnicka M, Kupiec T, Parys-Proszek A, Makowska Z, Paleczka A, et al. Development of a forensically useful age prediction method based on DNA

methylation analysis. Forensic Sci Int Genet. 2015;17:173-9.

51. Fernandez-Rebollo E, Eipel M, Seefried L, Hoffmann P, Strathmann K, Jakob F, et al. Primary Osteoporosis Is Not Reflected by Disease-Specific DNA Methylation or Accelerated Epigenetic Age in Blood. J Bone Miner Res. 2018;33(2):356-61.
52. Vidal-Bralo L, Lopez-Golan Y, Mera-Varela A, Rego-Perez I, Horvath S, Zhang Y, et al. Specific premature epigenetic aging of cartilage in osteoarthritis. Aging. 2016;8(9):2222-31.
53. Fleckhaus J, Schneider PM. Novel multiplex strategy for DNA methylation-based age prediction from small amounts of DNA via Pyrosequencing. Forensic Science International: Genetics. 2020;44:102189.
54. Montesanto A, D'Aquila P, Lagani V, Paparazzo E, Geracitano S, Formentini L, et al. A New Robust Epigenetic Model for Forensic Age Prediction. Journal of forensic sciences. 2020;65(5):1424-31.
55. Naue J, Lee HY. Considerations for the need of recommendations for the research and publication of DNA methylation results. Forensic Science International: Genetics. 2018;37:e12-e4.
56. Naue J, Hoefsloot HCJ, Kloosterman AD, Verschure PJ. Forensic DNA methylation profiling from minimal traces: How low can we go? Forensic Sci Int Genet. 2018;33:17-23.
57. Grunau C, Clark SJ, Rosenthal A. Bisulfite genomic sequencing: systematic investigation of critical experimental parameters. Nucleic Acids Research. 2001;29(13):e65.
58. Tanaka K, Okamoto A. Degradation of DNA by bisulfite treatment. Bioorg Med Chem Lett. 2007;17(7):1912-5.
59. Holmes EE, Jung M, Meller S, Leisse A, Sailer V, Zech J, et al. Performance evaluation of kits for bisulfite-conversion of DNA from tissues, cell lines, FFPE tissues, aspirates, lavages, effusions, plasma, serum, and urine. PLoS One. 2014;9(4):e93933.

60. Bryzgunova O. Efficacy of Bisulfite Modification and DNA Recovery Using Commercial Kits from Samples of Genomic and Circulating DNA. Computational Biology and Bioinformatics. 2013;1(6).
61. Izzi B, Binder AM, Michels KB. Pyrosequencing Evaluation of Widely Available Bisulfite Conversion Methods: Considerations for Application. Med Epigenet. 2014;2(1):28-36.
62. Leontiou CA, Hadjidaniel MD, Mina P, Antoniou P, Ioannides M, Patsalis PC. Bisulfite Conversion of DNA: Performance Comparison of Different Kits and Methylation Quantitation of Epigenetic Biomarkers that Have the Potential to Be Used in Non-Invasive Prenatal Testing. Plos One. 2015;10(8).
63. Worm Ørntoft M-B, Jensen SØ, Hansen TB, Bramsen JB, Andersen CL. Comparative analysis of 12 different kits for bisulfite conversion of circulating cell-free DNA. Epigenetics. 2017;12(8):626-36.
64. Kint S, De Spiegelaere W, De Kesel J, Vandekerckhove L, Van Criekinge W. Evaluation of bisulfite kits for DNA methylation profiling in terms of DNA fragmentation and DNA recovery using digital PCR. PLoS One. 2018;13(6):e0199091.
65. Tierling S, Schmitt B, Walter J. Comprehensive Evaluation of Commercial Bisulfite-Based DNA Methylation Kits and Development of an Alternative Protocol With Improved Conversion Performance. Genet Epigenet. 2018;10:1179237X18766097.
66. Hong SR, Shin KJ. Bisulfite-Converted DNA Quantity Evaluation: A Multiplex Quantitative Real-Time PCR System for Evaluation of Bisulfite Conversion. Front Genet. 2021;12:618955.
67. Sudmant PH, Kitzman JO, Antonacci F, Alkan C, Malig M, Tsalenko A, et al. Diversity of Human Copy Number Variation and Multicopy Genes. Science. 2010;330(6004):641-6.
68. Koo TK, Li MY. A Guideline of Selecting and Reporting Intraclass Correlation Coefficients for Reliability Research. J Chiropr Med. 2016;15(2):155-63.
69. Passing H, Bablok W. A New Biometrical Procedure for Testing the Equality of

Measurements from Two Different Analytical Methods. Application of linear regression procedures for method comparison studies in Clinical Chemistry, Part I1983.

70. Kurdyukov S, Bullock M. DNA Methylation Analysis: Choosing the Right Method. Biology (Basel). 2016;5(1).
71. Naue J, Lee HY. Considerations for the need of recommendations for the research and publication of DNA methylation results. Forensic Sci Int Genet. 2018;37:e12-e4.
72. So MH, Lee HY. Genetic analyzer-dependent DNA methylation detection and its application to existing age prediction models. ELECTROPHORESIS.n/a(n/a).
73. Sanchez JJ, Borsting C, Balogh K, Berger B, Bogus M, Butler JM, et al. Forensic typing of autosomal SNPs with a 29 SNP-multiplex--results of a collaborative EDNAP exercise. Forensic Sci Int Genet. 2008;2(3):176-83.
74. Lou C, Cong B, Li S, Fu L, Zhang X, Feng T, et al. A SNaPshot assay for genotyping 44 individual identification single nucleotide polymorphisms. Electrophoresis. 2011;32(3-4):368-78.
75. Watkins NE, Jr., SantaLucia J, Jr. Nearest-neighbor thermodynamics of deoxyinosine pairs in DNA duplexes. Nucleic Acids Res. 2005;33(19):6258-67.
76. BLUEPRINT consortium. Quantitative comparison of DNA methylation assays for biomarker development and clinical applications. Nat Biotechnol. 2016;34(7):726-37.

APPENDICES

Appendix 1. Six BS conversion kits and its' instructions.

Abb.	Manufacturer	Kit name	DNA Input	Input vol. (µl)	Elution vol. (µl)
Z-EZ	Zymo Research	EZ DNA Methlyation-Lightning Kit	100 pg - 2 µg	20	10
D-PB	Diagenode	Premium Bisulfite kit	100 pg - 2 µg	20	10
P-ME	Promega	MethylEdge Bisulfite Conversion System	100 pg - 2 µg	20	10-20
T-EJ	Thermo Fisher Scientific	EpiJET Bisulfite Conversion Kit	50 pg - 2 µg	20	10-20
Q-EF	Qiagen	EpiTect Fast Bisulfite kit	1 ng – 2 µg	40	10-15
N-NE	New England Biolabs	NEBNext Enzymatic Methyl-seq Conversion Module	10 ng - 200 ng	29	20

Appendix 2. DNAm percentage of 5 CpG sites from SBE data

ID*	Age	ELOVL2	FHL2	KLF14	MIR29B2C	TRIM59
1	20	26.27	18.04	4.69	90.52	24.73
2	20	27.95	23.97	3.51	100	20.48
3	21	29.51	21.43	3.98	88.65	19.42
4	21	25.56	25.41	3.74	90.76	28.73
5	21	26.35	21.70	0	83.10	21.27
6	22	30.73	24.78	6.43	88.84	25.98
7	22	24.69	24.36	3.52	89.70	27.71
8	22	30.31	19.46	0	85.15	25.21
9	23	33.00	20.89	3.11	92.32	28.83
10	23	23.85	20.42	4.13	93.10	34.45
11	24	29.95	25.28	3.68	88.74	29.08
12	24	34.92	21.37	0	92.09	21.56
13	24	33.81	20.68	4.67	89.95	29.36
14	25	29.95	24.72	2.54	88.81	23.41
15	25	30.28	24.03	3.13	90.01	23.84
16	26	37.93	25.95	5.93	89.54	26.99
17	26	24.66	22.76	5.58	88.94	32.18
18	26	37.41	23.56	5.24	86.33	31.34
19	27	33.02	26.09	2.53	84.29	30.28
20	27	29.29	22.84	4.46	88.42	25.23
21	28	29.85	26.46	4.55	88.61	29.39
22	28	34.97	26.02	4.18	86.66	33.21
23	28	30.71	24.17	3.84	88.98	33.18
24	29	31.18	23.45	3.66	86.50	28.49
25	29	35.84	21.73	6.10	79.33	28.76
26	30	34.11	22.95	3.33	80.69	31.06
27	30	37.92	21.80	4.32	82.61	33.35
28	30	36.80	25.72	4.77	86.58	29.61
29	30	38.14	23.48	3.36	91.75	24.89
30	31	34.73	26.49	3.90	88.37	29.63
31	31	32.62	25.84	5.29	83.69	34.75
32	31	27.80	21.60	4.91	90.38	29.56
33	32	30.56	25.37	5.30	83.37	31.93
34	32	32.65	26.60	7.24	86.56	34.31

Appendix 2 (continued)

35	32	38.26	29.16	5.27	89.85	34.84
36	32	44.54	27.80	5.56	74.52	38.58
37	33	39.01	21.79	4.19	82.55	34.77
38	35	40.86	23.41	6.21	81.03	36.59
39	35	32.02	28.84	6.32	81.55	32.55
40	35	36.43	23.93	5.36	80.87	31.38
41	36	45.11	26.51	5.68	86.31	37.92
42	36	39.55	30.25	5.86	82.53	36.11
43	36	36.87	24.94	5.39	79.31	34.81
44	36	37.00	26.66	6.00	80.76	36.08
45	37	36.36	21.84	7.90	84.57	32.05
46	37	39.67	30.23	8.23	88.33	35.70
47	38	40.08	29.93	9.82	81.72	41.54
48	38	35.28	25.82	8.22	85.58	33.60
49	39	41.73	30.96	6.74	84.76	30.61
50	39	43.03	24.07	4.36	81.53	31.66
51	40	40.81	33.18	7.73	77.08	30.06
52	40	38.77	29.14	7.31	85.54	35.34
53	40	44.71	30.63	8.91	83.31	39.70
54	41	40.09	31.31	5.89	86.09	36.36
55	42	50.66	30.69	3.53	70.21	42.62
56	42	42.47	29.25	5.45	70.66	35.98
57	42	56.16	34.46	6.24	82.20	39.41
58	42	43.01	32.30	6.15	84.35	34.10
59	43	44.19	26.88	7.51	81.03	34.78
60	43	44.29	33.20	10.18	64.13	37.23
61	44	49.23	25.37	6.90	78.54	36.54
62	44	42.63	33.12	5.68	83.11	43.09
63	45	48.92	28.21	6.34	70.41	34.27
64	45	38.76	32.37	11.66	79.67	38.62
65	45	45.55	31.92	9.09	76.46	33.86
66	47	51.44	32.29	5.93	85.16	41.26
67	47	43.61	28.27	5.54	79.09	34.08
68	47	48.55	26.02	4.56	61.36	36.72
69	48	32.06	18.40	4.07	66.83	25.72
70	48	51.17	29.61	7.11	75.08	41.71

Appendix 2 (continued)

71	48	44.03	32.84	8.12	80.40	38.24
72	49	41.36	32.08	8.84	77.57	42.01
73	49	50.74	35.23	7.26	75.58	45.95
74	49	53.53	35.20	10.81	73.21	42.58
75	49	50.06	31.37	7.71	76.09	37.99
76	50	44.87	33.04	10.31	62.07	50.97
77	50	46.15	33.92	7.16	78.86	39.43
78	50	51.91	35.15	8.88	75.15	42.25
79	50	47.31	32.97	9.22	82.13	44.53
80	51	49.17	31.44	10.09	64.61	40.82
81	51	51.06	32.40	10.01	71.67	42.95
82	51	46.55	30.32	8.64	73.06	40.49
83	52	48.36	34.43	10.51	78.86	39.58
84	52	46.47	29.63	7.14	66.93	39.55
85	52	50.34	34.74	10.36	75.26	42.81
86	53	45.64	40.50	10.28	48.23	46.92
87	53	44.08	39.13	12.49	65.21	43.24
88	53	52.56	32.08	9.87	73.57	42.19
89	53	59.20	31.25	6.65	81.01	41.16
90	53	47.74	34.78	12.42	70.85	35.64
91	54	47.72	33.14	11.20	72.77	45.78
92	55	57.86	39.13	9.70	78.86	35.62
93	55	46.65	35.57	10.99	70.28	45.95
94	55	47.59	32.83	12.41	75.67	43.28
95	56	52.81	41.08	13.85	75.45	48.77
96	57	48.37	33.54	11.48	71.13	40.08
97	57	49.92	36.42	7.83	80.70	42.40
98	57	56.06	33.58	9.02	62.42	46.21
99	58	46.90	39.36	10.76	67.54	39.66
100	58	53.81	37.30	12.94	68.93	42.36
101	60	53.18	36.52	12.68	65.23	44.32
102	60	60.70	51.16	13.10	73.48	48.27
103	60	50.65	36.45	8.01	74.62	52.48
104	61	56.25	38.49	9.14	56.07	56.57
105	62	61.77	38.92	14.45	64.27	45.76
106	62	53.00	31.66	12.73	67.58	40.91

Appendix 2 (continued)

107	62	53.10	38.23	11.13	68.50	39.81
108	62	60.66	41.08	14.92	68.22	54.57
109	62	53.06	29.91	12.11	56.26	51.29
110	62	59.31	39.68	14.04	73.85	46.66
111	63	61.71	30.45	11.95	70.35	43.05
112	64	51.88	34.66	10.34	67.72	42.06
113	65	57.39	35.76	11.23	72.06	48.28
114	65	52.81	36.00	11.75	68.44	43.74
115	66	55.77	39.71	10.86	69.69	45.06
116	66	52.04	37.10	8.51	49.03	51.63
117	69	54.90	41.37	10.21	61.73	42.71
118	69	60.69	42.22	12.37	49.50	46.56
119	69	60.86	35.64	17.07	57.81	49.88
120	70	58.63	39.93	15.32	44.16	51.64
121	73	58.99	41.30	14.58	56.38	60.02
122	74	56.75	44.09	15.57	55.82	52.53
123	74	55.98	39.44	15.27	52.21	44.88
124	75	62.29	46.71	16.13	48.54	49.71
125	76	53.74	40.87	13.18	59.50	48.71
126	20	28.46	23.65	3.21	92.20	25.51
127	20	28.52	22.22	4.16	91.94	28.59
128	21	22.57	21.19	4.80	89.21	31.73
129	21	32.78	24.72	2.74	92.59	25.92
130	22	28.14	20.47	3.63	91.74	28.61
131	22	25.86	19.10	3.25	94.15	25.26
132	22	29.69	24.66	2.73	94.09	31.18
133	23	32.15	20.94	3.79	91.23	22.99
134	23	29.75	20.70	5.02	88.50	16.12
135	23	31.49	24.11	2.56	88.43	27.92
136	23	30.14	24.49	3.32	89.30	26.57
137	24	34.34	23.65	5.46	87.80	21.85
138	24	30.01	28.30	4.98	92.34	30.70
139	25	27.85	21.24	4.17	88.19	30.46
140	25	35.61	25.35	3.69	89.13	29.02
141	26	42.74	25.98	6.48	100	31.42
142	26	32.10	20.80	2.76	87.93	32.03

Appendix 2 (continued)

143	26	33.78	21.13	5.06	84.23	24.31
144	27	32.83	30.43	6.40	92.66	32.41
145	27	32.16	27.31	5.98	91.46	29.43
146	28	41.74	28.51	5.21	87.32	29.64
147	28	34.43	27.48	5.10	84.75	31.96
148	29	35.49	29.57	3.86	88.84	30.30
149	29	39.58	28.63	6.31	80.71	33.48
150	29	31.72	23.29	4.78	90.83	36.93
151	30	42.96	25.42	5.78	87.11	32.65
152	30	40.68	26.53	6.49	89.00	30.60
153	31	35.74	27.51	4.62	88.33	32.45
154	31	34.39	30.08	6.03	82.92	34.90
155	32	27.74	24.43	5.11	83.14	31.40
156	32	41.08	26.52	5.16	89.57	29.16
157	32	35.38	23.38	4.72	78.46	34.44
158	33	42.48	26.51	5.08	85.73	35.03
159	33	35.74	24.80	4.73	87.02	33.06
160	33	42.65	29.18	6.98	87.55	35.98
161	34	36.18	29.15	6.96	85.93	34.24
162	34	40.60	27.04	5.46	84.03	29.06
163	34	43.83	33.31	5.89	79.47	29.14
164	34	39.91	30.34	4.66	83.94	26.93
165	35	41.50	29.29	5.56	90.98	26.55
166	35	43.18	27.60	5.30	85.70	32.85
167	36	48.74	30.95	4.36	89.93	37.44
168	36	37.58	29.74	6.70	81.61	35.44
169	37	32.25	32.43	4.03	85.70	33.71
170	37	42.74	31.01	5.47	80.21	37.78
171	38	48.25	35.57	6.55	87.67	35.12
172	38	59.24	53.90	2.18	91.74	51.33
173	39	36.59	30.35	7.20	82.57	35.76
174	39	45.84	29.87	8.69	78.72	35.98
175	39	44.49	29.13	5.87	79.20	40.35
176	40	44.04	29.83	5.27	72.30	37.38
177	40	42.98	29.07	7.09	80.40	37.88
178	40	39.90	30.43	7.04	79.55	34.54

Appendix 2 (continued)

179	41	43.74	29.79	6.68	79.63	37.05
180	41	43.44	29.43	5.88	82.65	44.60
181	42	45.23	33.98	4.60	73.63	37.30
182	42	44.31	26.22	5.03	80.23	31.29
183	43	50.76	38.45	7.27	76.17	39.74
184	43	54.21	33.13	5.84	84.12	37.75
185	44	40.40	31.03	3.50	81.65	41.57
186	44	48.57	31.77	4.62	78.91	40.05
187	45	37.98	30.81	8.37	76.55	37.07
188	45	44.98	35.33	8.61	70.25	37.55
189	45	48.50	33.29	7.13	77.57	37.64
190	46	49.02	36.19	5.75	76.46	40.26
191	46	45.34	37.09	8.48	73.43	36.77
192	46	50.19	33.50	10.41	72.97	39.53
193	47	46.06	35.98	10.63	82.63	36.59
194	47	41.13	35.19	5.58	74.89	39.45
195	48	48.07	34.10	6.04	80.29	39.09
196	48	50.21	33.69	6.00	80.35	42.21
197	49	51.01	37.58	7.84	79.30	39.78
198	49	47.16	37.52	11.06	75.50	41.24
199	49	43.80	31.11	6.75	79.59	39.66
200	49	49.54	36.94	8.19	66.74	43.35
201	50	38.03	34.37	7.78	70.42	46.06
202	50	45.87	29.30	4.97	75.68	36.57
203	50	44.73	29.00	11.68	70.67	22.24
204	51	50.21	40.04	9.39	74.29	42.34
205	51	38.74	28.95	10.52	74.57	47.29
206	51	51.70	31.70	7.16	77.85	33.98
207	52	53.25	34.46	7.17	76.13	37.24
208	52	58.31	35.72	12.52	73.57	48.94
209	52	56.80	37.48	4.02	58.49	41.28
210	53	58.71	32.88	9.74	79.84	39.94
211	53	44.92	34.44	11.70	73.71	40.18
212	54	49.01	38.36	10.90	71.60	40.25
213	54	50.13	50.16	6.62	76.55	39.57
214	54	47.51	32.82	6.43	76.03	38.68

Appendix 2 (continued)

215	55	55.43	36.97	8.99	62.97	35.58
216	55	45.03	31.38	11.29	72.40	40.74
217	55	59.20	32.27	8.16	66.00	44.59
218	56	54.75	39.54	10.97	68.32	38.78
219	56	57.61	35.36	9.82	71.59	42.70
220	57	52.54	35.92	7.59	69.47	43.43
221	57	54.27	39.75	8.78	71.06	44.13
222	58	46.57	37.06	6.03	71.88	42.35
223	58	51.72	44.66	9.81	72.03	42.09
224	59	50.13	35.30	7.99	52.81	40.19
225	59	52.52	40.48	10.25	70.81	47.95
226	60	49.59	44.03	10.07	63.60	42.46
227	60	56.01	36.25	3.01	52.94	35.00
228	61	57.75	39.35	12.01	76.51	44.32
229	61	53.33	32.80	8.57	72.81	45.19
230	61	45.54	34.48	8.13	63.18	45.55
231	62	55.33	36.01	8.73	70.83	44.58
232	63	54.50	40.05	10.86	76.00	46.89
233	63	51.69	33.53	6.73	64.64	45.66
234	64	52.95	34.65	10.64	61.43	40.77
235	64	51.53	47.19	11.76	68.90	52.46
236	64	58.93	40.15	11.61	57.86	40.70
237	65	52.98	39.75	10.03	65.21	47.61
238	65	48.44	40.23	13.81	66.80	40.81
239	65	62.70	40.86	15.33	63.88	45.75
240	65	49.02	43.24	12.00	74.67	40.95
241	67	50.88	43.32	11.98	66.83	50.57
242	67	47.45	37.04	10.90	55.20	51.96
243	68	53.95	34.55	7.23	75.22	49.26
244	68	60.99	38.86	12.04	48.21	51.22
245	69	53.42	37.30	13.50	73.17	47.58
246	70	55.80	39.86	8.98	55.37	47.88
247	71	46.04	42.28	12.33	54.57	48.02
248	72	56.37	41.90	14.11	58.26	47.71
249	72	61.46	43.59	12.06	76.44	53.74
250	73	39.91	37.55	8.30	54.25	47.22

*50 samples of the test set were in bold.

Appendix 3. DNAm of 20 samples from pyrosequencing data

ID		001	013	026	041	054	065	081	098	109	122	138	149	161	172	183	192	211	220	234	245
Age		20	24	30	36	41	45	51	57	62	74	24	29	34	38	43	46	53	57	64	69
Gene	No.																				
ELOVL2	P1	28.05	35.85	36.58	46.33	41.72	45.77	52.50	59.85	55.89	55.86	30.44	37.20	36.82	61.11	51.67	48.95	46.82	51.82	55.52	52.51
	P2	22.98	26.07	18.82	30.34	29.44	29.20	35.91	38.88	38.36	40.79	20.14	24.56	27.04	40.65	32.21	30.67	32.89	30.97	38.52	37.12
	P3	54.30	63.99	61.05	75.93	73.78	70.56	83.71	83.21	80.97	88.33	63.81	58.25	64.37	85.94	74.44	75.26	74.04	81.89	83.98	79.72
	P4	45.27	59.97	49.02	62.35	62.04	63.84	71.71	73.67	73.28	81.29	56.03	50.94	55.81	75.84	68.98	62.49	62.92	70.32	72.53	80.71
	P5	14.69	25.60	17.70	27.99	25.80	24.09	36.87	39.00	33.96	41.40	14.32	24.32	28.09	43.52	33.66	25.31	30.82	35.16	33.74	42.53
	P6	32.63	65.46	39.68	52.29	48.66	47.82	61.98	63.40	62.13	70.58	40.87	44.69	49.13	81.29	59.06	55.01	57.85	64.87	67.07	72.00
	P7	46.56	60.11	54.88	64.70	62.24	71.16	73.16	71.99	70.33	76.18	54.18	61.44	58.21	78.99	72.80	66.15	64.85	76.12	73.22	71.81
	P8	19.81	58.24	23.37	32.16	35.79	31.42	38.51	33.61	35.98	38.74	23.52	23.11	25.71	45.50	36.10	27.88	35.41	40.68	38.51	41.70
	P9	24.03	29.02	22.86	40.24	36.41	34.58	40.58	40.30	40.87	46.68	27.68	26.41	33.10	66.33	39.89	33.62	36.36	48.77	44.04	44.04
FHL2	P1	25.83	30.91	34.95	38.91	43.34	41.16	43.71	45.28	45.25	56.16	38.05	39.48	36.91	65.41	49.67	42.04	46.19	44.26	47.01	50.88
	P2	32.99	30.60	33.90	38.64	42.25	43.35	43.94	51.30	50.71	60.26	37.91	41.57	38.81	71.35	51.27	44.42	50.85	48.92	52.88	61.26
	P3	27.19	29.17	35.53	35.64	39.89	40.00	40.37	46.60	45.54	58.20	35.95	38.79	38.56	74.67	46.77	42.02	43.98	47.27	47.98	56.84
	P4	50.23	56.52	67.66	68.91	69.34	72.68	69.50	78.64	72.38	77.95	65.75	62.42	66.94	88.82	70.20	66.98	72.77	67.92	70.17	77.10
	P5	21.87	25.55	29.25	32.57	35.20	36.21	36.52	43.11	39.78	49.55	31.26	33.96	32.19	64.74	40.97	38.61	39.25	43.27	44.33	46.26
	P6	34.91	38.00	43.63	46.14	48.25	48.86	48.01	55.90	50.88	64.79	44.94	45.09	42.87	73.22	51.95	46.85	53.34	51.25	50.19	55.97
	P7	13.85	17.98	19.63	21.90	24.10	22.60	23.44	27.39	24.22	30.53	24.36	21.95	20.02	41.73	24.48	24.70	25.04	27.20	27.30	31.31
	P8	11.56	12.17	15.37	14.70	16.04	16.12	15.78	19.19	19.27	23.75	15.00	17.86	14.86	33.66	20.11	16.71	18.94	19.75	20.67	24.55
	P9	31.29	33.07	40.14	35.60	42.11	41.32	36.08	39.78	41.77	49.18	37.00	38.69	34.22	64.32	43.77	37.94	43.06	41.16	41.82	44.45
	P10	9.89	7.10	10.35	12.18	12.18	11.46	12.43	14.87	11.36	17.23	11.73	12.58	11.75	20.74	14.56	9.42	14.17	13.50	14.06	17.74
	P11	17.98	16.42	21.84	19.82	18.92	20.30	17.03	22.95	17.81	22.62	21.35	21.07	19.15	26.85	20.89	16.20	19.90	23.55	21.20	26.53
	P12	9.18	9.23	11.50	10.29	10.47	10.28	10.69	13.71	8.91	12.80	10.26	9.85	12.04	11.10	11.68	9.25	13.11	13.02	11.53	15.71

Appendix 3 (continued)

KLF14	P1	4.30	4.44	3.53	5.83	5.74	7.36	8.84	8.96	10.26	12.54	3.70	4.53	5.24	2.21	6.05	8.96	9.45	6.84	9.03	11.93
	P2	2.45	3.84	2.65	4.29	4.49	5.29	4.91	4.81	6.45	6.65	1.95	2.07	2.79	1.76	3.74	4.00	5.14	4.57	5.55	7.84
	P3	4.55	4.44	5.91	5.28	6.66	5.97	6.82	5.48	7.36	8.49	3.40	4.48	3.09	3.06	6.60	5.54	5.76	6.28	7.56	7.84
	P4	4.89	3.71	3.37	4.06	2.98	3.52	3.57	4.33	4.42	4.01	2.22	2.03	2.38	1.79	3.07	2.26	3.83	3.86	5.14	5.62
	P5	2.96	3.94	0.60	3.12	3.94	4.10	4.95	0.52	4.53	5.07	2.24	1.96	2.11	2.17	3.40	3.76	3.90	4.30	5.99	3.92
MIR29B2C	P1	92.60	88.80	79.70	85.61	85.28	74.01	71.00	59.80	51.91	51.90	78.69	85.03	90.04	92.09	75.53	72.03	70.13	67.05	58.10	72.46
	P2	62.45	63.72	51.38	61.87	55.40	46.67	48.94	40.52	35.80	35.56	55.08	60.12	68.37	64.83	56.53	47.96	44.43	49.61	33.12	49.66
	P3	58.73	56.69	47.30	54.71	52.83	40.09	47.38	37.66	31.43	34.76	49.23	55.26	66.62	60.67	52.18	46.48	44.86	44.31	31.19	48.62
	P4	44.25	51.32	32.61	45.86	39.77	29.13	34.86	30.42	23.00	24.05	38.98	44.30	53.42	47.75	40.55	33.36	33.51	34.94	23.61	33.84
	P5	38.36	51.20	29.99	42.16	41.79	27.39	33.79	29.87	21.15	22.57	36.01	41.70	48.02	41.50	38.22	30.19	30.28	35.91	22.48	35.40
TRIM59	P1	15.55	17.47	18.57	22.13	22.24	17.88	25.57	23.43	26.54	24.95	14.24	21.71	19.86	44.52	23.14	22.27	25.25	23.64	25.33	25.31
	P2	10.30	12.91	10.63	12.62	15.68	11.07	18.04	18.43	20.22	16.90	7.54	12.97	13.45	24.98	12.92	14.35	17.42	15.73	14.60	16.16
	P3	16.03	22.23	17.56	19.54	24.15	22.32	30.94	27.98	35.36	32.68	16.54	21.32	23.28	39.52	23.06	26.06	30.61	27.40	30.38	31.77
	P4	31.18	37.87	37.92	42.35	41.87	40.60	48.62	52.28	52.80	54.73	32.34	38.27	35.91	69.33	43.81	43.80	51.16	46.67	48.95	51.46
	P5	32.78	33.90	35.54	39.66	40.18	36.77	48.72	49.92	51.84	54.52	32.89	36.93	36.73	56.66	43.91	43.55	45.96	46.19	47.09	51.17
	P6	24.59	30.04	30.09	37.40	34.53	33.63	42.94	42.87	46.46	49.95	23.26	29.71	33.29	50.88	41.47	39.45	43.91	44.94	43.93	45.60
	P7	23.90	32.32	31.73	39.59	34.73	32.37	42.87	42.39	50.19	50.36	27.27	33.67	33.84	60.37	38.98	41.38	47.39	46.24	41.52	47.25
	P8	17.39	25.06	20.70	27.02	27.77	24.66	35.99	33.07	35.16	37.50	17.73	25.36	23.13	42.10	28.25	29.37	33.17	33.11	32.35	40.07
	P9	15.57	22.60	19.09	25.04	21.95	19.33	28.41	26.17	26.79	23.60	15.80	24.17	21.09	36.85	22.40	22.91	29.75	22.34	26.45	25.70

Appendix 4. 40 Common CpG makers of MPS (x-axis) and pyrosequencing (y-axis) from 20 samples.

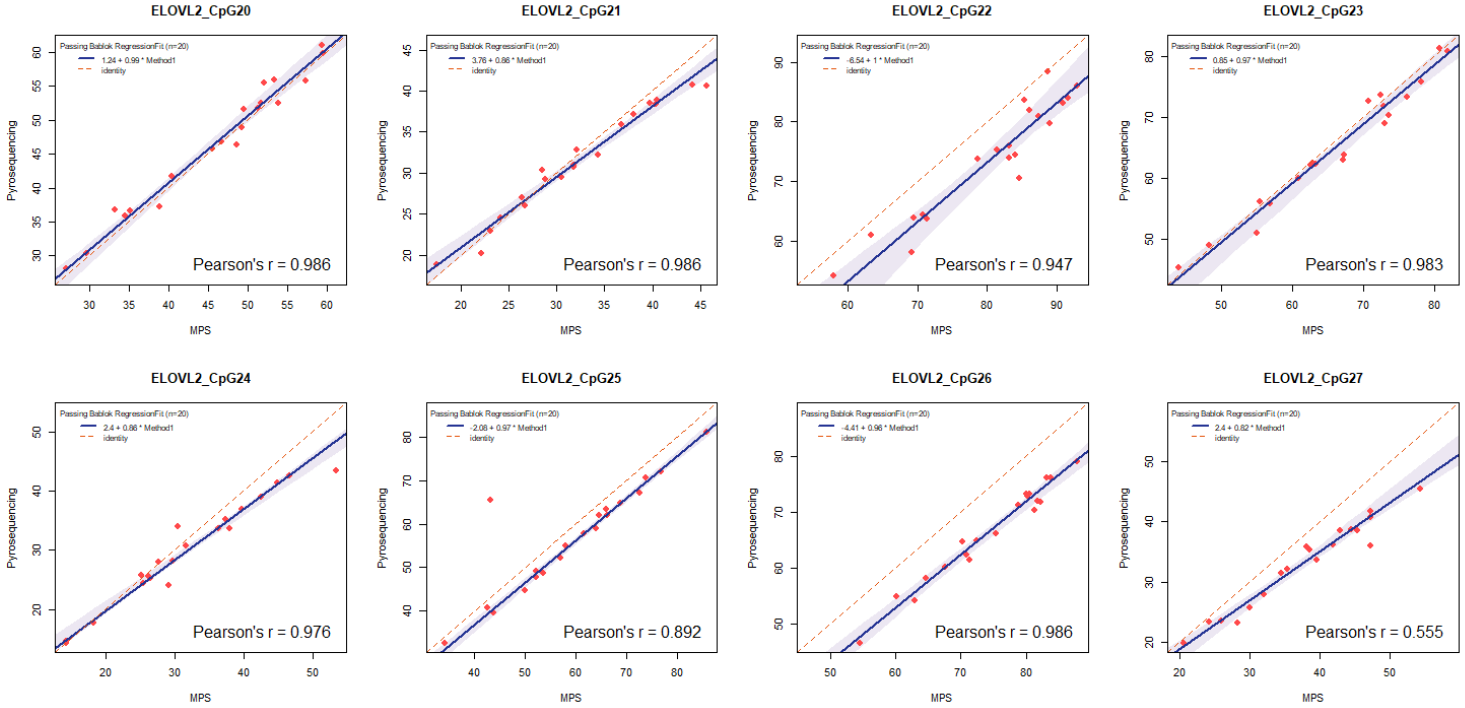

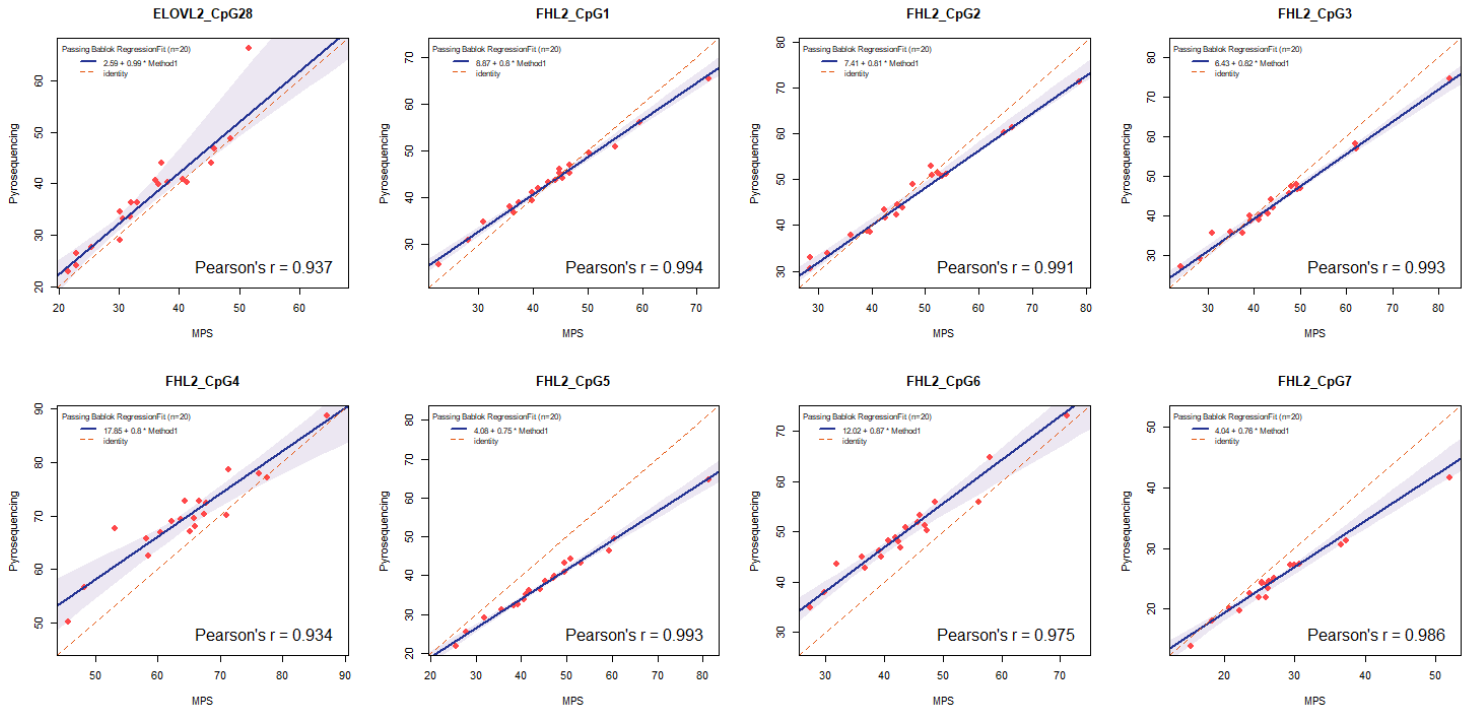

Appendix 4 (continued)

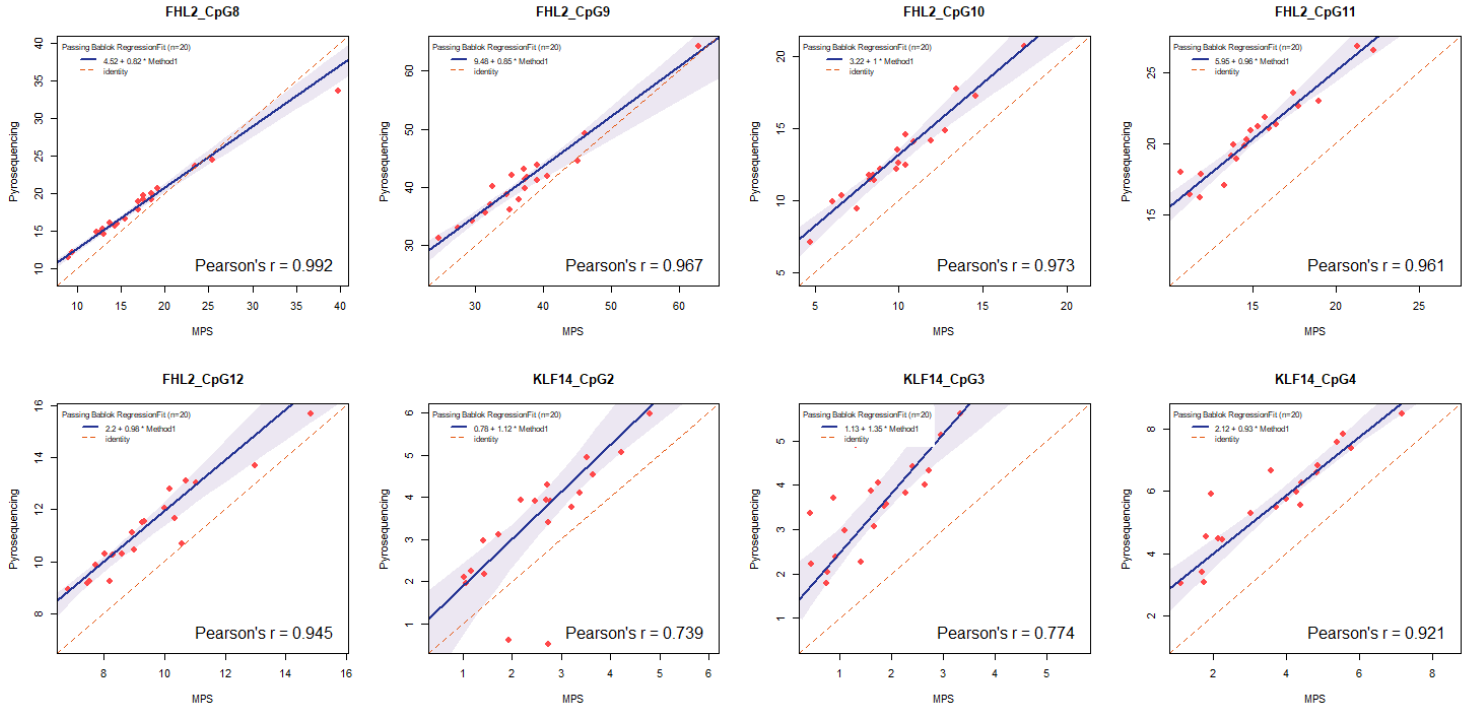

Appendix 4 (continued)

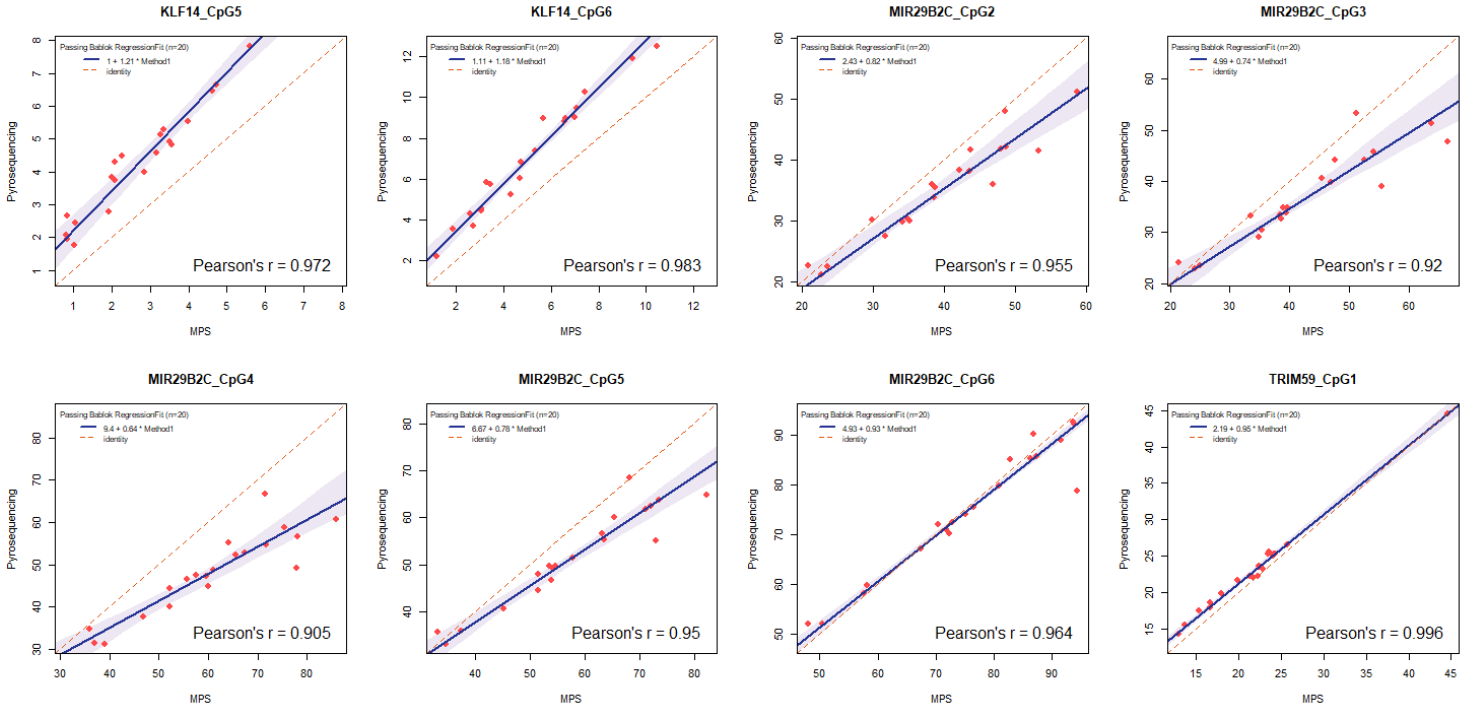

Appendix 4 (continued)

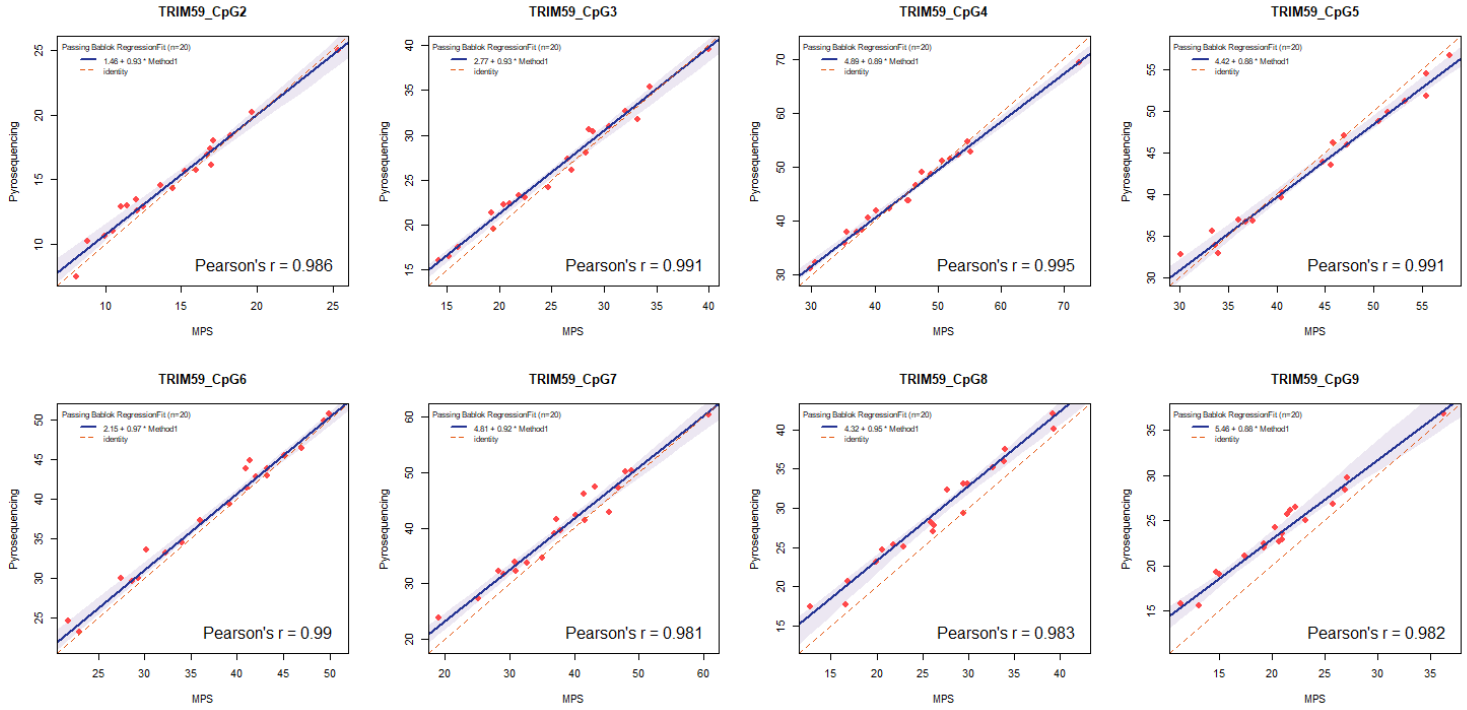

Appendix 4. 40 Common CpG makers of MPS (x-axis) and pyrosequencing (y-axis) from 20 samples.

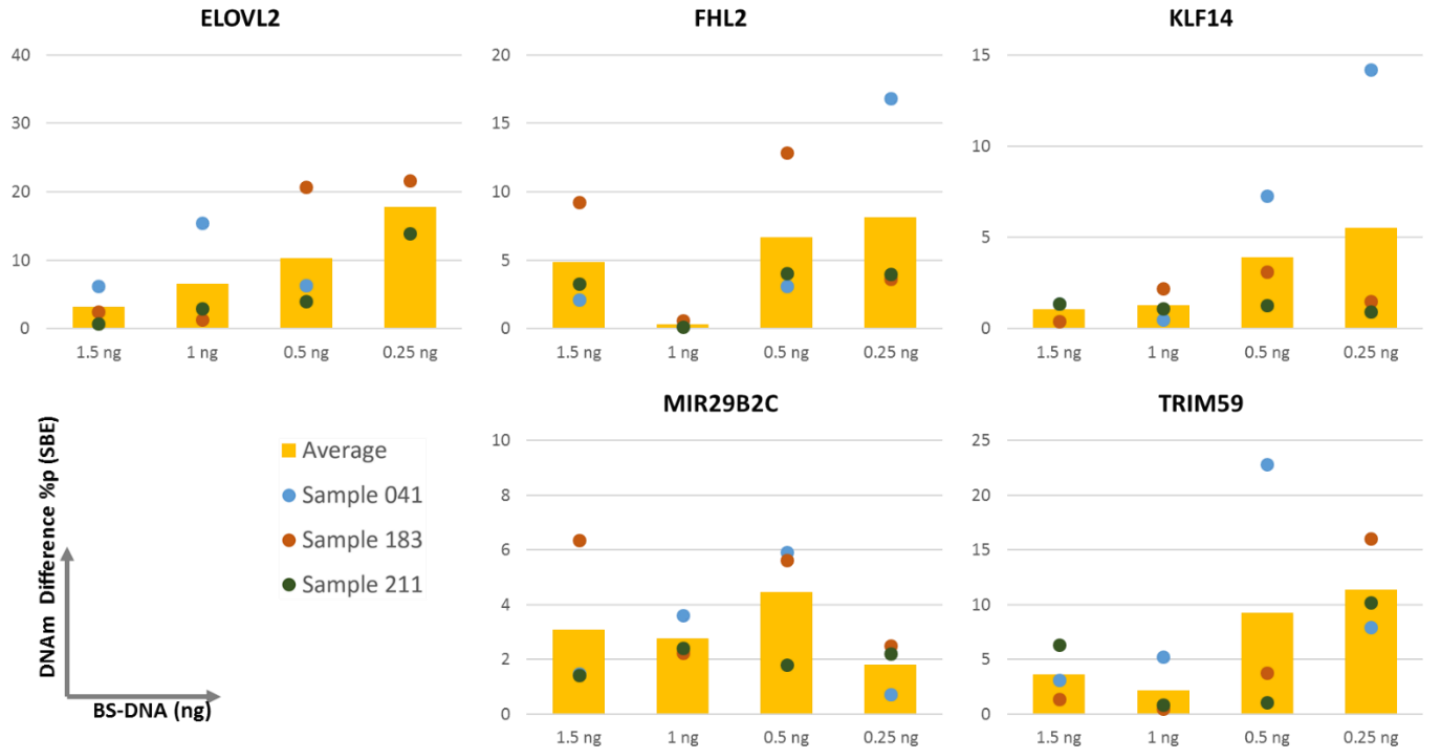

Appendix 5. Sensitivity test of constructed SBE. Based on DNAm level of 5 ng of BS-DNA, differences between 5 ng and each diluted BS-DNA were presented: 1.5 ng, 1 ng, 0.5 ng, and 0.25 ng. All BS-DNA samples were diluted and amplified based on the BisQuE result. There were tendencies that the difference was bigger when the amount of BS-DNA was smaller. Particularly, 0.25 ng data of *ELOVL2* from sample 041 was not detected at all.

Appendix 6. DNAm percentage of 5 CpG sites and predicted age using SBE primers of Jung et al.[33]

ID	Age	ELOVL2	FHL2	KLF14	MIR29B2C	TRIM59	Predicted Age*
13	24	36.51%	27.83%	5.42%	70.96%	28.77%	31.09
26	30	39.24%	22.03%	3.49%	70.36%	28.30%	28.72
39	35	34.08%	28.21%	7.28%	67.76%	30.81%	32.50
41	36	51.13%	25.95%	7.10%	71.92%	33.70%	40.28
54	41	42.69%	29.41%	6.79%	70.64%	33.07%	37.25
65	45	46.15%	28.51%	9.76%	63.35%	32.71%	42.65
74	49	54.27%	32.76%	12.09%	60.26%	39.75%	53.20
81	51	53.96%	30.14%	11.62%	58.62%	39.27%	51.87
86	53	49.54%	39.21%	11.84%	40.76%	42.49%	59.76
98	57	61.42%	31.70%	9.93%	54.01%	40.83%	57.39
109	62	55.05%	29.54%	12.29%	46.19%	42.30%	56.94
122	74	58.59%	44.13%	15.56%	45.76%	44.10%	68.39
133	23	31.43%	27.54%	5.11%	76.85%	29.48%	26.38
161	34	36.44%	26.21%	7.62%	72.98%	33.86%	32.28
183	43	51.47%	34.03%	7.78%	66.30%	34.93%	46.63
192	46	51.01%	29.63%	11.60%	59.75%	37.69%	49.25
213	54	51.06%	45.89%	7.57%	61.58%	40.00%	54.44
220	57	53.72%	33.07%	8.30%	52.46%	37.92%	52.49
221	57	54.94%	36.06%	9.43%	52.02%	40.43%	56.02
234	64	54.19%	31.47%	11.37%	50.00%	40.59%	55.27

*Predicted age was calculated with the blood age model of Jung et al.[33].

ABSTRACT(IN KOREAN)

바이설파이트 변환된 DNA의 정량과 플랫폼 간 분석을 이용한 법과학적 연령 추정

<지도교수 신 경 진>

연세대학교 대학원 의과학과

홍 새 롬

최근 DNA 메틸화는 최근 법의유전학에서 수사 단서로써 연령 추정 등 그 잠재성으로 인해 활발히 연구되고 있다. 여러 DNA 메틸화 분석 플랫폼을 이용해서 혈액과 같이 법과학적으로 관련도가 높은 체액의 연령 추정 모델이 많이 제안되었다. 많은 연령 추정 모델이 제안되었으나, 법과학적 맥락을 감안해 낮은 질과 적은 농도의 DNA, 연령과 DNA 메틸화의 연속성, 그리고 타 플랫폼의 모델 적용 시 낮아지는 정확도와 같은 고려 사항이 있다. 이런 점을 해결하기 위해, 바이설파이트 (BS) 변환된 DNA의 정량, 초병렬 시퀀싱 (massively parallel sequencing; MPS) 데이터를 바탕으로 하는 법과학적 연령 추정 모델, 그리고 널리 사용되는 단일 염기 연장 (single-base extension) 및 파이로시퀀싱의 플랫폼 간 분석을 위한 보정 방법을 다루었다.

우선, BS 변환은 대부분의 DNA 메틸화 분석법의 필수 요건이며, DNA의 분해와 손실을 유도해서 이후 분석 과정을 저해할 수 있다. 또한, 불완전한 바이설파이트 변환은 DNA 메틸화 정도를 과장하는 결과를 초래할 수 있어 매우 중대한 문제이다. 길이가 다른 두 multicopy영역에 대해 사이토신이

없는 중합효소연쇄반응(PCR) 프라이머를 도입해, BisQuE라고 명명된 다중 정량 실시간 중합효소연쇄반응(multiplex quantitative real-time PCR)을 개발했고, 이 시스템은 바이설파이트 변환 과정의 세 가지 중요한 요소인 바이설파이트 변환 효율, 회수율, 그리고 분해된 정도를 동시에 확인할 수 있었다. 개발된 BisQuE를 이용해 여섯 가지의 바이설파이트 변환 키트를 20개의 샘플에 대해 테스트 했다.

관찰된 DNA 메틸화 정도는 분석 방법에 따라 값이 달라질 수 있으므로, 본 연구에서는 자주 사용되는 MPS, SBE 및 파이로시퀀싱 플랫폼을 위한 동일 증폭산물 전략을 개발했다. 이 시스템은 ELOVL2, FHL2, KLF14, MIR29B2C와 TRIM59 상의 다섯 가지 증폭산물을 포함했다. 긴 길이의 BisQuE 결과를 바탕으로 250명의 혈액 DNA를 변환하고 BS 변환된 DNA를 신뢰도 있는 DNAm 결과를 갖는 최소량인 1.5 ng으로 준비했다.

250명의 DNA 메틸화 데이터를 MPS와 SBE에서 성공적으로 획득했고, 또한 20명에서의 5개의 마커에 대해 파이로시퀀싱을 진행해 같이 분석했다. 동일 증폭산물 전략으로 인해, 플랫폼에 따른 DNA 메틸화의 차이를 비교했고 이 중 ELOVL2 마커가 세 방법에서 서로 상호 교환이 됨을 확인했다. 그러나 나머지 마커에 대해서는 MPS 데이터에 맞추기 위해 SBE와 파이로시퀀싱 모두 보정 모델을 생성했다.

마지막으로, 연령과 DNA 메틸화의 연속성을 고려해, MPS를 바탕으로 하는 두 연령 추정 모델, 5-CpG 모델과 다중 CpG 모델을 구축했다. 5-CpG 모델은 단순화된 모델로 SBE와 공통으로 하는 5 종의 마커를 포함하며, 보정된 SBE 데이터에서 평균 절대 오차가 3.99세로 높은 정확도를 보였다. 다중 CpG 모델은 MPS와 파이로시퀀싱에 적용할 수 있으며 각각 2.85세와 5.43세의 오차를 나타냈다.

본 연구는 BS 변환된 DNA의 정량과 동일 증폭산물 전략을 바탕으로 법과학적 상황에서 연령 추정 모델링을 할 때의 지침을 제공하며, 모든 BS 변환된 DNA의 정량과 동일 증폭산물을 이용한 플랫폼 별 DNA 메틸화 차이를 분석한 첫 연구이다. 제안된 방법을 활용한다면 법과학 분야에서 모델을 제시하고자 하는 연구자는 정확하고 신뢰도 높은 연령 추정 모델링이 가능하며, 범죄 현장에서 나온 DNA를 다루는 연구자는 믿을 만한 연령 추정 결과를 보고할 수 있다.

핵심되는 말 : 연령 추정, 바이설파이트 변환, DNA 메틸화, 초병렬 시퀀싱, 파이로 시퀀싱, 정량 실시간 중합효소연쇄반응, 단일 염기 연장

PUBLICATION LIST

1. Hong SR, Jung SE, Lee EH, Shin KJ, Yang WI, Lee HY. DNA methylation-based age prediction from saliva: High age predictability by combination of 7 CpG markers. Forensic Sci Int Genet. 2017;29:118-125.
2. Cho S, Jung SE, Hong SR, Lee EH, Lee JH, Lee SD, et al. Independent validation of DNA-based approaches for age prediction in blood. Forensic Sci Int Genet. 2017;29:250-256.
3. Jung SE, Lim SM, Hong SR, Lee EH, Shin KJ, Lee HY. DNA methylation of the ELOVL2, FHL2, KLF14, C1orf132/MIR29B2C, and TRIM59 genes for age prediction from blood, saliva, and buccal swab samples. Forensic Sci Int Genet. 2019;38:1-8.
4. Hong SR, Shin KJ, Jung SE, Lee EH, Lee HY. Platform-independent models for age prediction using DNA methylation data. Forensic Sci Int Genet. 2019;38:39-47.
5. Lee HY, Hong SR, Lee JE, Hwang IK, Kim NY, Lee JM, et al. Epigenetic age signatures in bones. Forensic Sci Int Genet. 2020;46:102261.
6. Hong SR, Shin KJ. Bisulfite-Converted DNA Quantity Evaluation: A Multiplex Quantitative Real-Time PCR System for Evaluation of Bisulfite Conversion. Front. Genet. 2021;12:618955.